2006

Sources and Deposition Processes Linking Atmospheric Chemistry and Firn Records from Four Glacier Accumulation Zones in the McMurdo Dry Valleys, Antarctica

Bruce R. Williamson

SOURCES AND DEPOSITION PROCESSES LINKING ATMOSPHERIC CHEMISTRY AND FIRN RECORDS FROM FOUR GLACIER ACCUMULATION ZONES IN THE MCMURDO DRY VALLEYS, ANTARCTICA

By

Bruce R. Williamson

B.S. University of Washington, 2003

A THESIS

Submitted in Partial Fulfillment of the

Requirements for the Degree of

Master of Science

(in Earth Sciences)

The Graduate School

The University of Maine

August, 2006

Advisory Committee:

Karl J. Kreutz, Assistant Professor, Department of Earth Science, and the Climate Change Institute, Advisor

Paul A. Mayewski, Professor, Department of Earth Science, and Director of the Climate Change Institute

Stephen A. Norton, Professor, Department of Earth Science, and the Climate Change Institute

SOURCES AND DEPOSITION PROCESSES LINKING ATMOSPHERIC CHEMISTRY AND FIRN RECORDS FROM FOUR GLACIER ACCUMULATION ZONES IN THE MCMURDO DRY VALLEYS, ANTARCTICA

By Bruce R. Williamson

Thesis Advisor: Dr. Karl Kreutz

An Abstract of the Thesis Presented
in Partial Fulfillment of the Requirements for the
Degree of Master of Science
(in Earth Sciences)
August, 2006

Samples of snow and firn from accumulation zones on the Victoria Upper Glacier, the Clark Glacier, the Commonwealth Glacier and the Blue Glacier in the McMurdo Dry Valleys (~77 to 78° S and 161 to 164° E), Antarctica, are evaluated chemically and isotopically to determine the relative importance of local (site-specific) factors versus regional-scale climatic influences in defining regional glaciochemistry. Two approaches for distinguishing these controls are examined: comparing chemical concentrations using multivariate statistical analysis, and examining the effect of physical filtration (capturing particulate material largely originating in close proximity to each site) on sample values. These techniques provide constraints for interpretation of connections between Dry Valleys climate and the broader Ross Sea and East Antarctic Ice Sheet climate systems.

and Sr, on the other hand, are either completely or dominantly (average 65% - 85%) present in dissolved or soluble particulate form.

Statistical analysis and physical filtration together demonstrate that in areas where glaciochemical signals are influenced by locally derived particulates, interpreting regional trends requires caution. Differences in local effects between two locations may overwhelm broader climate signals. In areas of complex topography and terrain, the influence of these local factors must be understood before climate inferences can be drawn.

ACKNOWLEDGEMENTS

This material is based upon work supported by the National Science Foundation under Grant No. 0228052. I thank all of the people without whom this work would certainly not have been possible. The comments of my thesis committee, and in particular my advisor, Karl Kreutz, have taken a series of broad ideas and given them a form that I did not anticipate when I began the project, and which is far superior to my original thinking regarding Dry Valleys climate and chemistry. In addition, the Climate Change Institute and University of Maine laboratory staff spent a great deal of time introducing me to the meaning and the quirks of data generated by the instruments described in these chapters; I especially thank Mike Handley, Doug (Cap) Introne, Sharon Sneed and Tiffany Wilson for the hours of analysis for this project and for listening as I repeated the same questions multiple times until I finally had an adequate grasp of these instruments to work with the data they generate. The collection of field samples and understanding of the surrounding field conditions was possible only with the help and teaching of Steve Arcone, Terry Gacke, Erich Osterberg and Mike Waskiewicz. Help with maps and site locations was provided by Jessica Walker, with the United States Antarctic Program at McMurdo Station. GPS location surveys for satellite sites were conducted by Beth Bartel, from UNAVCO, also based out of McMurdo. Finally, Alison Williamson spent many hours working with my text to improve the language and organization, making the structure and grammar more comprehensible. The help of all

these individuals and the support of many more in providing background information regarding Antarctica, firn chemistry and meteorology is reflected here and is greatly appreciated.

TABLE OF CONTENTS

LIST OF TABLES

LIST OF FIGURES

INTRODUCTION

Nearly a century since Amundsen and Scott first arrived at the South Pole, Antarctica remains remote. Researchers have taken advantage of the continent's resulting minimal human fingerprint to catalog information stored in Antarctic ice regarding the history of the planet's atmosphere [e.g. *Mayewski et al.*, 1995; *Kreutz et al.*, 1997; *Petit et al.*, 1999; *Steig et al.*, 2000; *Augustin et al.*, 2004]. Ice core sites used to develop paleo-atmospheric proxy records have been chosen both in the interior of the continent [*Petit et al.*, 1999; *Augustin et al.*, 2004] and closer to the coast [*Mayewski et al.*, 1995; *Kreutz et al.*, 1997; *Steig et al.*, 2000] to provide decadal to millennial records of air masses reflecting both continental and marine processes. At the same time that deeper core sites permit a survey of changes in atmospheric chemistry through time, substantial work has filled in spatial gaps between core locations and led to a better understanding of the broader context of Antarctic climate [e.g. *Boutron and Martin*, 1980; *Mulvaney and Wolff*, 1994; *Mayewski*, 2003; *Dixon et al.*, 2004; *Bertler et al.*, 2005].

Among the coastal areas of Antarctica, the McMurdo Dry Valleys (MDV), southern Victoria Land, are of interest because they combine proximity to the Ross Sea with ~4800 km^2 of ice-free area, making this one of the largest areas of exposed terrain on the continent [*LTER*, 2005]. Investigators have worked extensively in this region to describe the chemistry of lakes, streams, and soils and how each of these chemistries affects local biology [*Welch et al.*, 1994; *Lyons et al.*, 2001; *DeCarlo and Green*, 2002; *Gooseff et al.*, 2003; *Lyons et al.*, 2003]. In between these areas of exposed rock and soil,

several alpine glaciers occupy the ridges separating individual valleys, some with separate accumulation zones and some with ice originating on the polar plateau to the west. These glaciers have provided datasets used to demonstrate increases in ice-free terrain and in the transport of marine tropospheric air into the region covering the past ~150 years, to describe a historical pattern of monsoonal circulation in the Dry Valleys, and to link recent regional temperature history to the El Niño Southern Oscillation [*Mayewski and Lyons*, 1982; *Mayewski et al.*, 1995; *Bertler et al.*, 2004*a*; *Bertler et al.*, 2004*b*].

The presence of extensive exposed rock and soil in the Dry Valleys creates opportunities and challenges in interpreting climate proxies from local snow accumulation zones. In particular, opportunities exist for examining local-scale climate patterns because of separation between the alpine glaciers of the Dry Valleys, yielding spatially distinct accumulation zones within a small geographic area, unusual in Antarctica. In addition, the soils present in the region provide the opportunity for a better understanding of the ebb and flow of regional ice cover [*Mayewski and Lyons*, 1982; *Mayewski et al.*, 1995].

Exposed soils also, however, create complications in understanding MDV climate records. The valleys occupy an area within 100 km of the coast, so it is not surprising that many studies have documented a strong marine signature in MDV snow and ice chemistry [*Welch et al.*, 1993; *Mayewski et al.*, 1995; *Lyons et al.*, 2003; *Bertler et al.*, 2004*b*]. On the other hand, these same authors note high terrestrial loads at many sites and remark on the differences in the resulting chemical datasets relative to sites on the polar plateau, characterized by the absence of significant local particle sources [*Mayewski*

and Lyons, 1982; *Lyons et al.*, 2003; *Bertler et al.*, 2004*b*]. For this reason, investigators continue to refine methods for separately identifying local soil and marine inputs to allow a more complete understanding of climate proxies recovered from the Dry Valleys glaciers.

Recent advances in the measurement of trace metals have created the opportunity to measure with great precision a variety of elements associated predominantly with terrestrial dust inputs. In areas of Antarctica far from particulate sources, trace metal concentrations can be well below the parts per trillion (ppt) level [*Planchon et al.*, 2002]; sources for these materials may include volcanic emissions [*Matsumoto and Hinkley*, 2001] and human pollution [*Planchon et al.*, 2002], as well as terrestrial soil materials [*Matsumoto and Hinkley*, 2001; *Planchon et al.*, 2002]. Sea water provides only a very small component for many of these metals, even over the open ocean; in lower marine air over the North Atlantic, for example, Al and Fe are enriched relative to Na^+ ~5000x and ~10000x above the concentrations of these species associated with sea-salt [*Weisel et al.*, 1984]. Similar ratios can be derived using published concentrations for Southern Ocean water and air [*Dick and Peel*, 1985; *Abollino et al.*, 2001].

In this thesis, I examine the upper two meters of surface snow and firn from four sites in the Dry Valleys – the Clark Glacier, the Commonwealth Glacier, the Blue Glacier, and the Victoria Upper Glacier (Figure I.1) – using a combination of trace metal, major ion and stable isotope analysis. The material collected at these sites represents precipitation deposited from 1989 to 2002 at all sites; at some sites, the period from 1980 to 1989 is covered as well. These sites comprise four glaciologically separate accumulation zones (they are distinct alpine glaciers, separated by ridges and valleys of

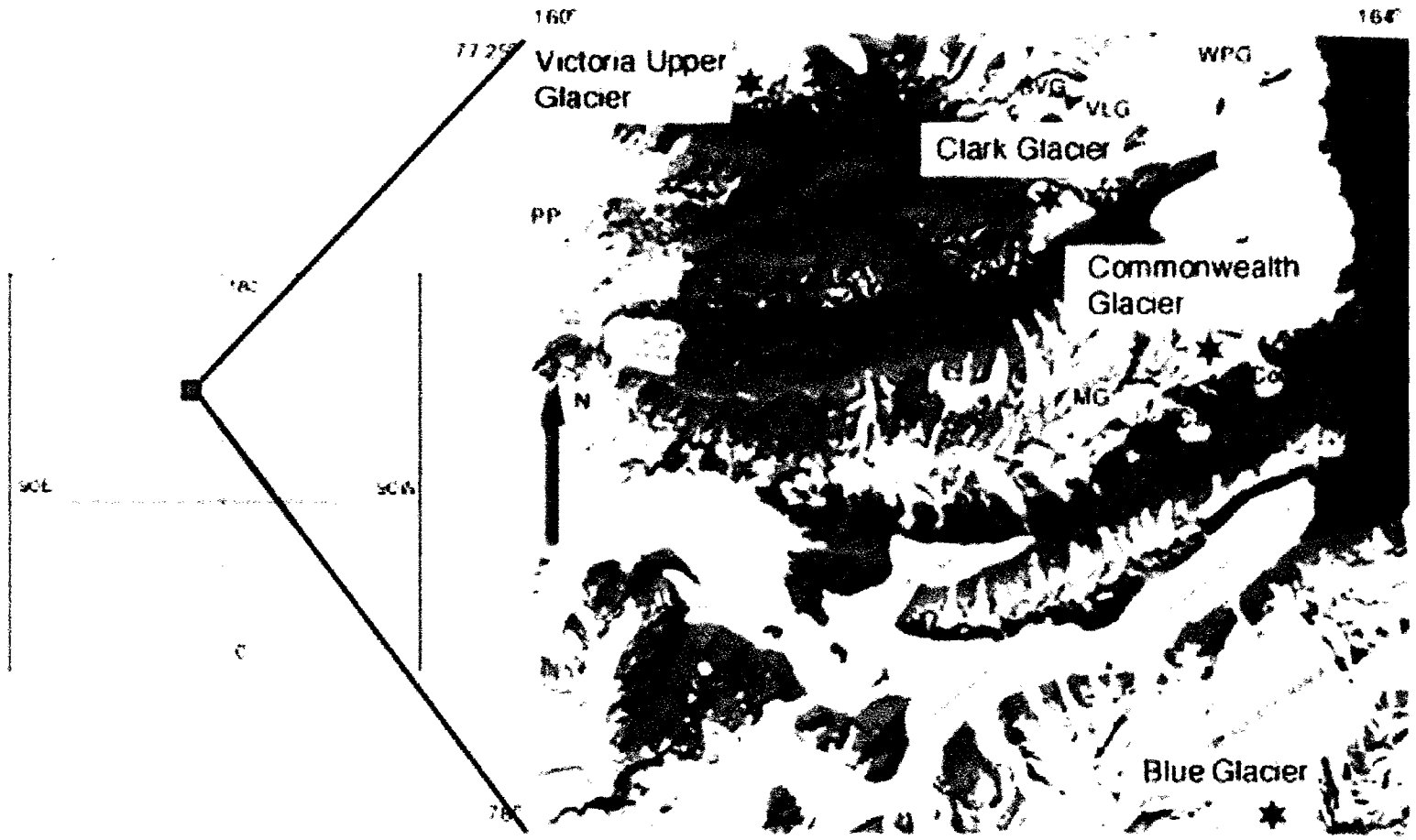

Figure I.1. Index map showing locations of Victoria Upper, Clark, Commonwealth, and Blue Glaciers. Base Map by GeographX, 2006.

exposed rock and soil), allowing study of precipitation and material input potentially unique to each area. The chemical signals for each glacier are derived from marine and terrestrial inputs varying in intensity based on proximity to the Ross Sea and to the valley floors, and with the transport histories associated with each location. Records for three of the sites are new, while the fourth – the Commonwealth Glacier – supplements ongoing research conducted as part of the Long Term Ecological Research (LTER) program [*Lyons et al.*, 2003]. The results of this work improve our ability to interpret atmospheric reconstructions based on regional ice cores and LTER data; these interpretations, in turn, will enable us to better understand the interplay between marine and continental air masses in a critical coastal area at the junction of the East Antarctic Ice Sheet and the Ross Sea.

Treatment of the results is divided into two parts. The first chapter uses the relationship among trends in three data sets – trace metal data from inductively-coupled plasma mass spectrometry (ICP-MS), major ion data from ion chromatography (IC) and stable isotope data from isotope ratio mass spectrometry (IRMS) – to interpret regional patterns in atmospheric deposition. First, an estimated accumulation rate is provided for each site based on seasonal variation in the concentration of sodium ion; this accumulation rate is confirmed by comparing it to physical accumulation records conducted alongside chemical sampling sites. Next, patterns in intra-site and inter-site chemistry deposition are presented and compared to previous authors' work in the region. The ratio of sea-salt (ss) to non-sea-salt (nss) fractions of species aids in the interpretation of spatial patterns in chemistry deposition [*Legrand and Mayewski*, 1997]. Finally, using

the statistical tool of Empirical Orthogonal Function (EOF) analysis, data for a selection of chemical species and elements are compared to examine relationships among the timing of species input at each location. At many sites in Antarctica and in the Dry Valleys, gradients in chemical concentrations have been documented relative to distance from the coast or to elevation [*Legrand and Delmas*, 1985; *Legrand and Delmas*, 1988; *Mulvaney and Wolff*, 1994; *Kreutz and Mayewski*, 1999; *Lyons et al.*, 2003; *Bertler et al.*, 2004b; *Bertler et al.*, 2005]. Based on the results of the above analyses, however, along the north-south coastal axis traced by the sites examined here, these gradients play a secondary role in predicting chemical concentrations. Primary controls explaining variation along this axis instead include local (site-specific) exposures to the marine source and to dust sources surrounding each site.

The second chapter focuses on the relative strengths and weaknesses of three different sample preparation procedures used to measure 35 different elements from the Victoria Upper Glacier. In particular, this work addresses the effects of sample filtering and acidification for high-particulate-load samples prior to analysis by ICP-MS. Values for the filtrate fraction and for the insoluble particulate fraction (defined here as the fraction of each element found in particle sizes >0.4 μm, an intermediate pore size filter among values found in the literature from 0.2 μm to 45 μm [*Abollino et al.*, 1995; *Edwards and Sedwick*, 2001; *Knusel et al.*, 2003]) are examined separately to determine the reproducibility of each measurement and the relative amount of each element found in soluble and insoluble form. This analysis tests the possibility of using this procedure to yield separate and complementary records for "soluble" and "insoluble" particulate in snow and ice with high particulate content. Because local exposed rock and soil provide

the most likely sources for insoluble particulate material, this procedure provides insight into the distinction between input of local terrestrial materials and input of marine materials in the Dry Valleys.

Chapter 1:

A COASTAL TRANSECT OF MCMURDO DRY VALLEYS SNOW AND FIRN: MARINE AND VALLEY INFLUENCES ON GLACIOCHEMISTRY

The Dry Valleys provide an unusual opportunity to study the interplay between local- and regional-scale spatial trends in Antarctic climate. Several studies in the region show a combination of marine and continental air masses influencing local climate with seasonality, external forcings, and site-specific factors creating diverse conditions [*Welch et al.*, 1993; *Mayewski et al.*, 1995; *Doran et al.*, 2002; *Bertler et al.*, 2004]. In addition to information regarding local climate, for the Newall Glacier in the MDV and for nearby Taylor Dome, there is a growing body of literature examining regional climate as it relates to global signals [*Mayewski et al.*, 1995; *Mayewski et al.*, 1996; *Steig et al.*, 1998; *Steig et al.*, 2000].

The Dry Valleys are of particular interest to Antarctic researchers because this region contains records of marine, aeolian, lacustrine and fluvial processes within a small geographic area [*Hall et al.*, 2000; *Armienti et al.*, 2001; *DeCarlo and Green*, 2002; *Hall et al.*, 2002; *Lancaster*, 2002; *Green et al.*, 2005; *Hall and Denton*, 2005]. In addition, although the area is known for research on the exposed valley floors, there are several alpine glaciers residing on ridges separating the individual valleys. Ice cores from sites on several of these glaciers have provided records of atmospheric chemistry showing connections between local snow and ice composition and marine ionic chemistry [*Mayewski et al.*, 1995; *Lyons et al.*, 2003] marine biological activity and sea ice extent [*Welch et al.*, 1993], and local aerosol transport [*Mayewski and Lyons*, 1982; *Bertler et al.*, 2004].

This chapter focuses on evidence used to isolate local input of aerosols to MDV glaciers, including effects based on differing site exposures to marine airflow and proximity to differing soil sources, from the effects of regional climatic variables such as distance from the coast or elevation. This question is complicated by the fact that significant concentrations of the analytes found in MDV ice derive both from marine species associated with the nearby Ross Sea and from soluble and insoluble materials present within the valleys themselves [*Mayewski and Lyons*, 1982; *Welch*, 1993; *Welch et al.*, 1993; *Mayewski et al.*, 1995; *Lyons et al.*, 2003; *Bertler et al.*, 2004]. Interpreting chemical records in this area therefore requires techniques to separate these local terrestrial signals from the regional marine signal.

In this work, I discuss the chemical composition of snow and firn from four sites in the region – the Clark Glacier, the Commonwealth Glacier, the Blue Glacier, and the Victoria Upper Glacier. The first three of these sites trace a north-south transect within 30 km of the coast of the Dry Valleys region and are in close proximity to three of the primary valleys in the MDV network – the Victoria Valley, the Wright Valley, and the Taylor Valley – and three smaller size (~10 km) valleys – the Garwood Valley, the Marshall Valley, and the Miers Valley. The Victoria Upper Glacier is located at the western end of the Victoria Valley, near the junction between the polar plateau and the MDV. Chemistry data from snow and firn samples representing all sites were generated using ion chromatography (IC), inductively-coupled plasma mass spectrometry (ICP-MS), inductively-coupled plasma optical emission spectrometry (ICP-OES), and isotope ratio mass spectrometry (IRMS) to measure 43 elements, ions and isotope ratios. To assess trends in these data sets, mean values for a selection of species are first evaluated

to provide a picture of spatial variation in snow and ice chemistry on a local scale (within the accumulation zones of the Clark and the Commonwealth Glaciers), and on a regional scale (among the four sites). These mean values and the relationships between them are also compared to similar surveys conducted within individual valleys by other investigators. Finally, using Empirical Orthogonal Function (EOF) analysis, I observe which subsets of these species co-vary in their deposition, yielding information to help distinguish input timing for groups of analytes. Although several investigators in Antarctica and in the Dry Valleys have demonstrated links between species concentrations, elevation, distance from the coast, and distance to the sea-ice edge [*Legrand and Delmas*, 1984; *Legrand and Delmas*, 1988; *Welch et al.*, 1993; *Kreutz and Mayewski*, 1999; *Lyons et al.*, 2003; *Bertler et al.*, 2004], these trends are not present within this data set, indicating that differing soil sources and site exposures provide stronger influences on site chemistries along a north-south axis than do these regional-scale parameters.

Background

A number of researchers have discussed major ion chemistry in Dry Valleys snow and ice [*Mayewski et al.*, 1995; *Lyons et al.*, 2003; *Bertler et al.*, 2004], and in some cases have examined a selection of trace metals [*Mayewski and Lyons*, 1982; *Bertler et al.*, 2004]. All agree that local insoluble material plays a significant role in shaping the distribution of chemistry in MDV samples, and that dry periods combined with high winds likely deposit significant amounts of both soluble and insoluble species to glacier surfaces [*Mayewski and Lyons*, 1982; *Mayewski et al.*, 1995; *Lyons et al.*, 2003; *Bertler*

et al., 2004]. Refining the nature of these wind patterns in an examination of major ion, Al, and Fe input timing on the Victoria Lower Glacier, Bertler et al. [2004*b*] found that with few exceptions, concentration maxima occur at the same time for marine and terrestrial elements. They associated these shared maxima with a "monsoonal" circulation in Dry Valleys climate and suggested that local chemistry thus provides a glaciochemical record of onshore-offshore wind patterns known to function in modern MDV meteorology [*Thompson et al.*, 1971; *McKendry and Lewthwaite*, 1990; *Doran et al.*, 2002; *Bertler et al.*, 2004].

The Dry Valleys are characterized by high spatial variability in meteorology, with temperature differences as high as 30 C° and wind speed differences of up to 10 ms^{-1} within a 30 km distance [*Doran et al.*, 2002]. A shift from relatively calm warm summers to relatively windy cold winters defines the local climate. Katabatic winds, in particular, play a large role in determining temperatures and relative humidity, especially in the austral winter (June, July, and August [JJA]) [*Thompson et al.*, 1971; *Doran et al.*, 2002; *Nylen et al.*, 2004]. During the summer, katabatic winds are less important, with a larger role taken by onshore flow [*Thompson et al.*, 1971; *Doran et al.*, 2002; *Nylen et al.*, 2004].

Bedrock lithologies in the MDV include dolerites, tonalites and granodiorites, metamorphic suites, and sedimentary units associated with the Beacon Sandstone [*McKelvey and Webb*, 1959; *McKelvey and Webb*, 1962; *Claridge and Campbell*, 1977; *Keys and Williams*, 1981; *Smilley*, 1987]. Surficial material recording ice advance from the direction of the Ross Sea during the last glacial maximum includes moraines, deltaic sediments from ancient lakes, and assorted till units associated with a variety of glacial

pulses [*Hall et al.*, 2000; *Hall et al.*, 2002; *Hall and Denton*, 2005]. The lithology of these surficial units varies depending upon the extent of each glacial advance and the source of the rocks entrained [*Hall et al.*, 2000; *Hall and Denton*, 2005].

Soils in the Dry Valleys contain abundant water-soluble salts, derived primarily from atmospheric deposition and weathering [*Claridge and Campbell*, 1977; *Keys and Williams*, 1981; *Bockheim*, 1997; *Bockheim*, 2002]. Sodium and Cl- ions trace a negative concentration gradient moving away from the coast, suggestive of a marine source, while NO_3^- increases inland and SO_4^{2-} is relatively evenly distributed between the polar plateau and the coast [*Keys and Williams*, 1981; *Bockheim*, 1997]. The SO_4^{2-} signature suggests a combination of marine biogenic, sea-salt and local lithologic input, depending on location within the valleys [*Claridge and Campbell*, 1977; *Keys and Williams*, 1981; *Bao et al.*, 2000]. Wind transport of these soils generally leaves larger particles (>50 μm) near the valley floors, with nearby glaciers receiving dominantly silt and clay size (<50 μm) particles [*Lancaster*, 2002]. At Terra Nova Bay, a coastal site 250 km to the north that is also strongly affected by katabatic flow, airborne particles were very similar in character to local sediment samples (marine and lacustrine), with 98% of Na^+ and 80% of K^+ and Mg^{2+} derived from a marine source, while only 50% of SO_4^{2-} and 22% of Ca^{2+} came from this source; Al and Fe were derived entirely from crustal sources [*Guerzoni et al.*, 1992].

Sampling Locations and Techniques

Samples for this study were collected from accumulation zones on the Clark Glacier (77.4054° S, 162.3656° E, 816 m), the Commonwealth Glacier (77.5423° S, 163.0226°E, 723 m) the Blue Glacier (78.0830° S, 163.2932° E, 1022 m), and the Victoria Upper

Glacier (77.3005° S, 161.0419° E, 1350m), located in the Olympus Range, the Asgaard Range, the Royal Society Range, and the Clare Range, respectively (Figure I.1). These sites are all within 60 km of McMurdo Sound. Snowpits were excavated in November, 2003 at the Clark, Commonwealth and Blue locations and in November, 2004 at the Victoria Upper Glacier as part of efforts to determine suitability for future collection of medium-depth ice cores [*Kreutz and Mayewski* proposal, 2002].

Snowpits at the Clark, Blue, and Victoria Upper Glaciers were dug to depths of 200 cm, 226 cm and 224 cm respectively; the pit at the Commonwealth Glacier was dug to 304 cm. One wall of each pit was prepared for sampling by first removing the outer 10 cm of firn with a clean plastic shovel and then scraping with a pre-rinsed plastic scraper to remove another 2 cm of material so as to avoid contamination. During this preparation process and the sampling process, the person collecting samples wore a Tyvek ® clean suit and two pairs of clean polyethylene gloves. Using pre-cleaned titanium tools, samples were collected at 2-cm intervals for major ion and isotopic analysis and at 10-cm intervals for trace element analysis (a higher-volume, lower-resolution sample was collected to allow multiple tests of trace elements from each interval, discussed in chapter 2, while staying within the lateral area associated with the major ions data); samples were collected working from the surface to the pit base. Each major ion and isotope sample was collected into one 60 mL polypropylene cup and each trace element sample was collected into a separate 500 mL polypropylene bottle. Major ion/isotope containers were cleaned before use by rinsing 3 times with deionized water (DI) (>18 MΩ.cm resistivity), soaking for >8 hours in DI, rinsing again 3 times and drying in a clean laminar flow bench for two hours. Trace metal containers were soaked in 10% HNO_3 for

24 hours, rinsed once, soaked for 24 hours and rinsed again in DI before drying on the clean bench.

Following the collection of the chemistry samples, snow density and temperature were measured at 3-cm resolution next to the sampling line (Figure 1.1). Because temperature probes measured temperature ~10 cm into the snow surface, and temperature sampling required <15 min for each 2 m sampling wall, the effects of ambient air temperature equilibration are expected to be minor. Borehole temperature data were also collected using an RBR model TR-1050P temperature logger lowered into boreholes on the Clark, Commonwealth and Victoria Upper Glaciers in November, 2005. Borehole temperatures presented here represent equilibration for a minimum of 45 minutes at selected ice depths. Snowpit chemistry sampling was completed in one day for the Victoria Upper, Clark and Blue Glaciers (2 m snowpits) and in two days for the Commonwealth Glacier (3 m snowpit). After collection, samples were maintained at -20° C and shipped back to the University of Maine Climate Change Institute for analysis.

Mass balance pole networks in proximity to the snowpits described here included 4 pole x 5 pole grids on the Clark and Commonwealth Glaciers with 200-meter spacing between poles, and a 3 pole x 3 pole grid on the Victoria Upper Glacier with 100-meter spacing (Figure 1.2). These networks were left in place between the 2004 and 2005 seasons, yielding one year of data. Mass balance poles were also installed in the 2003 season at the Clark, Commonwealth, and Blue Glaciers, with greater and more irregular pole spacing (~500 meter); 2004-2005 data for the Blue Glacier comes from the November, 2005 measurements of these poles. Mass balance data collected by the LTER group for the Commonwealth Glacier is included here for comparison during time

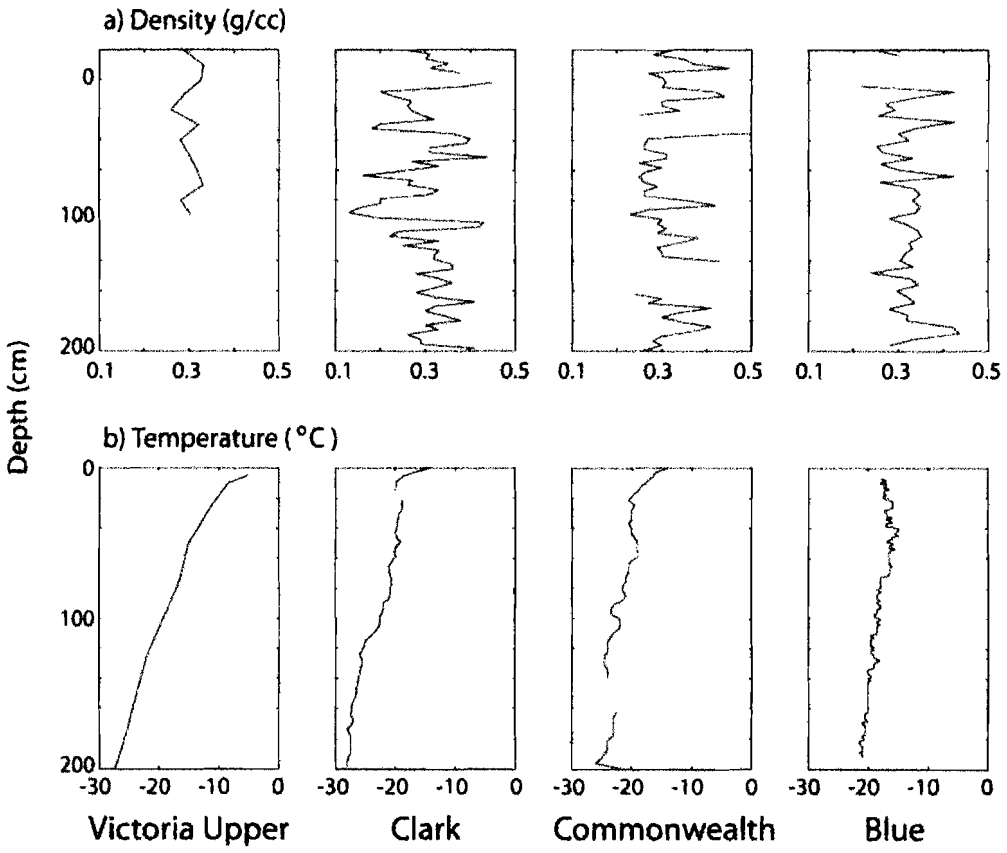

Figure 1.1. Density and temperature profiles for the Victoria Upper, Clark, Commonwealth, and Blue Glaciers. Density measurements were not collected for the Victoria Upper Glacier below 120 cm because firn density was too high for the equipment used.

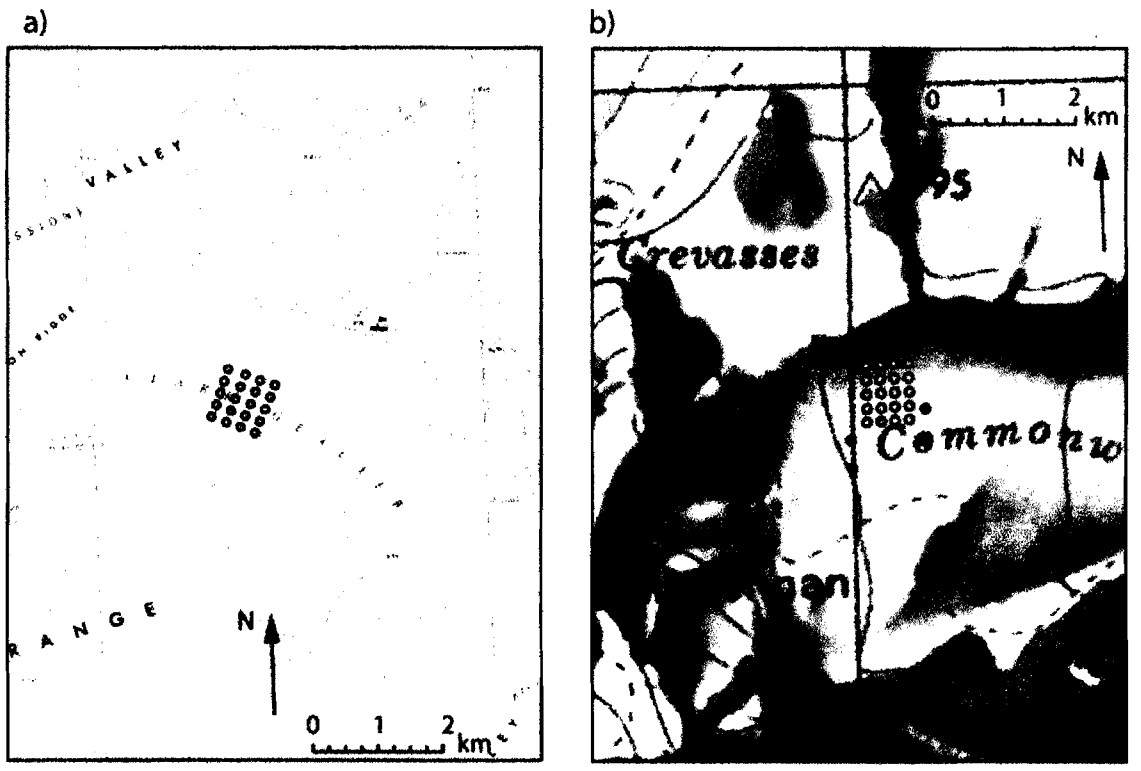

Figure 1.2. Mass balance pole networks for a) the Clark Glacier, b) the Commonwealth Glacier, c) the Blue Glacier, and d) the Victoria Upper Glacier. The area covered by the network (9 poles) on the Victoria Upper Glacier is represented as a square covering the approximate area of the network for clarity.

periods not covered by the above networks [*Fountain*, 2005]. Though there have been more than 20 LTER poles monitored on the Commonwealth Glacier on an intermittent basis, only four were located within 1500 meters of the snowpit; data from these four poles was used to ensure that the poles were measuring accumulation in areas of the glacier where there is net snow accumulation rather than net snow ablation.

Lastly, at the Clark and Commonwealth Glaciers, six additional pits (three at the Clark and three at the Commonwealth) were excavated and sampled during November 2004 using techniques identical to those used at the primary pits. These satellite pits were spaced 800 m apart to examine spatial variability within the area of each accumulation zone (Figures 1.3, 1.4). Five of the sites were sampled to 100 cm depth, while the sixth (one of three at the Commonwealth) was sampled to 60 cm depth. The pits at the Clark Glacier were sampled at 2-cm resolution, and those at the Commonwealth at 4-cm resolution, allowing comparison of mean chemistry values over a time period shared by the snowpits of 3 years at the Commonwealth Glacier and of 7 years at the Clark Glacier. Excavation and sampling required less than one day for each of these satellite pits.

Analysis

Major ion analysis was conducted using a Dionex™ DX-100 ion chromatograph after samples were melted and transferred via pipette to 8 mL mailing tubes used to introduce samples on to the column of the IC. These pipettes and mailing tubes were cleaned according to the same procedures used for the original sample containers. Anions (MS^-, Cl^-, NO_3^-, SO_4^{2-}) were measured using an AS-11 column and a Dionex™ Reagent

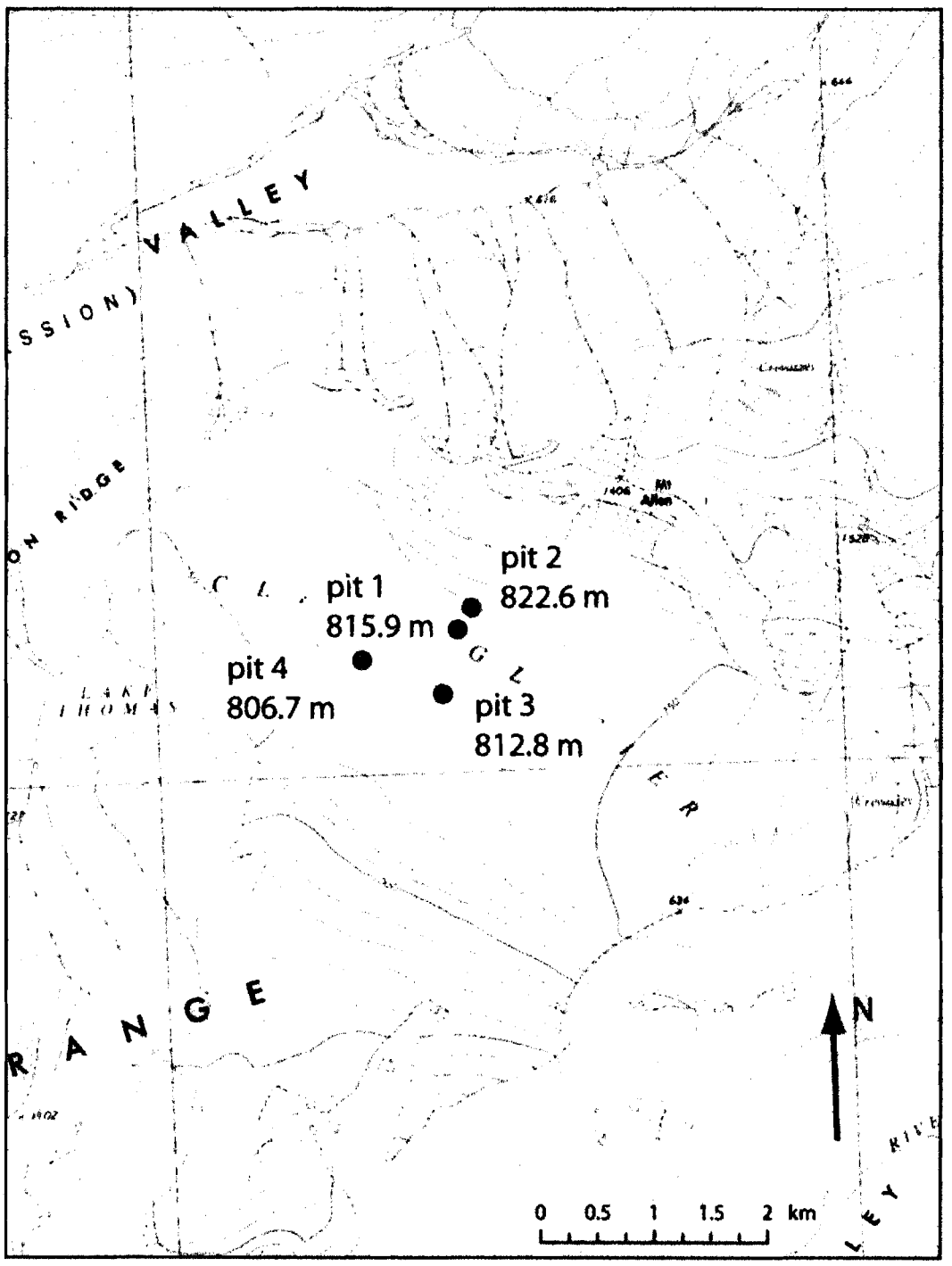

Figure 1.3. Locations of multiple one-meter pits on the Clark Glacier. The primary pit excavated in 2003 is shown in blue. The three pits excavated in 2004 to explore spatial variability are shown in red. Base map USGS Lake Brownworth quadrangle, 1977.

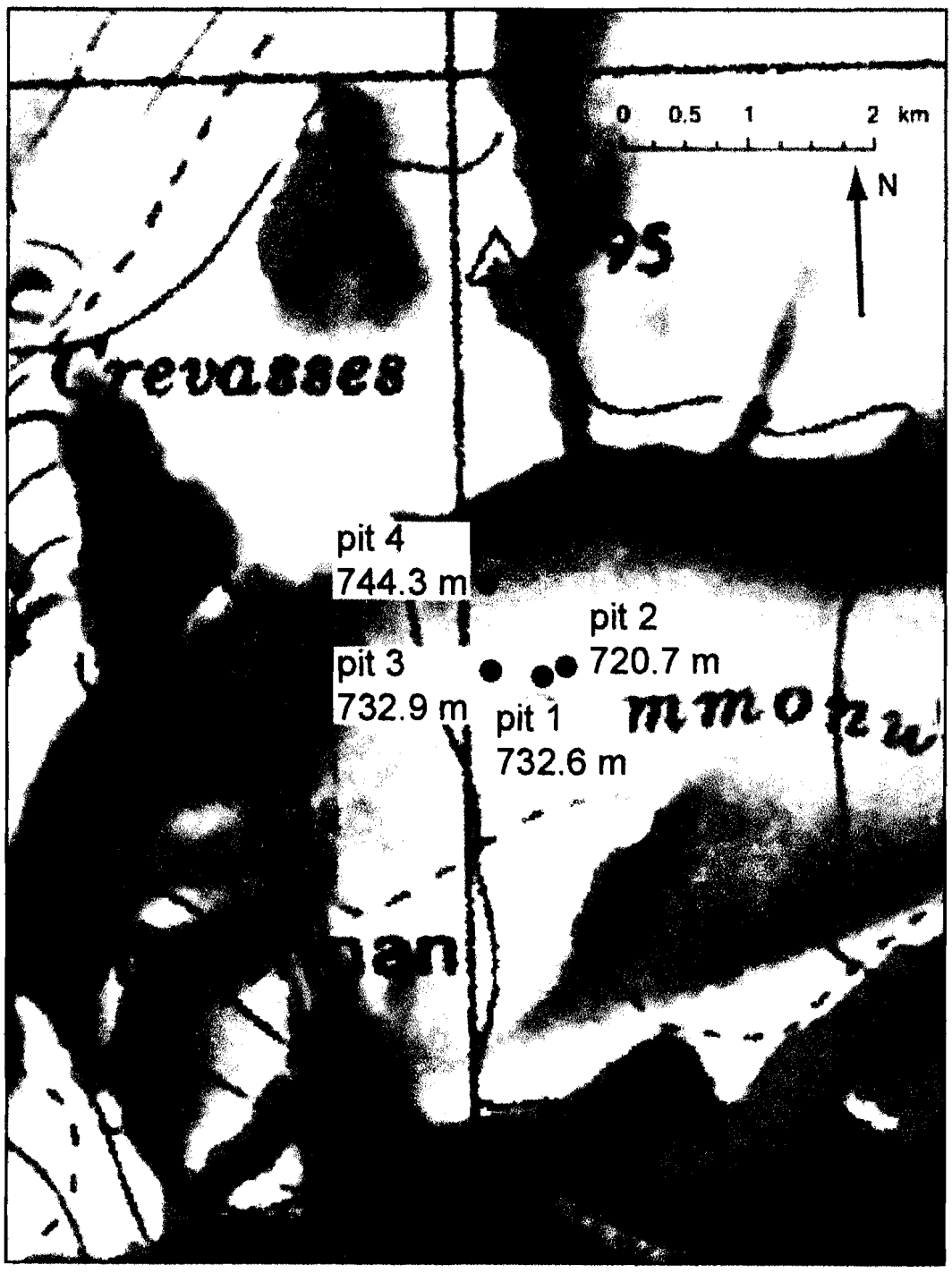

Figure 1.4. Locations of multiple one-meter pits on the Commonwealth Glacier. Base map USGS Ross Island and Vicinity, 1986.

Free Controller producing a KOH eluent gradient of 1 mM to 8 mM. Cations (Na^+, K^+, Mg^{2+}, Ca^{2+}) were measured using a CS-12A column with 25 mM methane sulfonic acid eluent (S. Sneed, personal communication). In addition to samples, 10 de-ionized water blanks were analyzed using the same methods. Values for the blanks were <1% of the lowest sample values for all species except for K^+, for which three of the blanks had values ~13% of the lowest sample or ~2% of the mean sample value. Duplicates were run every 20th sample; sample variability was <5% for all duplicates for all species except for Ca^{2+} (11%) and SO_4^{2-} (5.3%). Ion chromatography data represents the presence of major ions in dissolved form.

$^2H/^1H$ isotope ratios were determined using gas source mass spectrometry conducted on a Micromass Isoprime system configured for continuous flow, fitted with a EuroVector Pyr OH furnace and liquid autosampler running DataLynx software. Values are reported as a difference relative to the standard mean ocean water (SMOW) standard according to the formula

$$\delta D_{SMOW}\ (‰) = 1000 * \left(\frac{\left(^2H/_1H\right)_{SAMPLE} - \left(^2H/_1H\right)_{SMOW}}{\left(^2H/_1H\right)_{SMOW}} \right)$$

The long-term precision and duplicate variability using laboratory and international standards was 0.5‰ for δD_{SMOW}. Maximum duplicate variability (in only one duplicate pair) was < 2‰.

Trace metal concentrations were determined for samples from the Clark, Commonwealth and Blue glaciers using a ThermoFinnigan ELEMENT2™ inductively-coupled plasma mass spectrometer (ICP-MS) for Ba, Cd, Co, Cr, Cs, Cu, Mn, Pb, Sr, Ti, U, V, Zn and the rare earth elements (REE). A Perkin-Elmer Optima 3000

XL axial inductively coupled plasma optical emission spectroscope with a CETAC ultrasonic nebuliser (ICP-OES-USN) was used to determine values of Al, Ca, Fe and S. For samples from the Victoria Upper Glacier, concentrations of elements in both of the above lists were determined using ICP-MS. Preparation of samples for both instruments involved melting the original sample, agitating it to suspend sediment, and then immediately transferring an aliquot by pre-cleaned pipette from the original sample bottle to polypropylene analysis vials. For the ICP-MS, the aliquot was 3.5 mL, and for the ICP-OES, the aliquot was 10 mL. Analysis vials were then acidified to 1% HNO_3 using Fisher Optima® grade nitric acid to avoid material plating to the vial walls. Based on runs of several metals using both methods (Figure 1.5), values and trends are comparable between ICP-MS and ICP-OES; limited variability among the data likely relates to different amounts of particles being captured in separate runs (see chapter 2 for details). The overall good agreement demonstrates that data from these two instruments can be compared directly. Blank samples were again prepared using de-ionized water. For Al, Cu, Fe, Mn, Pb, S, Sr, Ti, and the rare earth elements (REE), blank values were <10% of average sample values at all sites. In all statistical analyses presented below, elements that do not meet this standard are not used. Data generated using the ICP-MS represents concentrations including both dissolved (ionic) and particulate modes for analyzed elements.

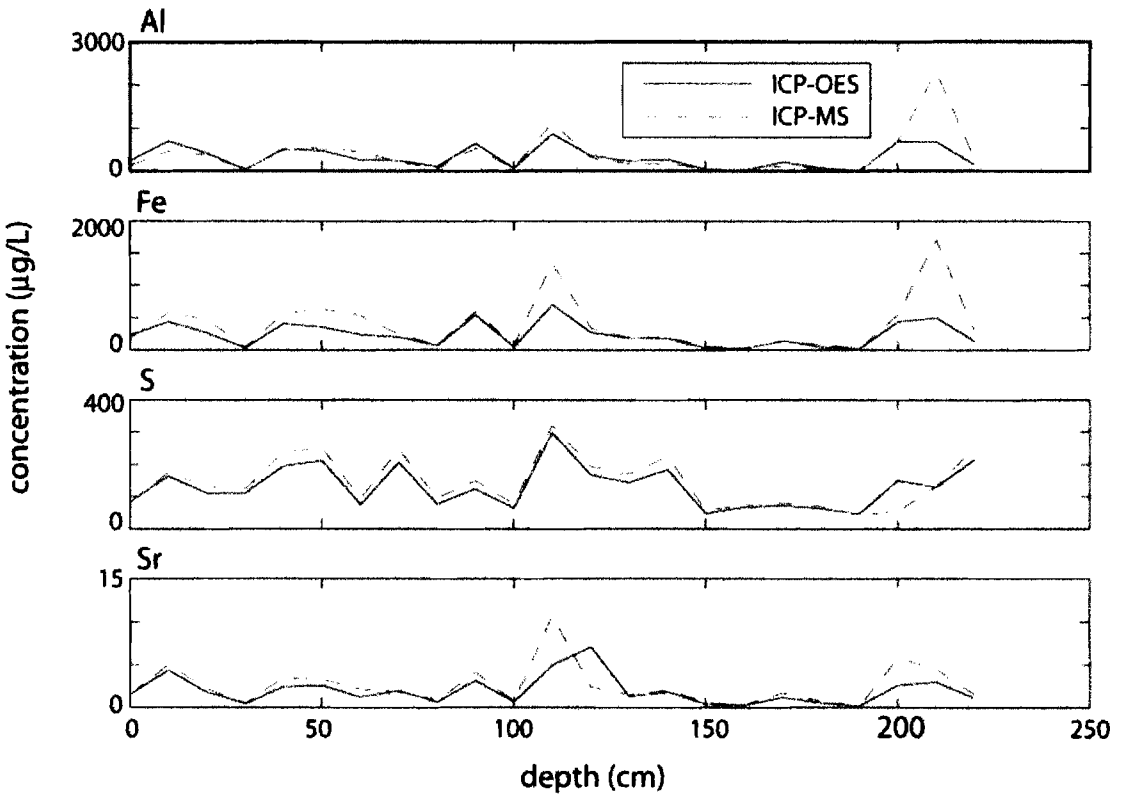

Figure 1.5. Comparison of Al, Fe, S and Sr measurements using the same samples analyzed with ICP-MS and ICP-OES. Samples come from the Clark Glacier. Similar behavior was seen in samples from the Commonwealth Glacier analyzed using both techniques.

Results

Chronologies/Accumulation rates

Prior investigations in Antarctica have depended on a variety of techniques for dating chemical profiles, including chrono-stratigraphic radioactive layers from atomic bomb testing [*Crozaz et al.*, 1966; *Boutron*, 1982; *Mayewski et al.*, 1995; *Bertler et al.*, 2004], strain-thickness calculation [*Mayewski and Lyons*, 1982], visual stratigraphy [*Boutron and Lorius*, 1979], and seasonal variations in the concentration and relative proportions of Na^+, Cl^-, methane sulfonate, and the stable isotopes of oxygen and hydrogen [*Boutron*, 1982; *Welch et al.*, 1993; *Kreutz et al.*, 2000; *Steig et al.*, 2000; *Bertler et al.*, 2004; *Dixon et al.*, 2005; *Steig et al.*, 2005]. For the sites described in this study, limitations exist for several of these methods. Deuterium ratios (δ^2H), for example, are modified after deposition by a smoothing effect thought to be related to low accumulation rate and diffusion processes [*Johnsen*, 1977; *Mayewski et al.*, 1995]. Stratigraphy is not well defined at the Victoria Upper Glacier site below 25 cm, with ice becoming a homogeneous hard mass with large crystal size (diameter = ~4 mm). As at other Dry Valleys sites, no surface melting was visible above the firn containing these crystals [*Lyons et al.*, 2003], and the top 25 cm appeared consistent with unmodified surface snowfall. Instead of liquid water at the surface, however, these conditions may represent subsurface melting [*Liston et al.*, 1999], and they dictate caution in interpreting chemistry at this site. While MS^- has been used at some coastal sites in Antarctica as a seasonal marker [*Legrand and Mayewski*, 1997], this species has been associated with vertical migration between seasonal ice layers at other sites, making proposed chronologies more complex [*Mulvaney et al.*, 1992; *Legrand and Mayewski*, 1997;

Pasteur and Mulvaney, 1999; *Pasteur and Mulvaney*, 2000; *Curran et al.*, 2002; *Smith*, 2004]. Given that Dry Valleys Glaciers have low accumulation rates [*Welch et al.*, 1993; *Mayewski et al.*, 1995; *Bertler et al.*, 2004], even a slight migration of MS^- could have a significant effect.

Because of uncertainties with these other methods, variations in sodium concentration, which reflect seasonal signals at a variety of sites in Antarctica [*Welch et al.*, 1993; *Legrand and Mayewski*, 1997; *Kreutz and Mayewski*, 1999; *Kreutz et al.*, 2000; *Bertler et al.*, 2004], including the Dry Valleys [*Welch et al.*, 1993; *Bertler et al.*, 2004], provide the most consistent chemical depth series with which to develop chronologies for the sites discussed here (Figures 1.6, 1.7, 1.8, 1.9). Because of potential issues with subsurface melt and percolation at the Victoria Upper Glacier, the sodium-based chronology for this site is considered more tentative than at the other three locations. Ongoing analysis of samples for beta activity will provide additional information to refine pit dating.

Snow pit samples for this study were collected in Antarctic Spring (November), and eight of ten pits sampled in the 2003 and 2004 seasons yielded Na^+ values which decrease with depth in surface snow; these findings support Bertler et al.'s [2004*b*] conclusion that peaks in Na^+ represent summer precipitation in the MDV, in contrast to winter Na^+ peaks found at many other sites in Antarctica [*Legrand and Delmas*, 1984; *Wagenbach et al.*, 1998]. Based on layer counting between peaks after adjusting for the density profile at each site, mean annual net mass balance is 2.5, 3.4, 3.1 and 4.6 cm water equivalent (w.e.) for the Clark, Commonwealth, Blue and Victoria Upper glaciers,

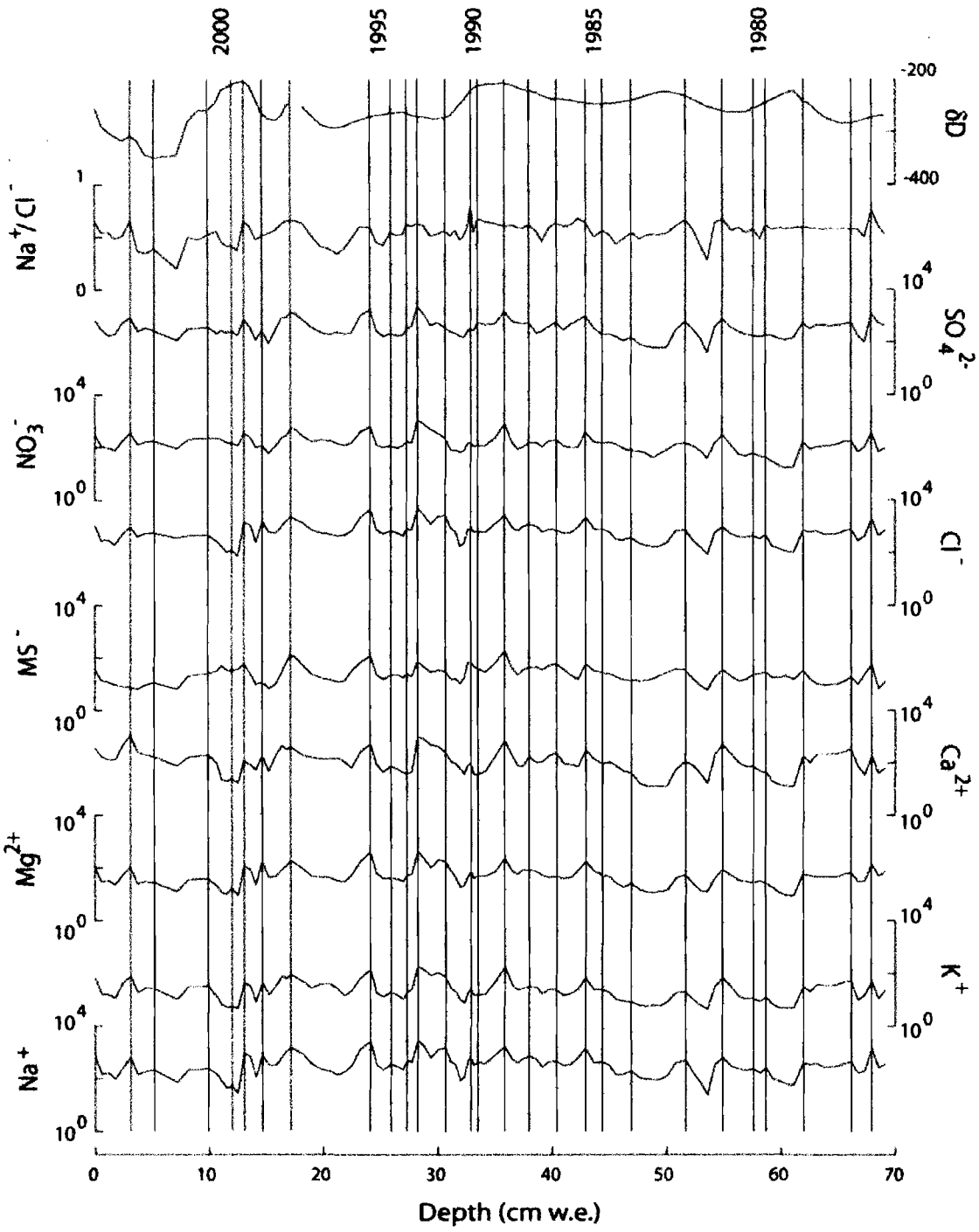

Figure 1.6. Major ions and isotope ratios for the Clark Glacier plotted with dates corresponding to summer (December, January, February [DJF]) peaks in sodium concentrations. Peaks are defined as snow or firn layers with concentrations >10% higher than the layers above or below. Ion concentrations are reported as the absolute concentration in ppb (scaled logarithmically), and isotope ratio δD (= Deuterium/Hydrogen) is reported as ‰VSMOW. Dating, supported by agreement with physical mass balance measurements, is estimated to be accurate to ±1yr.

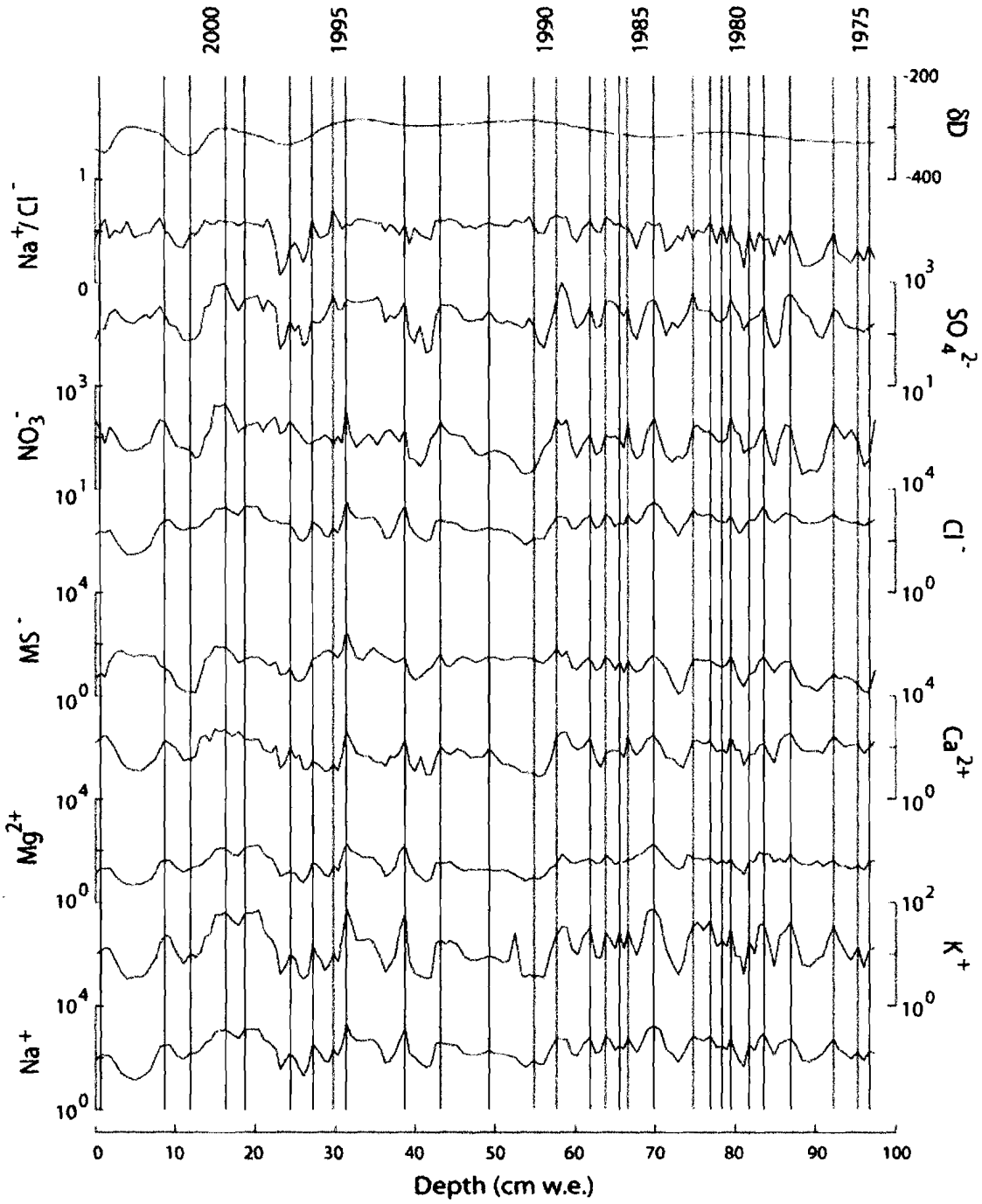

Figure 1.7. Major ions and isotope ratios for the Commonwealth Glacier plotted with dates corresponding to summer (DJF) peaks in sodium concentrations.

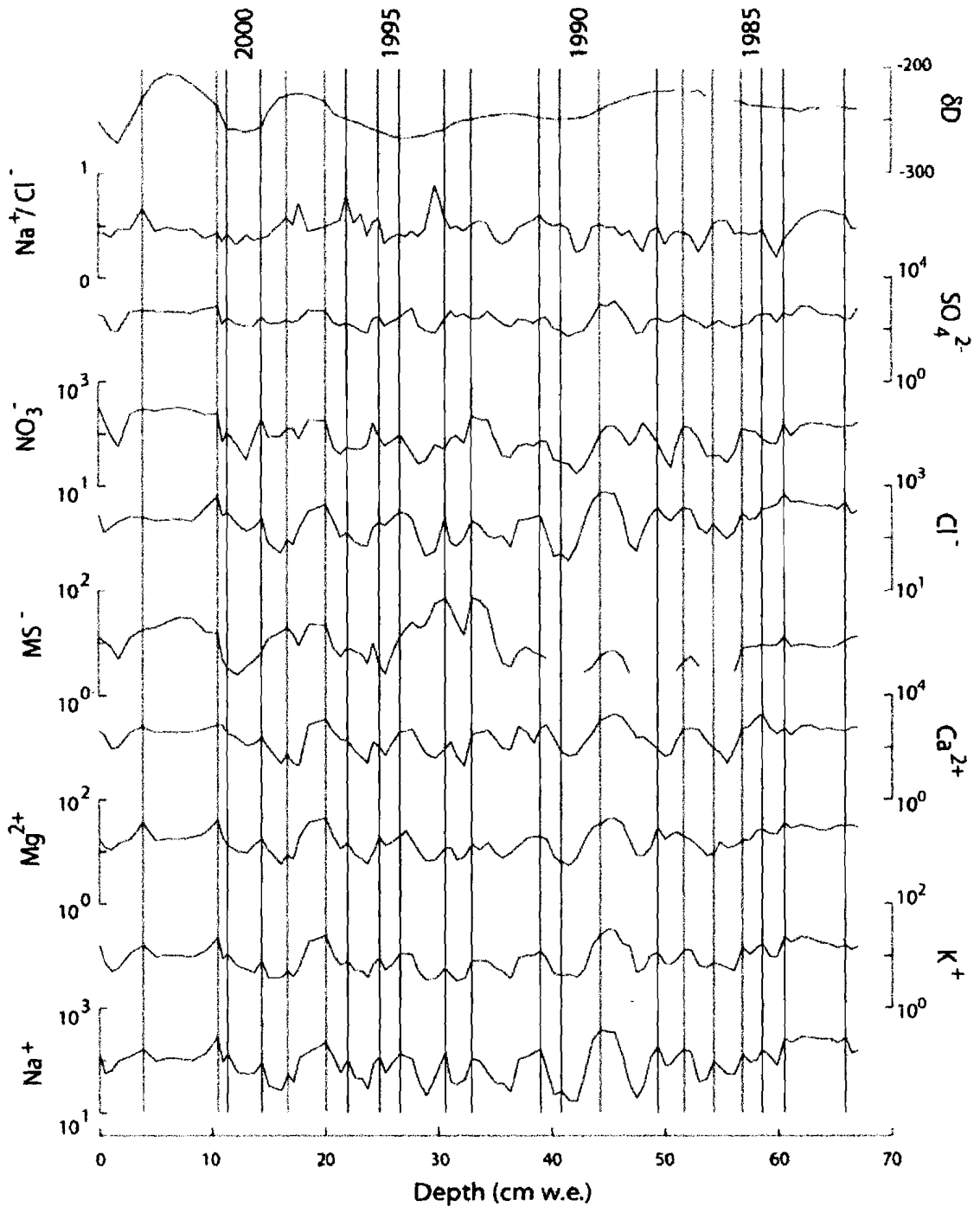

Figure 1.8. Major ions and isotope ratios for the Blue Glacier plotted with dates corresponding to summer (DJF) peaks in sodium concentrations.

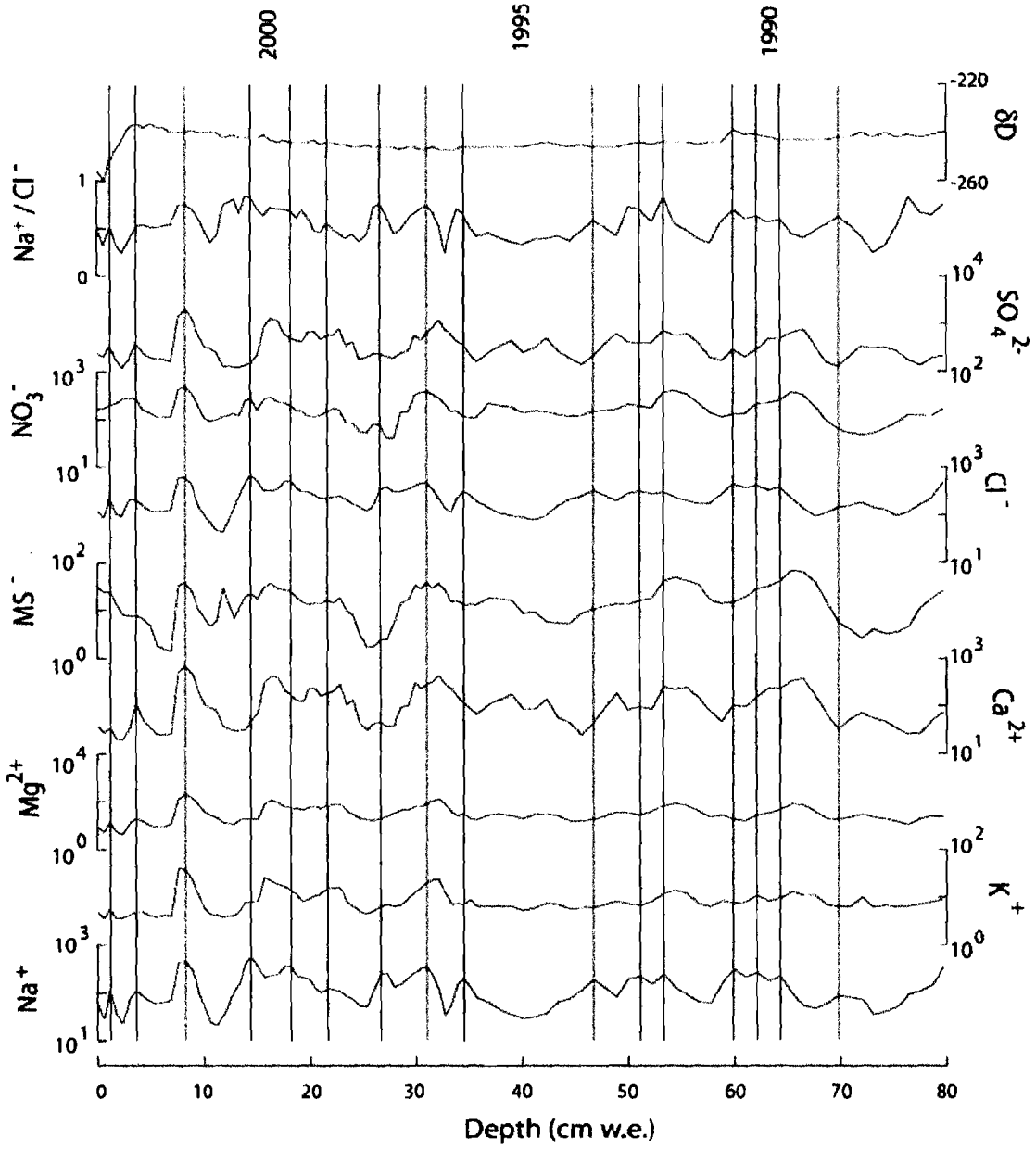

Figure 1.9. Major ions and isotope ratios for the Victoria Upper Glacier plotted with dates corresponding to summer (DJF) peaks in sodium concentrations.

respectively. The range of accumulations found within the depth series for each snowpit was 1 to 7 cm w.e. at the Clark, Commonwealth and Blue glaciers and from 1 to 12 cm w.e. at the Victoria Upper Glacier.

Networks of mass balance poles installed near the four snow pits provide a complementary geophysical data set with which to check accumulation rate histories derived from chemical measurements. At all four sites, I examine data collected from poles installed in 2003 or 2004 and removed in 2005. Data from poles within 800 meters of the pit site (i.e., within the dimensions of the pole grid) are used for comparison at the Clark, Commonwealth and Victoria Upper Glaciers, where the proximity of pole networks with pole spacing of 200 meters (100 meters at the Victoria Upper site) allowed high spatial resolution. For the Blue Glacier, a closely-spaced network was not installed because no coring activity was conducted at this location; data here includes poles from within 1000 meters of the pit site. Only pole data for the year 2004-2005 is included to examine a common time period where data exists for all sites.

The range of values for mass balance from pole networks agrees well with the range of mass balance values derived from Na^+ measurements over the time period covered in the snowpits at all sites except for the Victoria Upper Glacier (Figure 1.10). Because 2004-2005 pole data represent a time period after the snowpit was sampled, however, they cannot provide a direct comparison of mass balance during the time period covered by the pits. At the Commonwealth Glacier, on the other hand, the LTER mass balance network covers several years included in the chronology presented here [*Fountain*, 2005]. These values, when compared to the net mass accumulation figure for

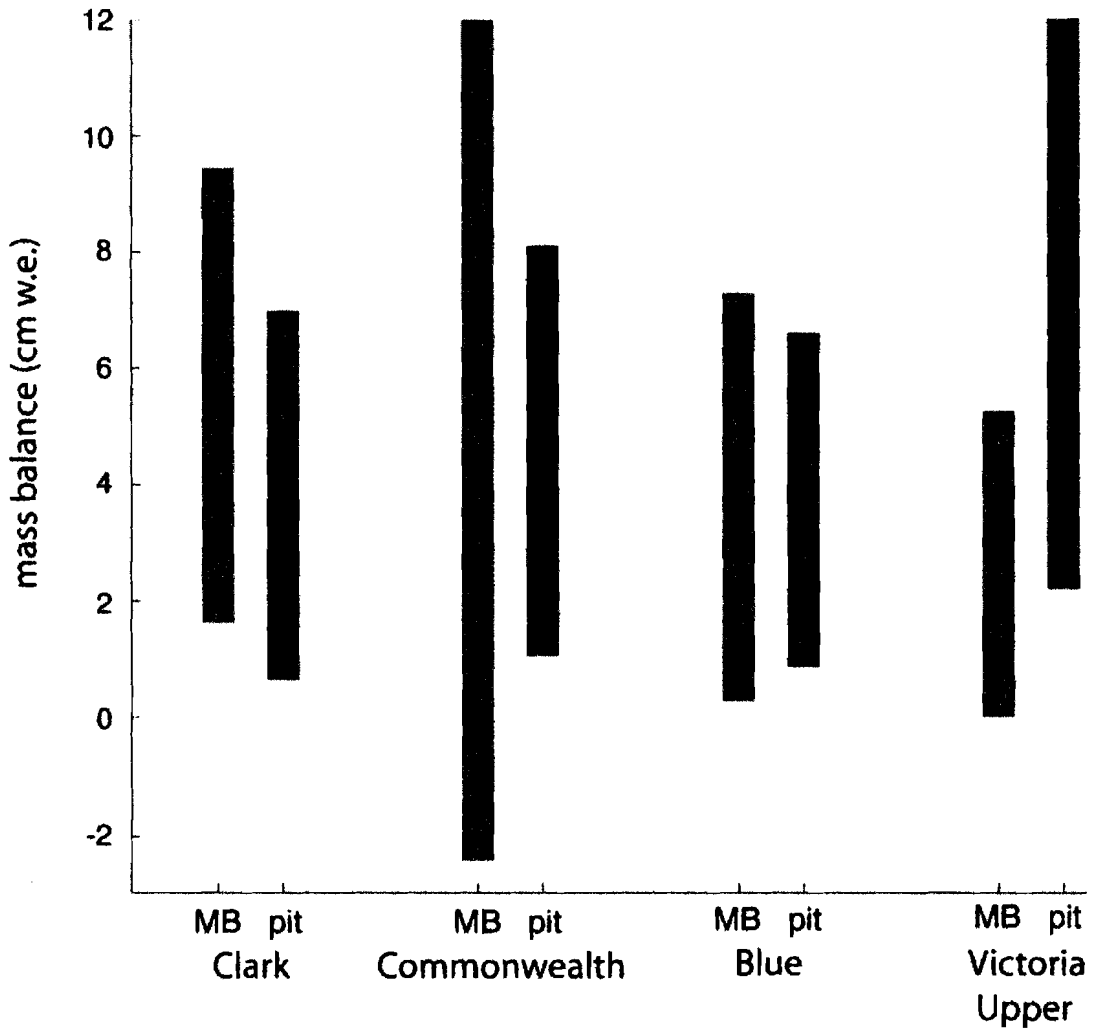

Figure 1.10. Measurements of mass balance by direct recording of mass balance poles ('MB') for 2004-2005 season (spatial range) compared to values determined according to mass differences between sodium peaks ('pit') (temporal range).

the corresponding years in the snow pit (Figure 1.11), provide additional confirmation that chemistry-based accumulation rates fall within the range of mass balances calculated from physical measurements.

Intra-site variability

Major ion concentrations measured in four pits separated by ~800 m at the Clark Glacier and from four similarly separated pits at the Commonwealth Glacier provide a measure of intra-site variability (Tables 1.1, 1.2). Mean values from snow and firn samples representing the time period 1996 - 2002 (depths from 10 cm to 96 cm, varying depending on the pit) were used for this comparison at the Clark site; mean values from samples representing 2000 - 2002 (depths from 4 cm to 58 cm) were used at the Commonwealth site. Concentrations within each of these sites vary across three orders of magnitude as they do at other Dry Valleys locations [*Lyons et al.*, 2003; *Bertler et al.*, 2004]; because lower concentrations are more prevalent than higher concentrations, this situation is best represented using a lognormal distribution (Figure 1.12). The geometric mean and standard deviation, designed to provide mean and variance values for lognormal distributions, are thus presented here instead of the arithmetic mean and standard deviation.

Both ion concentrations ($\mu g \cdot cm^{-3}$) and fluxes ($\mu g \cdot cm^{-2} \cdot yr^{-1}$) were considered in these comparisons. Because concentration differences can possibly be interpreted as either a change in the amount of a given species arriving at a site or as a change in the accumulation of ice surrounding the species creating a dilution effect, accounting for the accumulation rate is necessary to determine whether a dilution effect exists at a given

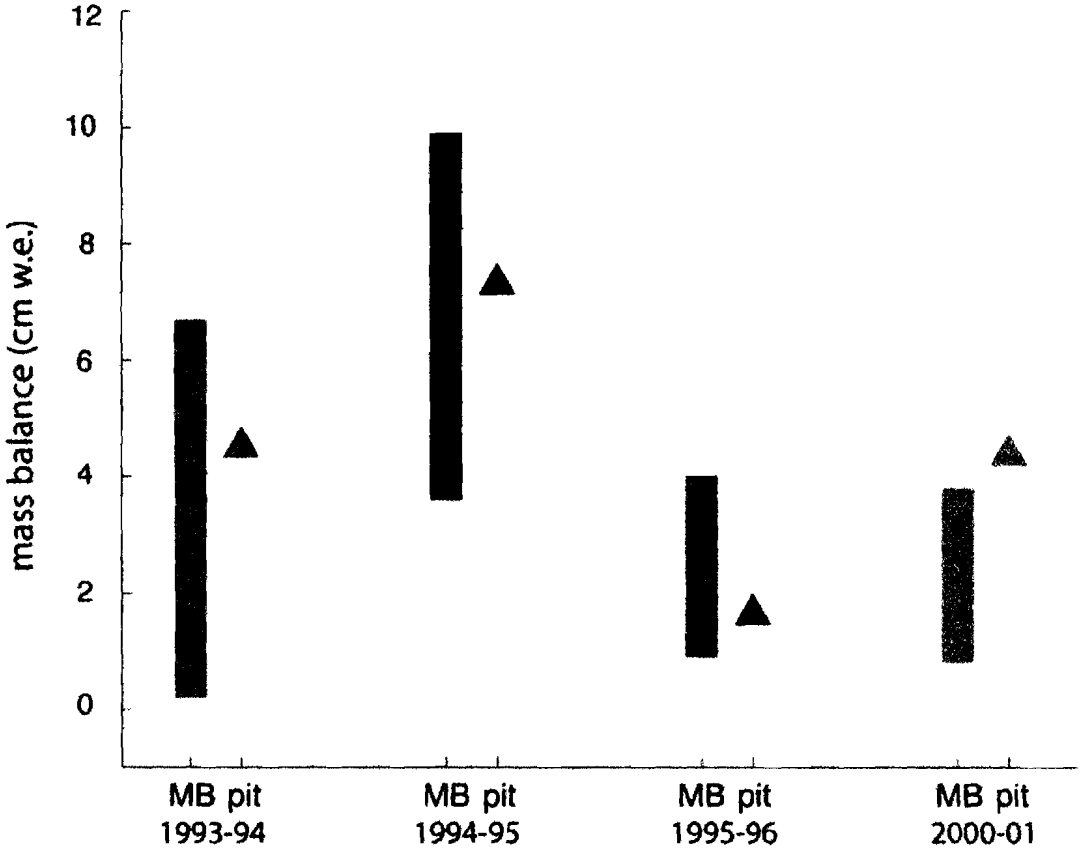

Figure 1.11. Mass balance ranges ('MB') compared to accumulation rates derived from pit chemistry ('pit' triangles) at the Commonwealth Glacier for each of the years shown. Mass balance data includes range of closest LTER stakes (n = 4) in place during each of these seasons [Fountain, 2005]. Pit data represents the corresponding accumulation derived according to figure 1.7.

Table 1.1. p values associated with two-tailed t-tests measuring variation in the means of major ionic species and ion ratios in snow representing 1996 - 2002 from four spatially separated pits (n = 31, 23, 24, and 28 samples) on the Clark Glacier. Differences between means indicated in red are significant at the 95% confidence level ($p < 0.05$) in a) Na^+:Cl^- ratio, b) Ca^{2+}:($Na^+ + K^+ + Mg^{2+}$) ratio, c) Na^+ concentration, d) MS^- concentration, e) K^+ concentration, f) Cl^- concentration, g) Mg^{2+} concentration, h) NO_3^- concentration, i) Ca^{2+} concentration, and j) SO_4^{2-} concentration. Geometric mean concentrations for each species in each pit are also indicated.

a)
$Na^+:Cl^-$

	pit 1	pit 2	pit 3	pit 4
pit 1 0.84 ± 0.14	1			
pit 2 0.85 ± 0.24	0.50	1		
pit 3 0.75 ± 0.20	<0.01	0.02	1	
pit 4 0.97 ± 0.11	<0.01	<0.01	<0.01	1
4 site mean: 0.85 ± 0.18				

b)
$Ca^{2+}:(Na^+ + K^+ + Mg^{2+})$

	pit 1	pit 2	pit 3	pit 4
pit 1 0.47 ± 0.32	1			
pit 2 0.45 ± 0.25	0.86	1		
pit 3 0.64 ± 0.49	0.11	0.11	1	
pit 4 0.32 ± 0.14	<0.01	<0.01	<0.01	1
4 site mean: 0.45 ± 0.33				

c)
Na^+

	pit 1	pit 2	pit 3	pit 4
pit 1 271.7 ± 417.9	1			
pit 2 246.0 ± 433.6	0.96	1		
pit 3 274.3 ± 313.5	0.97	0.98	1	
pit 4 506.1 ± 635.3	<0.01	0.03	<0.01	1
4 site mean: 327.3 ± 575.2				

d)
MS^-

	pit 1	pit 2	pit 3	pit 4
pit 1 31.47 ± 28.8	1			
pit 2 32.0 ± 21.4	0.37	1		
pit 3 18.0 ± 16.5	0.05	0.03	1	
pit 4 50.3 ± 43.5	0.04	0.07	<0.01	1
4 site mean: 35.1 ± 33.47				

e)
K^+

	pit 1	pit 2	pit 3	pit 4
pit 1 25.2 ± 33.2	1			
pit 2 20.5 ± 43.0	0.81	1		
pit 3 19.0 ± 16.8	0.21	0.47	1	
pit 4 26.1 ± 31.7	0.99	0.79	0.19	1
4 site mean: 23.1 ± 31.4				

f)
Cl^-

	pit 1	pit 2	pit 3	pit 4
pit 1 568.3 ± 785.8	1			
pit 2 470.7 ± 908.9	0.68	1		
pit 3 611.5 ± 486.7	0.71	0.47	1	
pit 4 812.4 ± 910.9	0.16	0.02	0.18	1
4 site mean: 617.5 ± 808.7				

g)
Mg^{2+}

	pit 1	pit 2	pit 3	pit 4
pit 1 45.8 ± 64.4	1			
pit 2 33.7 ± 86.3	0.46	1		
pit 3 46.6 ± 39.2	0.83	0.37	1	
pit 4 64.5 ± 70.7	0.11	0.01	0.15	1
4 site mean: 48.2 ± 69.2				

h)
NO_3^-

	pit 1	pit 2	pit 3	pit 4
pit 1 186.9 ± 120.3	1			
pit 2 160.3 ± 149.3	0.80	1		
pit 3 151.1 ± 96.1	0.04	0.17	1	
pit 4 156.5 ± 147.5	0.08	0.34	0.69	1
4 site mean: 160.7 ± 122.8				

i)
Ca^{2+}

	pit 1	pit 2	pit 3	pit 4
pit 1 130.7 ± 208.8	1			
pit 2 118.7 ± 278.4	0.95	1		
pit 3 169.0 ± 179.4	0.28	0.44	1	
pit 4 171.9 ± 295.5	0.26	0.39	0.93	1
4 site mean: 148.3 ± 253.4				

j)
SO_4^{2-}

	pit 1	pit 2	pit 3	pit 4
pit 1 333.7 ± 338.1	1			
pit 2 321.0 ± 619.9	0.65	1		
pit 3 297.4 ± 246.5	0.51	0.36	1	
pit 4 435.2 ± 480.4	0.13	0.36	0.02	1
4 site mean: 361.6 ± 415.5				

Table 1.2. p values associated with two-tailed t-tests measuring variation in the means of major ionic species and ion ratios in snow representing 2000 - 2002 from four spatially separated pits (n = 13, 11, 10, and 11 samples) on the Commonwealth Glacier. Differences between means indicated in red are significant at the 95% confidence level ($p < 0.05$) in a) Na^+:Cl^- ratio, b) Ca^{2+}:($Na^+ + K^+ + Mg^{2+}$) ratio, c) Na^+ concentration, d) MS^- concentration, e) K^+ concentration, f) Cl^- concentration, g) Mg^{2+} concentration, h) NO_3^- concentration, i) Ca^{2+} concentration, and j) SO_4^{2-} concentration.

a)
$Na^+:Cl^-$

	pit 1	pit 2	pit 3	pit 4
pit 1 0.80 ± 0.09	1			
pit 2 0.66 ± 0.21	0.04	1		
pit 3 0.57 ± 0.14	<0.01	0.23	1	
pit 4 0.62 ± 0.25	0.03	0.72	0.51	1
4 site mean: 0.67 ± 0.20				

b)
$Ca^{2+}:(Na^+ + K^+ + Mg^{2+})$

	pit 1	pit 2	pit 3	pit 4
pit 1 0.57 ± 0.38	1			
pit 2 0.29 ± 0.10	0.03	1		
pit 3 0.22 ± 0.12	<0.01	0.18	1	
pit 4 1.09 ± 0.55	0.01	<0.01	<0.01	1
4 site mean: 0.53 ± 0.47				

c)
Na^+

	pit 1	pit 2	pit 3	pit 4
pit 1 160.24 ± 490.8	1			
pit 2 172.5 ± 243.0	0.88	1		
pit 3 103.6 ± 247.3	0.43	0.27	1	
pit 4 120.2 ± 94.6	0.55	0.29	0.73	1
4 site mean: 137.6 ± 266.8				

d)
MS^-

	pit 1	pit 2	pit 3	pit 4
pit 1 29.6 ± 23.5	1			
pit 2 18.7 ± 10.7	0.69	1		
pit 3 26.4 ± 16.7	0.74	0.31	1	
pit 4 10.5 ± 8.2	0.07	0.04	<.01	1
4 site mean: 21.9 ± 17.6				

e)
K^+

	pit 1	pit 2	pit 3	pit 4
pit 1 13.7 ± 22.1	1			
pit 2 9.4 ± 5.5	0.24	1		
pit 3 8.6 ± 9.7	0.20	0.77	1	
pit 4 11.7 ± 6.1	0.63	0.26	0.27	1
4 site mean: 11.1 ± 10.8				

f)
Cl^-

	pit 1	pit 2	pit 3	pit 4
pit 1 311.1 ± 380.2	1			
pit 2 433.4 ± 426.2	0.46	1		
pit 3 290.8 ± 588.9	0.90	0.32	1	
pit 4 322.6 ± 130.3	0.93	0.23	0.78	1
4 site mean: 334.2 ± 540.7				

g)
Mg^{2+}

	pit 1	pit 2	pit 3	pit 4
pit 1 25.1 ± 46.6	1			
pit 2 27.1 ± 24.1	0.83	1		
pit 3 19.4 ± 27.8	0.53	0.32	1	
pit 4 23.5 ± 13.8	0.86	0.57	0.54	1
4 site mean: 23.7 ± 28.7				

h)
NO_3^-

	pit 1	pit 2	pit 3	pit 4
pit 1 114.4 ± 112.7	1			
pit 2 117.6 ± 77.6	0.91	1		
pit 3 98.4 ± 75.4	0.57	0.45	1	
pit 4 113.5 ± 38.8	0.97	0.85	0.49	1
4 site mean: 110.8 ± 77.8				

i)
Ca^{2+}

	pit 1	pit 2	pit 3	pit 4
pit 1 98.4 ± 232.0	1			
pit 2 57.5 ± 83.1	0.24	1		
pit 3 26.6 ± 69.2	0.02	0.12	1	
pit 4 157.1 ± 181.7	0.30	0.01	<0.01	1
4 site mean: 69.6 ± 167.3				

j)
SO_4^{2-}

	pit 1	pit 2	pit 3	pit 4
pit 1 244.8 ± 248.8	1			
pit 2 157.9 ± 182.0	0.16	1		
pit 3 186.4 ± 203.4	0.36	0.61	1	
pit 4 156.5 ± 180.0	0.16	0.98	0.60	1
4 site mean: 186.3 ± 204.0				

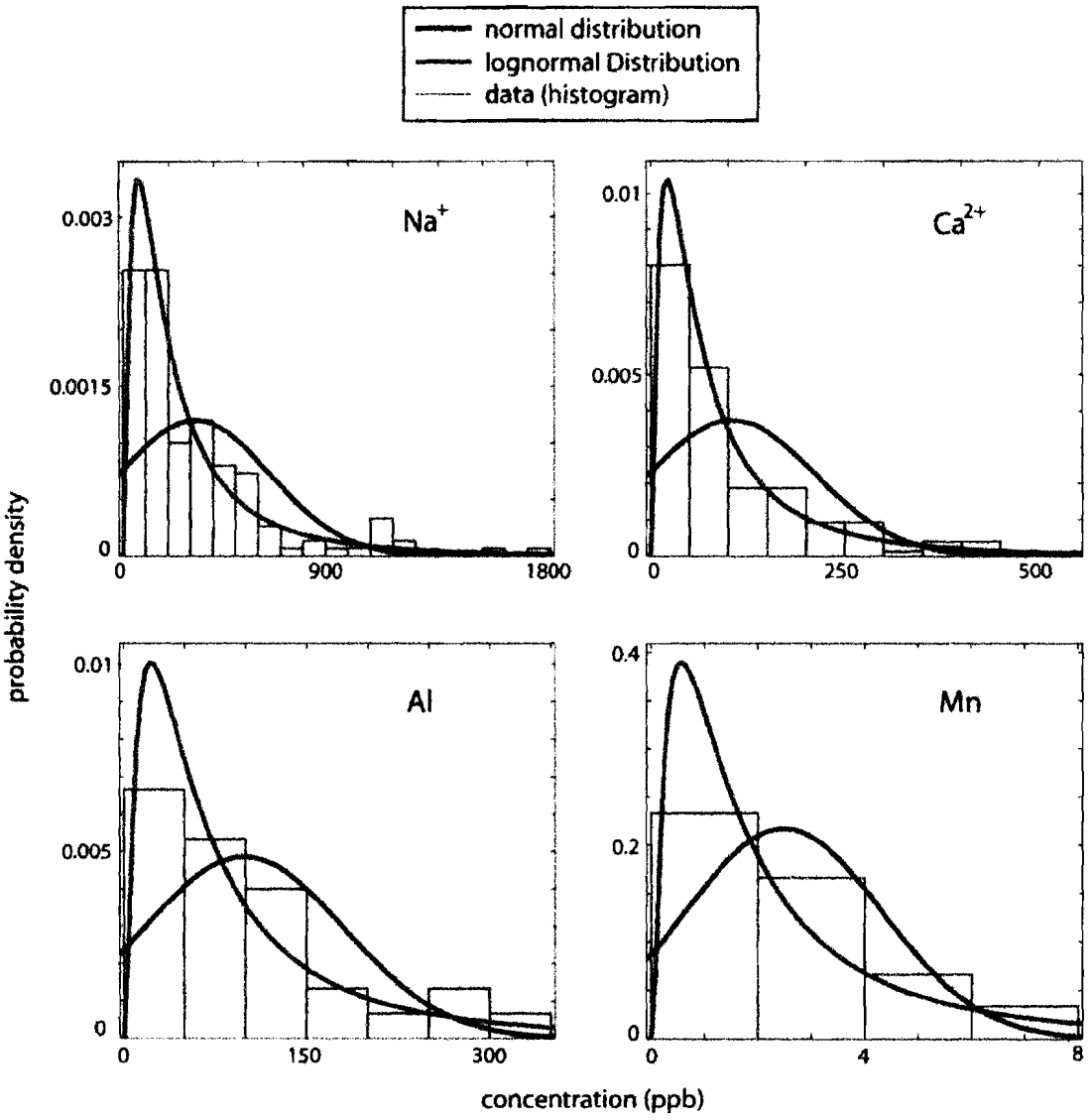

Figure 1.12. Major ion and trace metal concentrations at the Commonwealth Glacier compared to normal distributions and lognormal distributions based upon these data. Values from the Clark, Blue and Victoria Upper glaciers (not shown here) show similarly distributed values in most analytes.

location [*Mulvaney and Wolff*, 1994; *Yang et al.*, 1996; *Kreutz and Mayewski*, 1999]. This permits a more complete understanding of trends witnessed in the comparison of multiple sites. In the case of the snow pits at these locations, when flux and concentration are compared, the same statistically significant differences occur within and among the accumulation zones, arguing against a dilution effect. I will therefore use concentration values for the purposes of comparison. Mean Na:Cl and Ca:(Na + K + Mg) ratios for each site are also examined to provide information regarding the relative importance of sea-salt – with expected ratios of Na:Cl ~ 0.86 molar and Ca:(Na + K + Mg) ~ 0.06 molar – versus local soils and other atmospheric sources in determining snow and firn chemistry [*Mayewski et al.*, 1995; *Lyons et al.*, 2003].

On the Clark Glacier, concentrations of Na^+ and MS^- from pit 4 are significantly high relative to multiple pits, and MS^- concentrations at pit 3 are lower than those at the other three pits. There is also significant variation among the pits in the Na:Cl ratio and the Ca:(Na + K + Mg) ratios, with the Na:Cl ratio highest and the Ca:(Na + K + Mg) ratio lowest at pit 4. These trends cannot be explained either as a result of differences in distance from the coast, given that pit 4 is farthest from the coast, or by elevation, because the difference of < 6 m between pits 3 and 4 is smaller than the ~10 m difference between pits 2 and 3, with pit 2 at the highest elevation.

Instead, site-specific factors likely dictate these intra-site patterns. Causes may include varying exposures both to marine influence and to material inputs from the nearby valley floors. An example of potential marine effects is evident in an examination of austral summer wind data from the 2000 season. During a common time period from that summer for which wind direction measurements are available both from the Lake

Brownworth automatic weather station in Wright Valley (LB in figure I.1) and from a similar weather station on the ice divide of the Victoria Lower Glacier (VLG), a split in ground level wind direction was active, with winds at Lake Brownworth flowing predominantly from the east-northeast while winds at the Victoria Lower Glacier flowed predominantly from the east-southeast (Figure 1.13) [*Bertler et al.*, 2004*b*; *Fountain*, 2006]. This pattern would indicate that onshore winds flow around Mt. Allen, which lies between the Clark Glacier and the Ross Sea to the northeast. Because pit 4 was located in the least sheltered position relative to Mt. Allen and the closest to a direct pass to Victoria Valley (Figure 1.14), this pit would potentially have been exposed to a greater marine influence than the other locations sampled in the Clark accumulation zone.

A direct marine influence, however, does not explain the significantly high Na:Cl ratios at pit 4, well above what can be explained by pure sea-salt input. In addition, Ca:(Na + K + Mg) values for this and all other pits are an order of magnitude higher than marine values. These data require additional ion sources, and demonstrate that on an intra-site scale, relative exposure to the materials of the nearby Wright and Victoria Valleys also leads to differing major ion concentrations. The fact that the Ca:(Na + K + Mg) ratio is the lowest at pit 4, however, still supports the notion that the marine influence is strongest at this site, with relatively greater terrestrial inputs at pits 1, 2, and 3.

Data from the pit network at the Commonwealth Glacier also contain significant intra-site differences, with MS^- concentrations for pit 4 significantly lower than for pits 2 and 3, and concentrations of Ca^{2+} significantly higher at pit 4 than those at all other pits. Given that the Na:Cl and Ca:(Na + K + Mg) ratios are far from marine values, Ca^{2+}

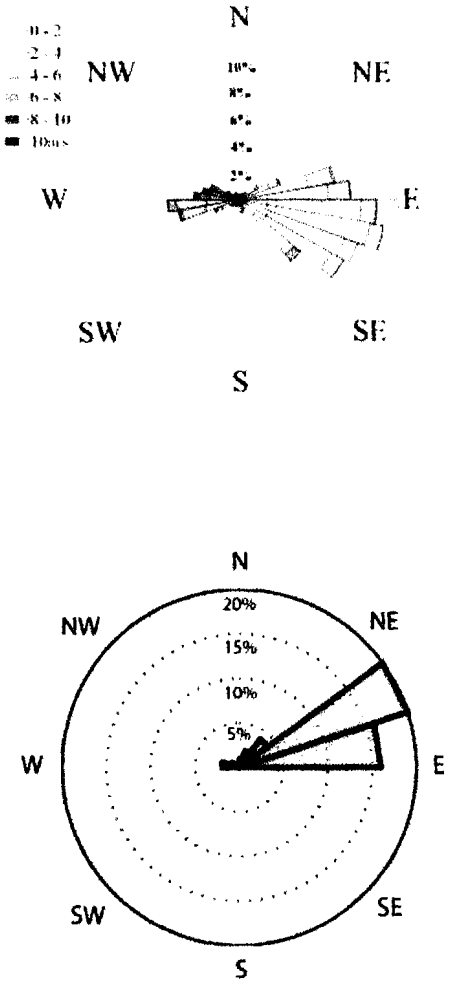

Figure 1.13. Wind direction data from a) the Victoria Lower Glacier (Bertler et al. [2004*b*]) and b) Lake Brownworth (Fountain [2006]). Both figures represent the percentage of wind originating in the direction shown by each bin. Bin size for Bertler et al. data is 10°; bin size for Lake Brownworth is 18°.

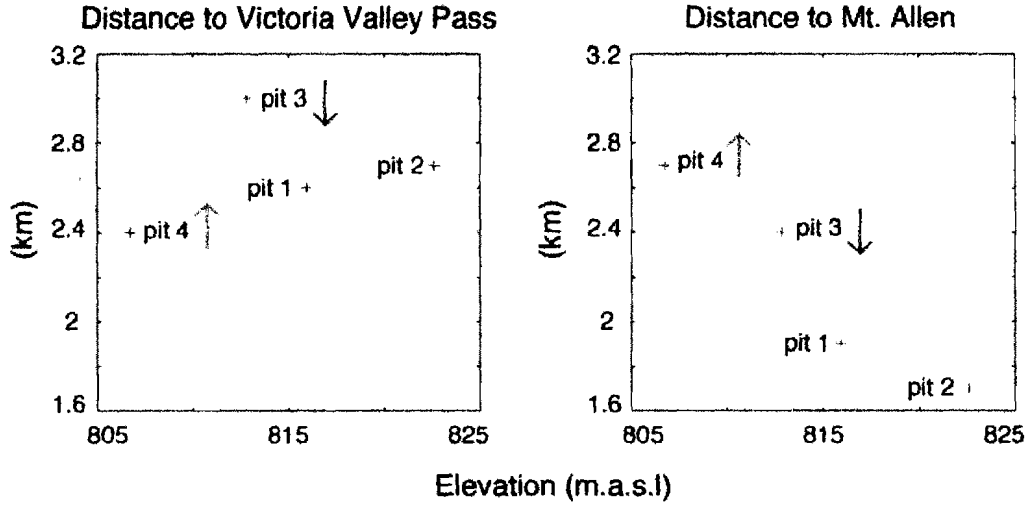

Figure 1.14. Pit elevations on the Clark Glacier relative to a) distance from the pass to Victoria Valley and b) distance from Mt. Allen to northeast. Arrows indicate pits with significantly high or low values.

variability at this site is likely associated with the proximity of pit 4 to the rock ridge on the north side of the glacier (<500 m distant) when compared with the locations of the other pits (>1 km distant). While it is interesting to note that MS^- values are again low in an area of the glacier that affords the possibility of shelter from marine-source winds, the fact that Na^+ values are not also significantly low at this site suggests that soil sources are dominant over the marine source for Na^+ at this location.

Regional Trends

Major Ions:

Sodium has been documented to provide a reliable proxy for sea-salt around Antarctica, with Cl^-, K^+, Mg^{2+}, Ca^{2+}, and SO_4^{2-} inputs being attributed in part to sea-salt and in part to terrestrial and atmospheric sources [*Legrand and Delmas*, 1988; *Mulvaney and Wolff*, 1994; *Legrand and Mayewski*, 1997; *Kreutz and Mayewski*, 1999; *Kreutz et al.*, 2000]. The adjacent exposed valleys and salt-rich soils of the MDV, however,

complicate this picture for the Clark, Commonwealth, Blue and Victoria Upper sites [*Mayewski and Lyons*, 1982; *Mayewski et al.*, 1995; *Lyons et al.*, 2003]. The seasonality of the Na^+ signal and the delineation by previous investigators of negative gradients in Na^+ concentration with distance from the coast along valley transects (also supported by the data here, discussed below) suggest that Na^+ variation in MDV ice reflects marine influence [*Lyons et al.*, 2003; *Bertler et al.*, 2004]. Along a north-south transect traced by the Clark, Commonwealth, and Blue Glacier sites, on the other hand, the lack of such gradients combined with evidence for substantial non-sea-salt inputs indicate that there are strong non-marine factors differentially affecting valley systems.

Several studies have demonstrated negative correlations between concentrations of marine species and distance from the coast and between these concentrations and increased elevation [*Legrand and Delmas*, 1984; *Legrand and Delmas*, 1985; *Mulvaney and Wolff*, 1994; *Kreutz and Mayewski*, 1999]. Mean ion concentrations from snow and firn representing the period 1989 - 2002 for the glaciers studied here provide confirmation that these same trends are evident within the Victoria Valley (Table 1.3) and among glaciers of the Asgaard Range (Table 1.4). In the Victoria Valley, results here for the Victoria Upper and the Clark Glaciers are in good agreement with those of Bertler et al. [2004*b*]; Na^+ and MS^-, in particular, fit well into the decreasing trend described in that work for the Wilson Piedmont (WPG), Victoria Lower (VLG) and Baldwin Valley Glaciers (BVG). Interestingly, data for K^+, Mg^{2+} and Sr at the Victoria Upper Glacier are higher than those at the BVG, as are Ca^{2+} values, indicating that K^+, Mg^{2+} and Sr may derive from a marine-terrestrial source similar to that associated with Ca^{2+} rather than

	WPG	VLG	CL	BVG	VU	PP	
Elev (m.a.s.l)	50	626	762	1150	1350	2400	
Distance to coast (km)	7.5	22.5	30	30	60	92.5	
Na^+	1698	889	350	166	118	45	marine + additional soil influence
MS^-	29	29	25	18	14	ND	marine
K^+	55	58	26	7	9	4	both
Mg^{2+}	198	126	55	17	35	6	both
Ca^{2+}	151	354	120	84	114	8	both
SO_4^{2-}	545	503	340	264	367	129	both
Sr	1.7	ND	1.9	0.5	0.8	0.03	both
Al	1.4	ND	233.6	2.8	115.2	1.2	terrestrial
Fe	1.0	ND	175	4.7	81	1.3	terrestrial

Table 1.3. Comparison of numerical mean concentrations (in μg/L) for ion and metal species from 5 sites in Victoria Valley and one site on the polar plateau. Data for Clark Glacier (CL) and Victoria Upper Glacier (VU) from this work. Data for Wilson Piedmont Glacier, Victoria Lower Glacier, Baldwin Valley Glacier and polar plateau (PP) from Bertler et al. [2004*b*]. Format is same as in Bertler's work, though some of the species designations regarding source have been altered based on results presented here.

	this work	Lyons	Welch
Na^+	166.8	489.7	37.2
K^+	11.4	46.9	2.7
Mg^{2+}	24.4	102.1	13.3
Ca^{2+}	51.8	284.7	19.2
Cl-	336.1	1040.2	149.4
SO_4^{2-}	219.2	202.6	29.1
NO_3^-	93.0	99.2	27.5
Na:Cl	0.79	0.73	0.5
xs-Ca	88.6	264.7	ND
MS	20.9	ND	7.9

Table 1.4. Mean values for major ions at the Commonwealth Glacier collected in this work, by Lyons [2003], and at the Newall Glacier by Welch [1993]. Lyons values are significantly higher than those here with the exceptions of SO_4^{2-} and NO_3^-. This relates to the collection season for their values, which was the austral summer, wheras this work includes data/samples spanning the entire year. The format of the chart is the same as that of Lyons et al. [2003]. xs-Ca (from Lyons) is equivalent to nss-Ca as defined here.

from a solely marine source. These data must be treated with caution, however, because of the possibility of melting and post-depositional effects at the Victoria Upper site.

A similar comparison can be made in the Asgaard Range using data collected from the Newall Glacier [*Welch*, 1993]. This comparison again confirms that given presumably similar soil influences (both sites reside on the ridge between the Taylor and Wright Valleys), opposing trends in elevation and species concentration dominate. The time period for the Newall record does not intersect with the time period covered here, but significantly lower values for all ions on the Newall Glacier relative to the Commonwealth likely represent a real trend, given the large difference in elevation and proximity to valley soil material between the two sites. The lower Na:Cl ratio also suggests more substantial sea-salt fractionation at the Newall Glacier than at the Commonwealth.

Comparison with major ion data from Lyons [2003] at the Commonwealth highlights high intra-annual and inter-annual variability in MDV chemistry. Disagreement between Lyons' data and the results here is likely because their study was conducted using surface samples, including in most cases ~5 cm of surface snow. As described above, surface snow in the MDV during austral summer has peaks in Na^+ and several other ionic species. This dictates that the Lyons means represent mean peak values, while the record presented here includes both lower "background" winter values and these peak values. When Lyons' values are compared to my peak values, the results generally agree within reasonable sampling / timing errors (Figure 1.15).

In contrast to these trends relating marine species, distance to the coast and elevation within each of the valleys, gradients follwing these variables are absent in a

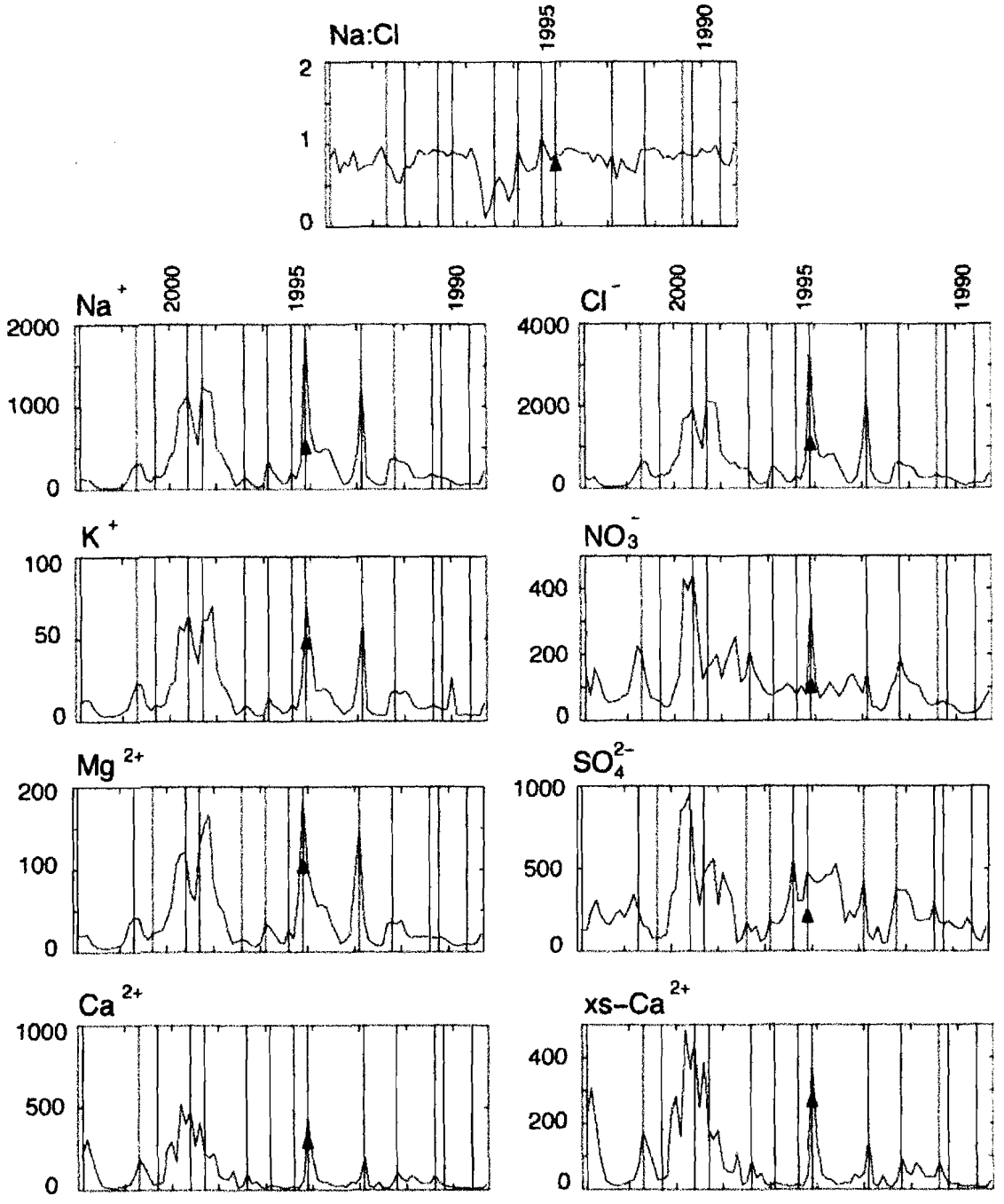

Figure 1.15. Mean major ion concentrations from Lyons et al. [2003] (red triangles) plotted within the annually dated ion records reported here. The Lyons data were collected in the three summer seasons surrounding 1994-1995. These seasons recorded some of the highest peaks in the record in most ions. Lyons data was translated from μmol/L to μg/L for comparison in all cases except Na:Cl, where the data presented here were translated into μmol/L to compare ratios.

comparison of sites comprising a coastal transect (Figure 1.16). The Commonwealth Glacier snowpit, for example, which is only 12.5 km from the coast and at an elevation above sea level of 680 m, has lower values for Na^+ than does the Clark Glacier pit, which is 30 km from the coast and 770 m in elevation. Though the Victoria Upper Glacier is outside of this coastal zone, the Blue Glacier, 25 km from the coast and at 990 m elevation, likewise yields lower values for Na^+, Cl^- and Mg^{2+} than does the Victoria Upper Glacier, 60 km from the coast and at 1350 m elevation.

Total chemical concentrations generally decrease from north to south within 30 km of the coast. The most northerly site, the Clark Glacier, has the highest values in seven of eight species and the most southerly site, the Blue Glacier, has the lowest values. Concentrations for the Commonwealth Glacier fall inside the range of values for the Blue Glacier and the Clark Glacier. Ca^{2+} provides the notable exception to this pattern, with the Blue Glacier having the highest mean concentrations, 50% higher than those found at the Clark Glacier and 400% higher than those of the Commonwealth.

The non-sea-salt (nss) fractions of Ca^{2+} and SO_4^{2-} have been used at sites in Antarctica and in the Dry Valleys to examine volcanic signatures and the influence of terrestrial dust on the ionic record [*Mayewski et al.*, 1995; *Lyons et al.*, 2003; *Dixon et al.*, 2004]. These concentrations are calculated here using the assumption that the conservative major ion – i.e., the ion which does not occur in excess of its ratio to other major ions as predicted by pure sea-salt input – represents the reference sea-salt indicator for each sample. Given the large amount of material in the Dry Valleys derived from local soils, volcanic signatures are not clear. While the Clark Glacier has an nss-SO_4^{2-} spike in 1992 that might arguably derive from the eruption of Pinatubo in 1991, for

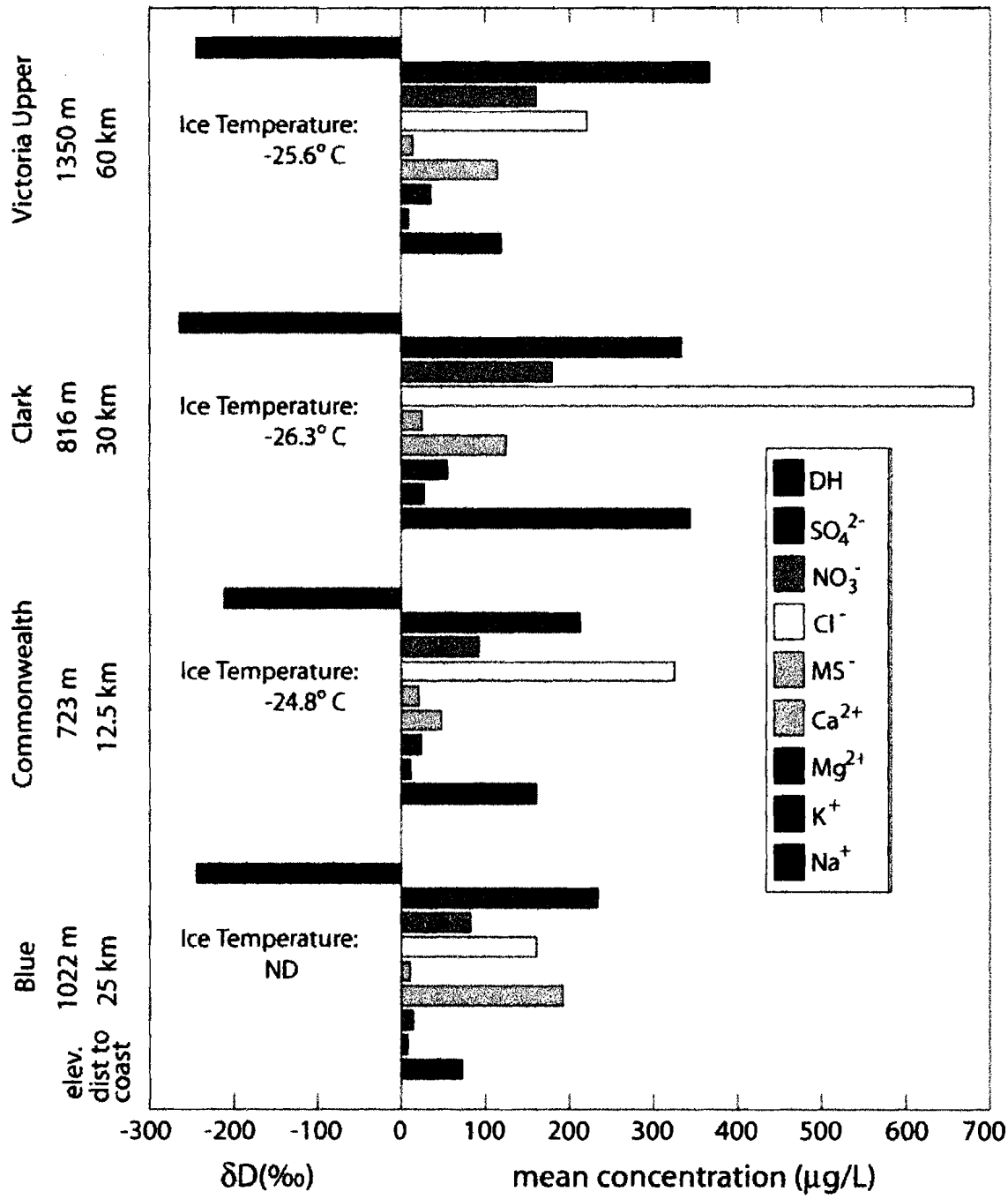

Figure 1.16. Comparison of mean major ion concentrations and $^{2}H/^{1}H$ (δD) isotope ratios from 1989 - 2002 for the Victoria Upper, Clark, Commonwealth and Blue Glaciers. Ice temperature is from 10 m depth, an approximation of mean annual temperature [Paterson, 1981].

example, a similar spike is not identifiable in either the Commonwealth or the Blue records (Figure 1.17). In addition, as the intra-site comparison makes clear, even Na^+ values (with a strong marine component) are strongly influenced by local soils, making a pure marine baseline – the assumed baseline in non-sea-salt analysis [*Legrand and Mayewski*, 1997] – unlikely. Although non-sea-salt analysis cannot therefore provide absolute percentages of the influence of marine versus soil influence at any given site, it will be used here instead to provide a comparison of the relative influence of these factors among site chemistries.

Differences between total and non-sea-salt concentrations at these sites are most pronounced at the Clark and Commonwealth, where Na^+ and Cl^- dominate the overall ion budget, but nss-SO_4^{2-} and nss-Ca^{2+} are the largest contributors for non-sea-salt species (Figure 1.18). Non-sea-salt Ca^{2+} and SO_4^{2-} in fact dominate both the total Ca^{2+} and SO_4^{2-} budgets (Table 1.5) and the total non-sea-salt ion budget at all four sites (though the mean nss-Cl^- concentration at the Commonwealth Glacier is not significantly different than that of nss-Ca^{2+}). Values for nss-Ca^{2+} and nss-SO_4^{2-} at the sites are also from 120% to >1000% higher than total (ss + nss) concentrations for these species on the nearby polar plateau [*Steig et al.*, 2000; *Bertler et al.*, 2004], indicating that MDV ice is reflecting local soil inputs rather than long-range transport. Although a positive relationship was found in this data between both total and nss-SO_4^{2-} concentrations and distance from the coast, the negative concentration gradient in this species within the Victoria and Taylor Valleys [*Lyons et al.*, 2003; *Bertler et al.*, 2004], suggests that this trend likely also relates to differing soil influences affecting glaciers in different valleys.

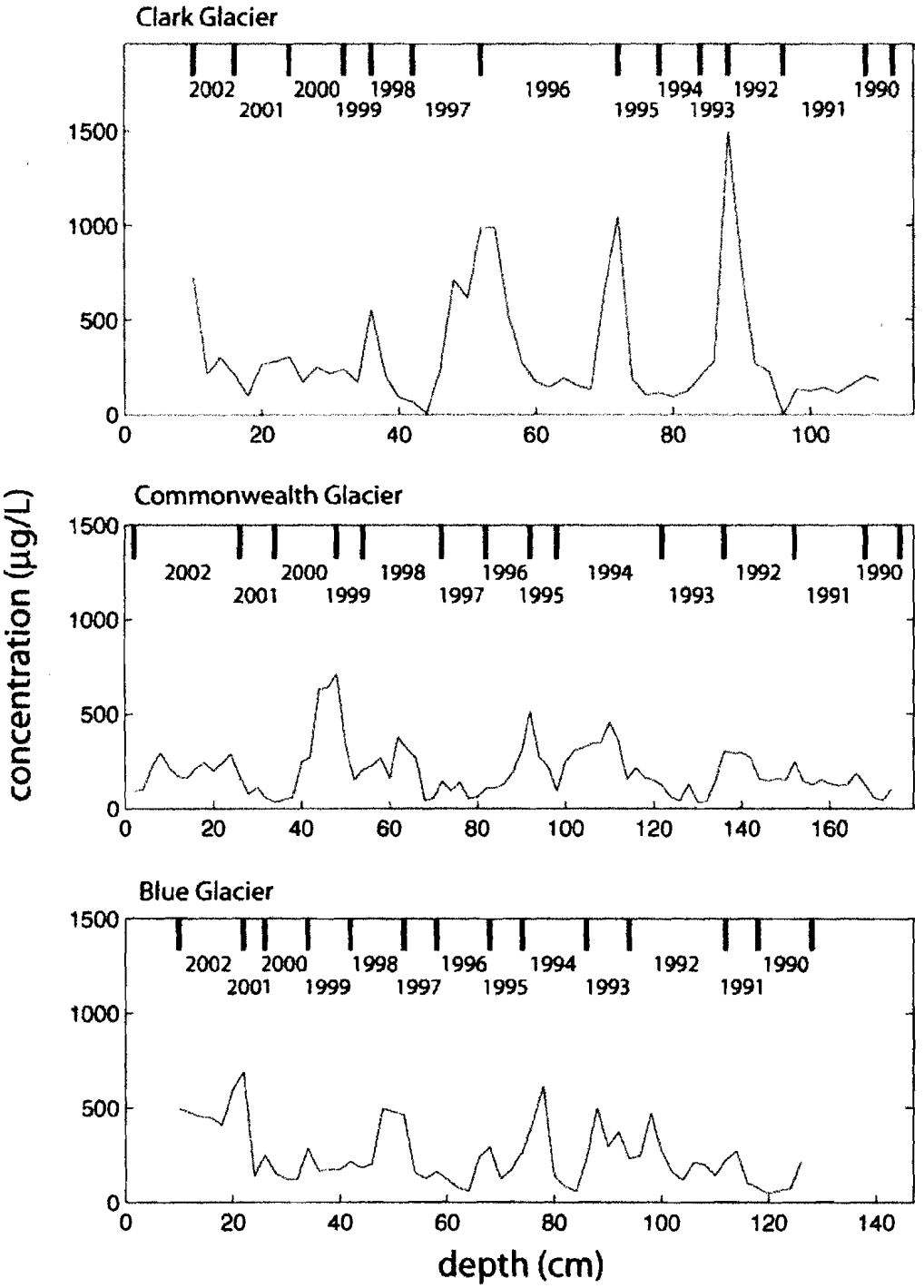

Figure 1.17. Non-sea-salt SO_4^{2-} concentrations at the Clark, Commonwealth, and Blue Glaciers from 1990 to 2002. As in the case of Na^+, peaks in SO_4^{2-} shown here are associated with austral summer (DJF) precipitation. While the unusually high peak in summer 1992-1993 at the Clark Glacier would be a long delay for the Pinatubo eruption (June, 1991), it might possibly be related. No such peaks exist in this time period at either the Commonwealth or the Blue Glacier sites.

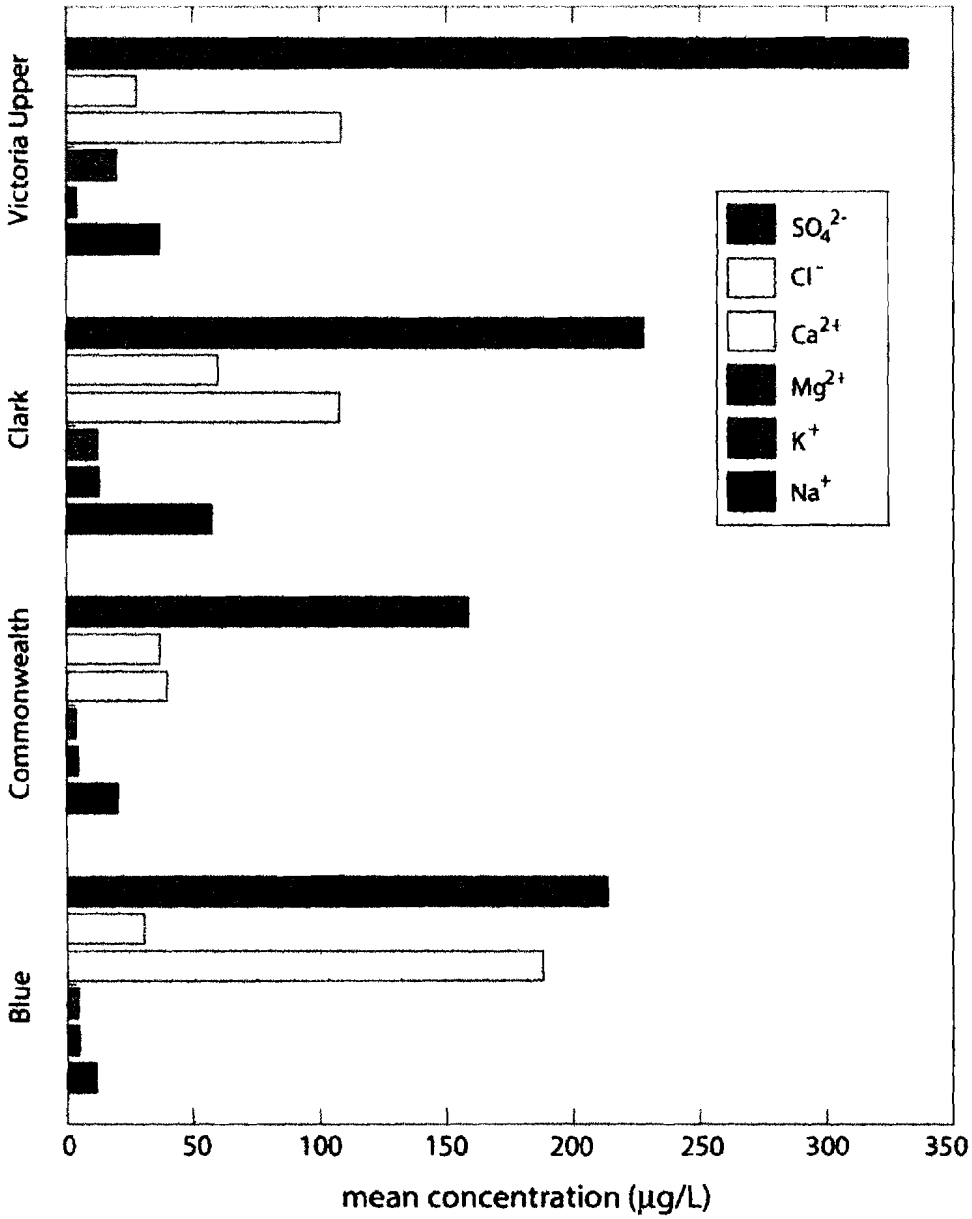

Figure 1.18. Non-sea-salt components of Na^+, K^+, Mg^{2+}, Ca^{2+}, Cl^- and SO_4^{2-} at Victoria Upper, Clark, Commonwealth and Blue glaciers.

	Blue	Commonwealth	Clark	Victoria Upper
Na^+	3.6	5.6	4.9	10.7
K^+	65.8	46.9	50.8	50.8
Mg^{2+}	19.9	19.9	25.4	54.9
Ca^{2+}	98.0	84.8	86.5	95.0
Cl^-	20.5	13.5	11.5	13.6
SO_4^{2-}	91.7	76.9	70.7	91.0

Table 1.5. Calculated percentage of non-sea-salt material at each site assuming that all marine aerosol species occur in the same ratios found in standard seawater.

Stable Isotopes and Ice Temperature:

Because isotope records are smoothed at these sites, lower frequency cycles in these records do not represent seasonal signals, making the mechanism for their variation unclear. In addition, as for the major ions, relationships between isotopic ratios, elevation, latitude and distance from the coast are not apparent. While the least negative mean isotopic signature occurs at the Commonwealth Glacier, which is closest to the coast and at the lowest elevation, the most negative isotopic signature comes from the Clark Glacier, which is neither at the highest elevation, nor at the farthest southern latitude, nor at the greatest distance from the coast. The Blue Glacier (the highest latitude site) and the Victoria Upper Glacier (the highest elevation site, also farthest from the coast) have similar intermediate values.

Stable isotopes reflect temperature, the amount of precipitation received, and isotopic conditions at the source of evaporation [*Dansgaard*, 1964; *Jouzel et al.*, 1982; *Grootes et al.*, 1989; *Jouzel et al.*, 1997]. To test the possibility of a stable isotope –temperature relationship at these sites, the spatial pattern in isotopic signatures was compared to the pattern of ten-meter-depth borehole temperatures measured in 2005 at

the Clark, Commonwealth, and Victoria Upper Glaciers as a proxy for mean annual temperature [*Paterson*, 1981]. The spatial pattern traced by these ice temperatures mirrors isotope patterns, with values of –25.6° C, -26.3° C and –24.8° C at the Victoria Upper, Clark, and Commonwealth sites, respectively. Although agreement between the pattern in ice temperatures and that of isotopic departures does not guarantee that deuterium values are providing a proxy for temperature at these locations, it leaves open this possibility. Additional high-resolution samples collected during the 2005 season directly underneath automatic weather stations operational from 2004 to 2005 on the Clark and Commonwealth Glaciers will allow more direct comparison of temperature-isotope relationships in future work.

Trace Metals:

Of the trace metals analyzed for these sites, 6 will be discussed here, chosen both for the highest quality data and for representation of a variety of metal species. Al and Fe, for example, represent the largest absolute contributions to the metal budget, Sr is abundant in both the terrestrial and the marine environment, and Mn is important in water chemistry in Dry Valleys lakes [*DeCarlo and Green*, 2002]. Cu and Nd here represent examples of trace constituents and the rare earth elements. All metals except Sr occur in MDV snow and ice in concentrations orders of magnitude higher than their presence in seawater (relative to the major ions) would support [*Weisel et al.*, 1984; *Abollino et al.*, 2001].

Samples from the Clark Glacier have either the highest or near-highest mean concentrations in all of these metals except Sr; samples from the Commonwealth Glacier have among the lowest metal concentrations (Figure 1.19). Concentrations of Fe at all

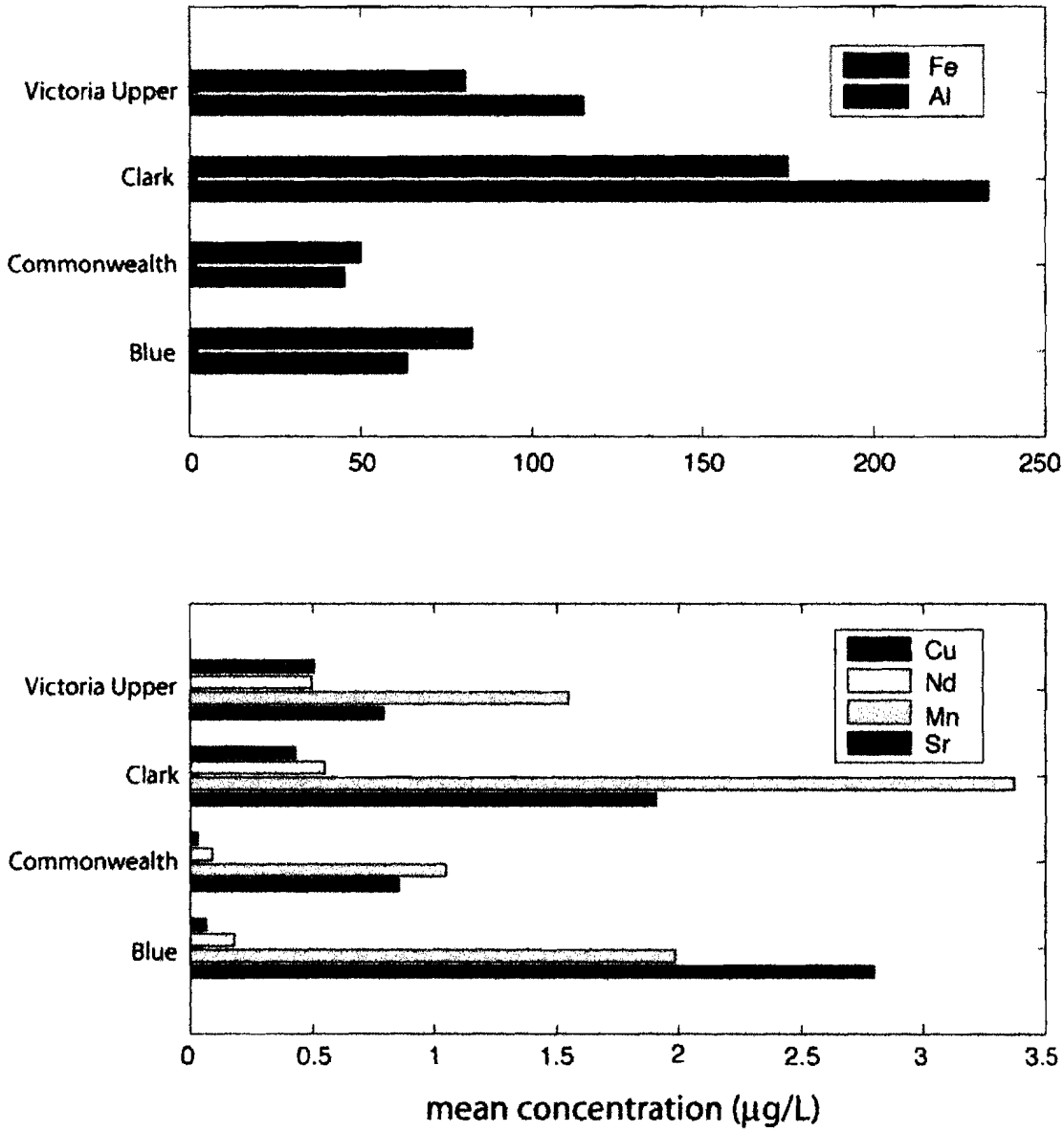

Figure 1.19. Mean concentrations of Al, Fe, Sr, Mn, Cu, and Nd at the Victoria Upper, Clark, Commonwealth and Blue glaciers.

sites are comparable to values found by Mayewski and Lyons [1982] (~20 to 270 μg/L) in a study of the Meserve Glacier. They are substantially higher, however, than concentrations reported by Bertler et al. [2004*b*] in a survey of four sites in the Victoria Valley. Because three of the sites in that study were either on the polar plateau or on glaciers in closer proximity to the coast, these concentrations may represent more direct coastal or plateau influences than do concentrations from the sites described here.

In order to examine chemical variation in the insoluble particulate fraction at these sites, enrichment factors relative to Al are defined as:

$$E_x = \frac{C_{x-sample} / C_{Al-sample}}{C_{x-upper\ crust} / C_{Al-upper\ crust}}$$

where C is the concentration of the metal in question (in μg/L), and listed in Table 1.6. These enrichment factors yield a complex picture, but among the four metals with the highest concentrations (Al, Fe, Sr, and Mn), ratios approach values for the upper crust [*Wedepohl*, 1995] to the north, with the Clark and Victoria Upper sites being closest to

	Clark	Commonwealth	Blue	Victoria Upper	Upper Crust
$C_{Fe}:C_{Al}$	0.76	1.11	1.33	0.66	0.40
$C_{Sr}:C_{Al}$	0.01	0.02	0.05	0.01	0.004
$C_{Mn}:C_{Al}$	0.01	0.02	0.03	0.01	0.01
$C_{Cu}:C_{Al}$	0.002	0.0004	0.0008	0.008	0.0001
$C_{Nd}:C_{Al}$	0.002	0.002	0.003	0.004	0.0003
E_{Fe}	1.9	2.775	3.325	1.65	
E_{Sr}	2.5	5.0	12.5	2.5	
E_{Mn}	1.0	2.0	3.0	1.0	
E_{Cu}	20.0	4.0	8.0	80.0	
E_{Nd}	6.7	6.7	10.0	13.3	

Table 1.6. Metal:Al ratios for the Clark, Commonwealth, Blue, and Victoria Upper Glaciers, and enrichment factors associated with these ratios. Upper crust values from Wedepohl [1995].

these values. These trends may represent either an increasing soil influence to the north, differing soil types at the four sites, or soil particulate fractionation during transport.

Temporal Variability

Examining the ion chronologies more closely, at the Clark, Commonwealth and Blue Glaciers, the Na^+ signal is well correlated with K^+, Mg^{2+}, and Cl^- for all samples in the record ($0.74 < r^2 < 0.98$, $p < 0.01$), indicating a similar seasonality for these ions as for Na^+; the Na/Cl ratio likewise shares concurrent peaks with Na^+ concentrations for most of the record. Ca^{2+}, NO_3^- and SO_4^{2-} concentrations, on the other hand, are less closely correlated with Na^+ ($0.36 < r^2 < 0.81$), likely showing a smaller marine influence for these species, and a correspondingly increased influence from the local dust sources in the MDV for Ca^{2+} and SO_4^{2-} (from stratospheric processes for NO_3^-) [*Mayewski et al.*, 1995; *Legrand and Mayewski*, 1997; *Bertler et al.*, 2004*b*]. Only at the Clark Glacier is Na^+ well-correlated with MS^- ($r^2 = 0.50$); at all other sites, Na^+ and MS^- are correlated with $0 < r^2 < 0.3$. Relatively low correlations between Na^+ and MS^- were also found by Bertler et al. [2004*b*] at the Victoria Lower Glacier, illustrating the possibility of post-depositional MS^- migration in MDV snow and firn.

At the Victoria Upper Glacier, other ions (with the exception of Cl^-) are not as strongly correlated to the Na^+ depth series ($0.11 < r^2 < .31$). Because the correlation with Cl^- remains high ($r^2 = 0.94$), and the Na:Cl ratio has a mean value of 0.86 and a median value of 0.84, identical to the seawater value (0.86) and similar to the other sites (Na:Cl between 0.70 and 0.84), variation in Na^+ concentrations likely represents marine seasonal variation. With the possibility of melting, however, lack of correlation among major ions

with both local soil and marine sources may reflect post-depositional effects at this location in addition to species input timing.

Al, Fe, Sr, and Mn (Figures 1.20, 1.21, 1.22, 1.23) are strongly inter-correlated ($0.59 < r^2 < 0.98$ for relationships among these four metals). Cu and Nd are less well correlated with each other and with all metals ($0.01 < r^2 < 0.92$). Possibly because trace metal samples were collected at 10 cm resolution, when these data are compared directly to the annual markers in the major ion datasets, metal peaks are offset. They are also not correlated with corresponding 10-cm averages in these annual markers.

Exploring these differences further, samples at the Clark Glacier analyzed for both ionic (dissolved) and total (dissolved plus particulate) calcium, magnesium and sodium (Figure 1.24) yield trends with similar patterns of variability ($0.62 < r < 0.84$), ruling out the possibility that phasing relationships between metals and ions are a result of the analytical process. In addition, for all three of these species values are similar on an absolute basis when concentrations are low. As concentrations increase, Ca and Mg values increase faster in the ICP-MS measurement than do Ca^{2+} and Mg^{2+} in the IC values. This indicates a large source of insoluble Ca^{2+} and Mg^{2+} present at the Clark Glacier, most likely related to local particulates.

To examine the relative input timing of major ions and metals together, separate empirical orthogonal function analyses are conducted for each of the sites examined in this study (Tables 1.7, 1.8, 1.9, 1.10). Empirical Orthogonal Function analysis (EOF) has been used in a variety of settings as a tool to examine datasets with large numbers of variables [*Peixoto and Oort*, 1992; *Meeker et al.*, 1995; *VonStorch and Zwiers*, 1999].

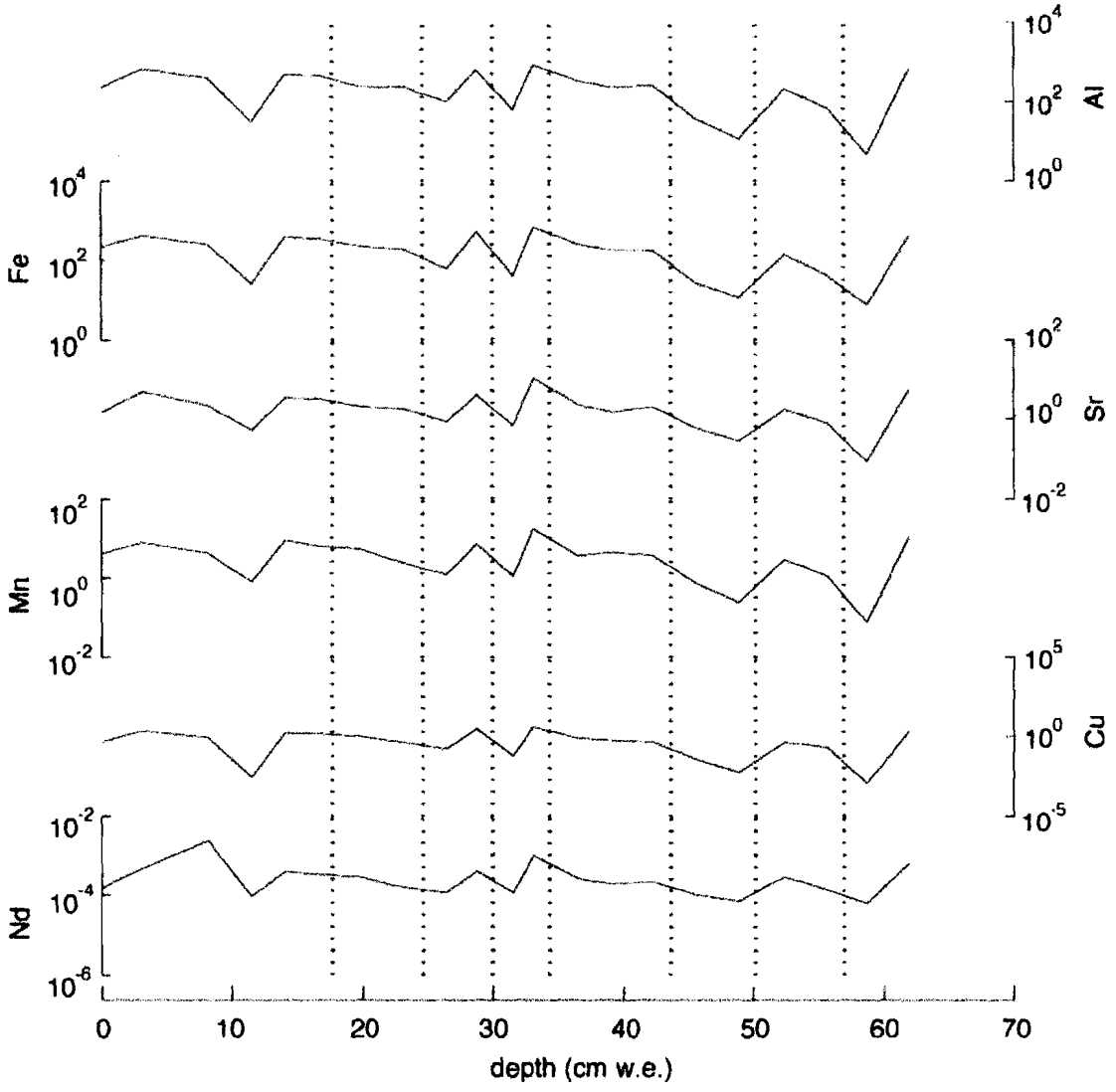

Figure 1.20. Variations in trace metal concentrations with depth at the Clark Glacier. All values are reported as the concentration in μg/L, scaled logarithmically. Dotted lines represent depths of peaks in 10-cm averaged concentrations of Na^+. Peaks in metals are not in phase with these peaks and also are not in phase with annual peaks in Na^+ (not shown here to maintain clarity).

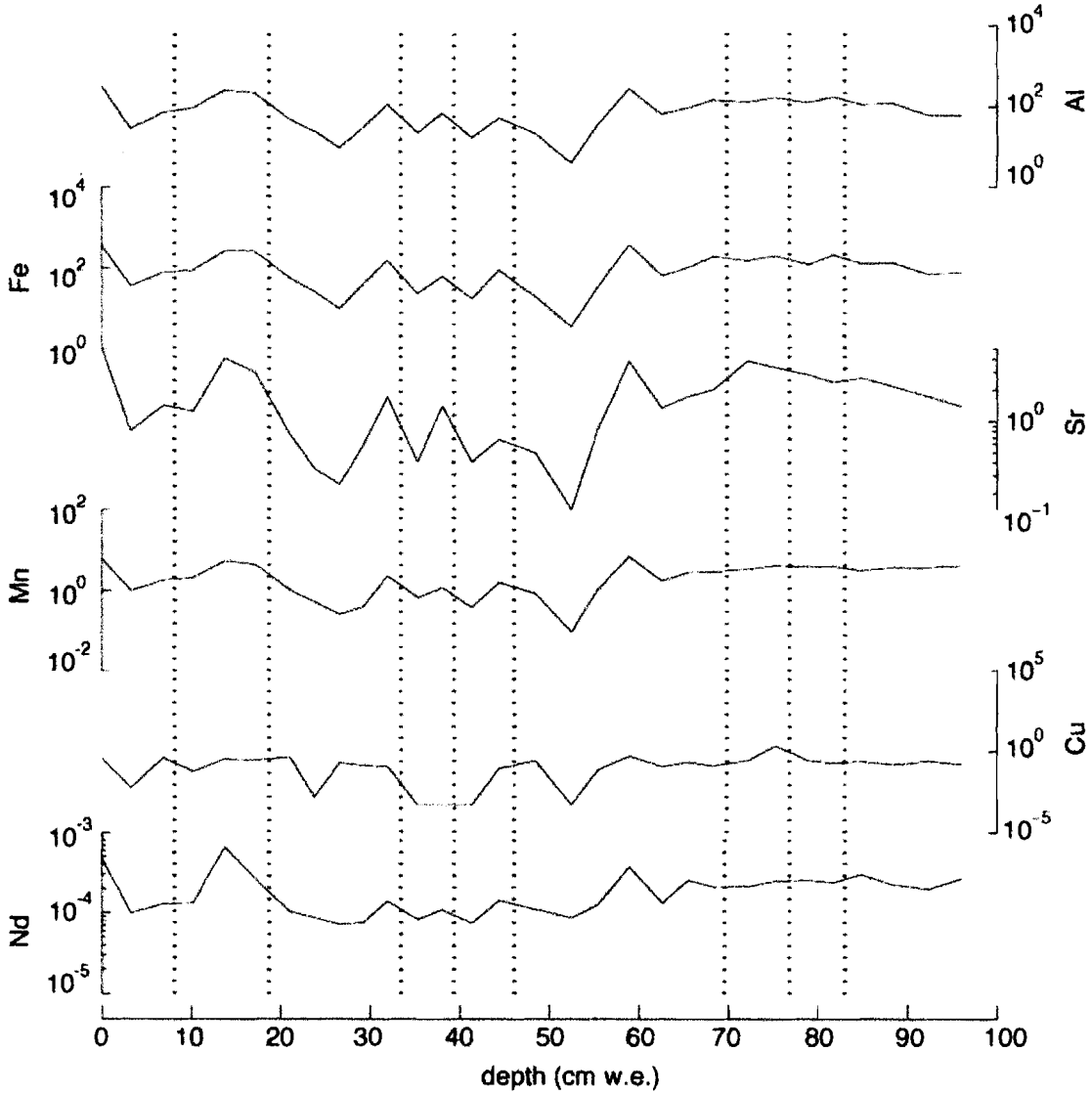

Figure 1.21. Variations in trace metal concentrations with depth at the Commonwealth Glacier.

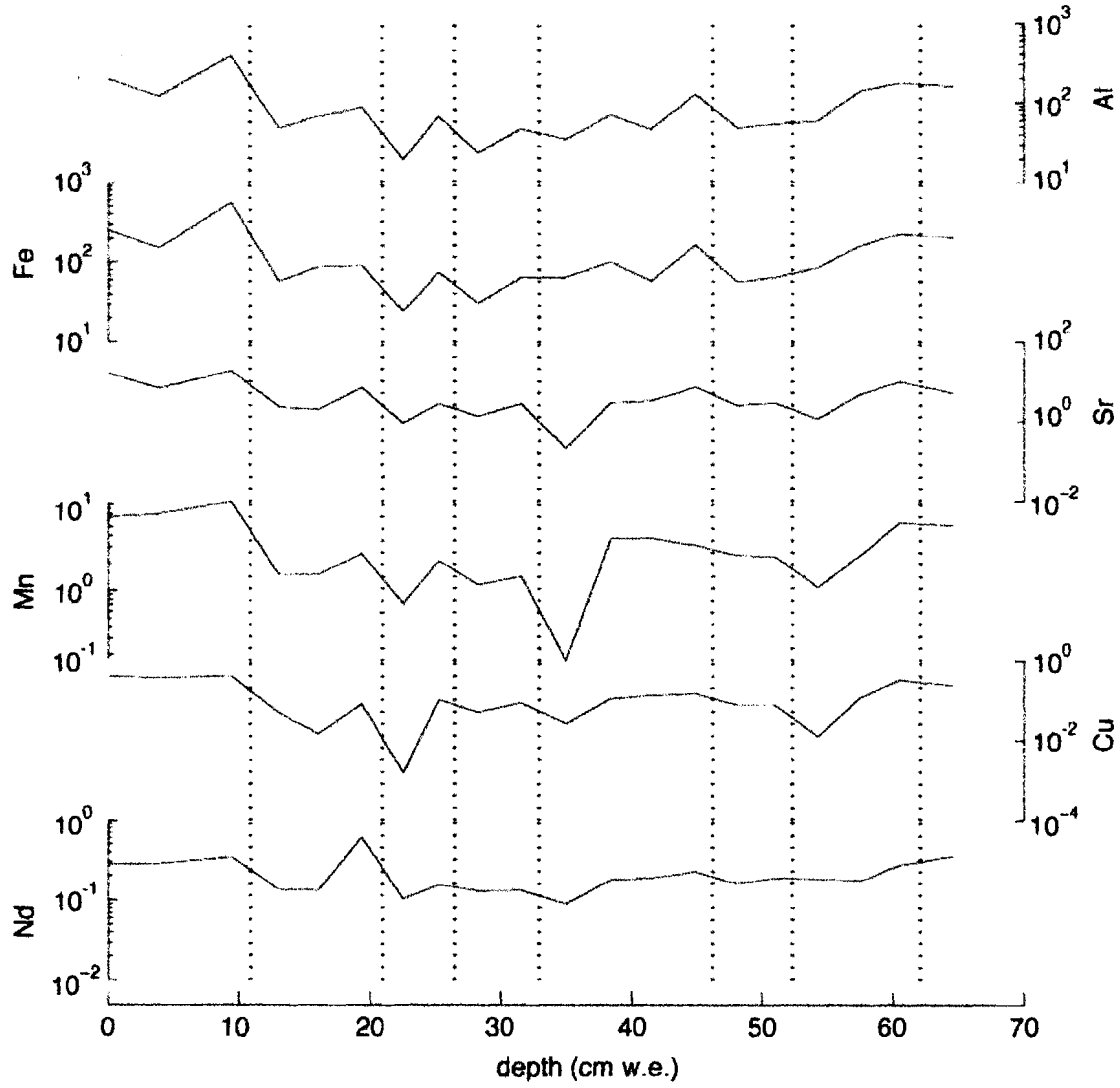

Figure 1.22. Variations in trace metal concentrations with depth at the Blue Glacier.

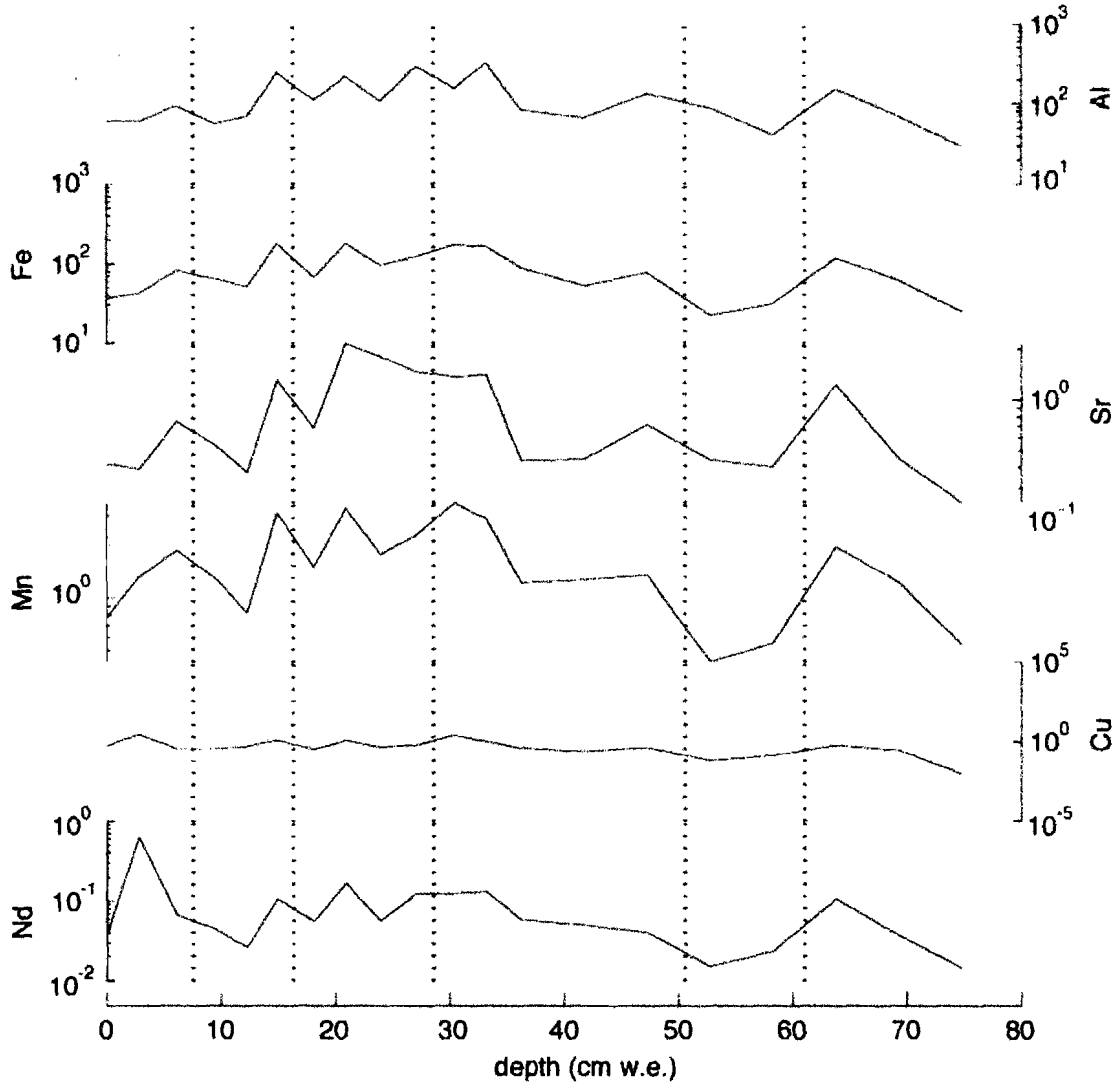

Figure 1.23. Variations in trace metal concentrations with depth at the Victoria Upper Glacier.

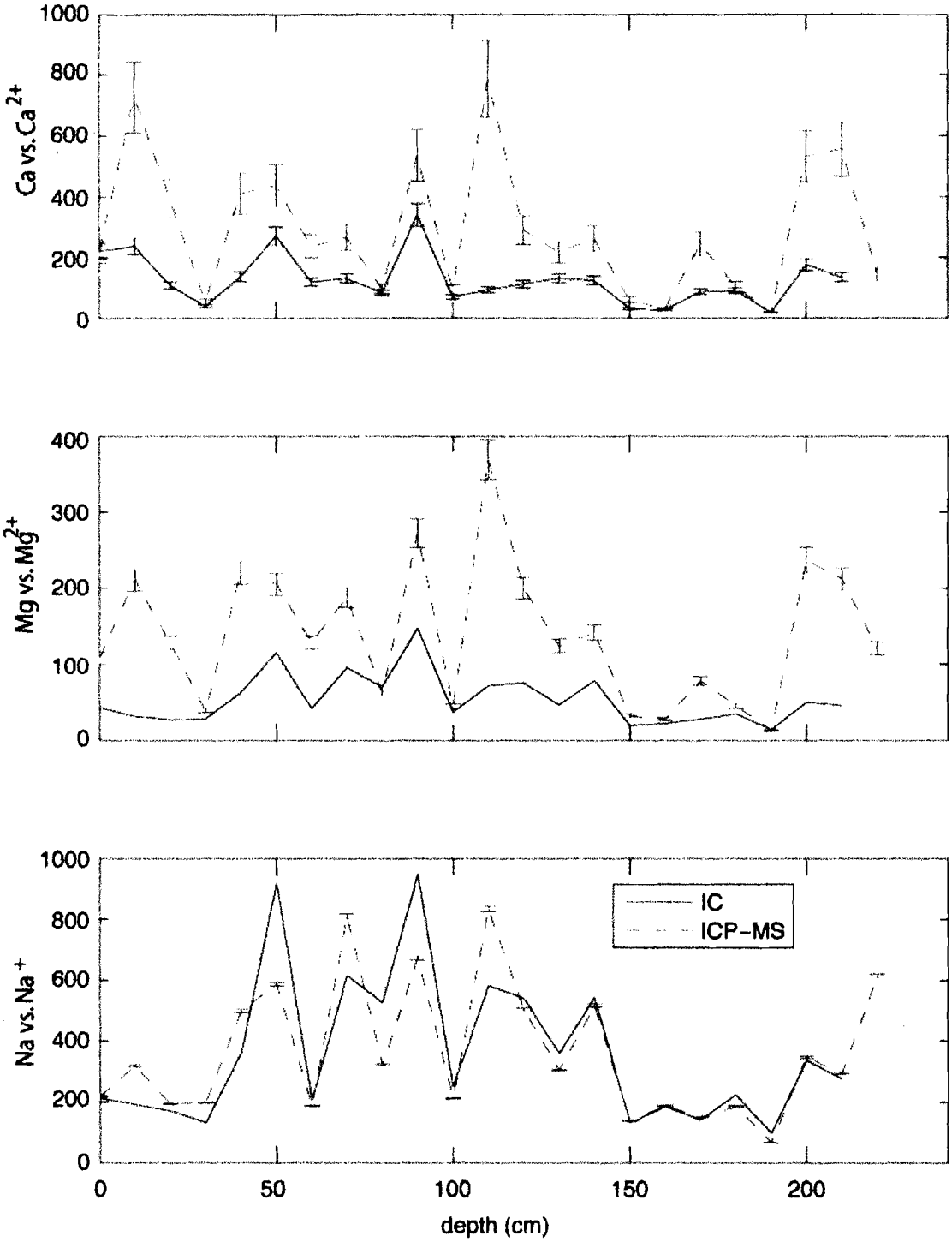

Figure 1.24. Concentrations of calcium, magnesium, and sodium at the Clark Glacier measured by ion chromatography (IC) and by inductively-coupled-plasma mass spectrometry (ICP-MS). IC samples measure soluble ions Ca^{2+}, Mg^{2+} and Na^{+}, while ICP-MS measures total presence of Ca, Mg and Na present in a sample. Data for Ca^{2+}, Mg^{2+} and Na^{+} represent geometric means of five 2-cm resolution samples within the same 10 cm of firn directly measured for total value by ICP-MS.

	EOF1	EOF2	EOF3	EOF4	EOF5	EOF6
total	62.59	28.90	5.83	1.35	0.73	0.41
Na^+	**60.88**	**32.77**	-4.76	0.19	-1.08	0.00
K^+	**84.00**	**7.81**	**-6.06**	-0.08	1.63	-0.15
Mg^{2+}	**63.07**	**23.54**	**-12.17**	0.48	-0.23	0.21
Ca^{2+}	**94.64**	-0.18	0.00	-4.00	0.49	-0.56
MS^-	**5.36**	**76.46**	**16.10**	0.29	1.38	0.26
SO_4^{2-}	**40.93**	**44.19**	**13.14**	-0.01	-1.22	-0.23
Al	**70.23**	**-25.33**	2.32	-0.56	-0.12	1.27
Fe	**80.32**	**-18.14**	0.01	0.40	0.43	0.65
Sr	**68.76**	**-27.28**	2.32	-0.64	-0.64	-0.06
Mn	**57.70**	**-33.28**	1.46	**6.83**	0.03	-0.67

Table 1.7. Percentage of total variance, and variance by variate, explained using the first six EOFs generated at the Clark Glacier. Positive and negative values represent the relative loading of each variate on each function (e.g. SO_4^{2-} is positively correlated with EOF2, to which Al is negatively correlated) The remaining six EOFs explained <5% of variance in all variates at all sites.

	EOF1	EOF2	EOF3	EOF4	EOF5	EOF6
total	68.60	16.60	6.71	5.53	1.78	0.40
Na^+	**69.40**	**21.25**	**-8.69**	0.35	-0.01	0.01
K^+	**76.35**	**13.40**	**-9.06**	0.00	0.09	-0.80
Mg^{2+}	**67.19**	**20.56**	**-10.71**	0.09	-0.68	0.15
Ca^{2+}	**92.70**	-0.32	-0.05	-0.11	**6.19**	-0.40
MS^-	**9.43**	**49.30**	**39.33**	-0.05	-1.02	0.85
SO_4^{2-}	**61.65**	**30.90**	4.13	0.36	0.16	-2.49
Al	**84.44**	**-12.84**	0.15	-1.13	-1.30	0.00
Fe	**84.26**	**-10.60**	0.22	-1.11	-3.23	0.00
Sr	**80.51**	**-15.37**	1.47	-0.71	-0.93	0.00
Cu	**34.26**	-4.26	0.04	**61.35**	0.07	0.01
Mn	**85.06**	**-12.94**	0.27	-0.65	-0.42	0.00
Nd	**77.94**	**-7.41**	**-6.36**	-0.45	**7.29**	0.06

Table 1.8. Percentage of total variance, and variance by variate, explained using the first six EOFs generated at the Commonwealth Glacier.

	EOF1	EOF2	EOF3	EOF4	EOF5	EOF6
total	64.63	13.30	10.66	6.32	2.76	1.50
Na^+	**87.20**	1.55	0.50	4.20	-2.04	2.98
K^+	**69.16**	**26.85**	0.02	-1.49	0.84	-0.48
Mg^{2+}	**74.64**	**22.40**	0.59	0.00	-0.48	0.00
Ca^{2+}	**63.24**	**23.10**	0.48	-4.62	**5.46**	-2.31
MS^-	-4.69	**-13.06**	**71.51**	4.84	4.55	-0.92
SO_4^{2-}	**47.85**	0.93	**41.35**	-3.50	-1.07	3.99
Al	**76.81**	**-15.43**	-3.54	-0.56	2.64	0.92
Fe	**70.25**	**-19.76**	-4.40	-1.45	3.22	0.76
Sr	**86.20**	**-8.17**	-2.16	0.54	2.34	0.01
Cu	**77.65**	**-11.39**	1.97	-0.76	**-5.28**	-2.29
Mn	**77.29**	**-13.45**	-0.19	-0.12	**-5.13**	-3.26
Nd	**40.60**	3.48	-1.22	**53.71**	0.07	-0.08

Table 1.9. Percentage of total variance, and variance by variate, explained using the first six EOFs generated at the Blue Glacier.

	EOF1	EOF2	EOF3	EOF4	EOF5	EOF6
total	50.82	19.55	12.70	7.76	4.55	1.82
Na^+	**10.25**	**-12.15**	-1.50	**73.26**	1.79	0.89
K^+	**83.00**	**-9.41**	1.82	1.93	-1.72	0.09
Mg^{2+}	**80.84**	**-9.37**	1.90	-0.64	-2.05	0.00
Ca^{2+}	**79.80**	**-11.46**	4.38	-3.04	0.06	-0.10
MS^-	**28.88**	**-28.63**	3.44	**-8.46**	**29.33**	0.96
SO_4^{2-}	**73.84**	**-9.22**	4.60	0.02	-6.79	-2.64
Al	**41.65**	**17.30**	**-21.59**	0.89	9.82	**-7.44**
Fe	**72.64**	**14.95**	**-7.49**	-0.26	0.03	0.00
Sr	**44.80**	**21.19**	**-18.90**	-1.88	-0.36	**8.32**
Cu	**18.32**	**33.65**	**41.28**	1.40	0.40	1.05
Mn	**75.76**	**19.26**	-1.64	0.00	-0.95	0.00
Nd	-0.08	**47.96**	**43.90**	1.40	1.28	-0.34

Table 1.10. Percentage of total variance, and variance by variate, explained using the first six EOFs generated at the Victoria Upper Glacier.

The technique is designed to generate a function explaining the maximum possible associated variance in a total dataset based on factors weighting linear correlations among individual variables. After generating this first function (EOF1) the procedure then generates a second function, orthogonal to the first, explaining the maximum possible variability in the remaining data (EOF2). This process is repeated until as many functions are generated as there are original variables. Because each function is orthogonal to all the others, each explains a unique portion of total data variance, which may then represent a common physical mechanism influencing that portion of data variability.

In practice, the majority of total data set variability is typically explained by the first few EOFs. Many of the higher order functions explain no total variance at all, but for individual variates they may capture significant portions of behavior not reflected in the variability of other components. To avoid spurious relationships, any EOF mode that explains less than 5% of variance in both the total dataset and in individual variates will not be considered in this analysis.

EOF1 explains 51%, 63%, 69% and 65% of total data variance at the Victoria, Clark, Commonwealth and Blue sites, respectively. At the coastal locations, this pattern of variation accounts for 34% to 86% of deposition variance in individual metals and 41% to 95% of variance in the deposition of individual ions (excluding MS^-). The Victoria Upper Glacier again shows a fundamentally different pattern, with noticeably lower loadings on the first mode, particularly for Na^+ (10%), Al (42%), Sr (45%) and Nd (0%). MS^- has only limited association with the first mode at any of the sites in this study.

EOF2 represents an additional dataset total variance of 20% at the Victoria Upper Glacier, 29% at the Clark Glacier, 17% at the Commonwealth Glacier and 13% at the Blue Glacier. Most variates still have appreciable loadings on this function at all sites, with the exceptions of Ca^{2+} at the Clark and the Commonwealth, Cu at the Commonwealth, and Na^{+}, Nd, and SO_4^{2-} at the Blue. Interestingly, at the Victoria Upper Glacier, the first two variability modes account for only ~ 22% of Na^{+} variance. MS^{-} variance, on the other hand, has a 77% loading on the second EOF at the Clark and a 49% loading on this mode at the Commonwealth, making this the dominant mode for variation of this species at these sites.

For the Clark and Commonwealth glaciers, MS^{-} is the only variate with a loading higher than 15% on any axis ≥ EOF3, with 16% of variation in this species on the Clark and 39% on the Commonwealth attributed to EOF3. Aside from MS^{-}, variability at these locations ranges from 6% to 13% on the third axis for a selection of the major ions (plus 6% of Nd variance at the Commonwealth). Total data set variability in all modes beyond EOF2 is less than 15%, and EOF3 accounts for only 6% at the Clark and 7% at the Commonwealth. For the Blue and Victoria Upper Glaciers, however, these higher modes contain 22% and 27% of total variability, with 72% of MS^{-} and 41% of SO_4^{2-} variance at the Blue site associated with EOF3, 54% of Nd associated with EOF4 at the Blue site and Na^{+}, MS^{-}, Al, Sr, Cu, and Nd demonstrating high variance associated with EOF3 through EOF6 at the Victoria Upper site. In particular, 74% of Na^{+} variance and 44% of Nd variance is accounted for in the third and fourth EOF on the Victoria Upper Glacier.

Discussion

While there is broad agreement that local particulate material exerts a strong influence on MDV snow and firn chemistry [*Mayewski and Lyons*, 1982; *Mayewski et al.*, 1995; *Lyons et al.*, 2003; *Bertler et al.*, 2004*b*], prior studies have focused either on one site in particular [*Mayewski and Lyons*, 1982; *Welch*, 1993; *Mayewski et al.*, 1995] or on east-west transects along the axis of the valleys [*Lyons et al.*, 2003; *Bertler et al.*, 2004*b*]. Among this second group, Lyons et al.'s [2003] surface survey along the axis of the Taylor Valley provides an excellent view of spatial patterns in major ion chemistry along that axis, but was not designed to address differences between metals (dominated by terrestrial insoluble particulate) and soluble ions (from both terrestrial and marine soluble aerosols). Their study also included only near surface (<50 cm) samples, making it impossible to test deposition timing among species [*Lyons et al.*, 2003]. Bertler et al. [2004*b*], on the other hand, developed a combined ions / metals record similar to that presented here for sites along the axis of the Victoria Valley, but three of the four sites are concentrated in a 25 km line nearest to the Ross Sea, while the fourth is on the polar plateau, intended to capture plateau rather than MDV processes. The work presented here bridges these data sets, with three sites along a north-south axis near the coast and the fourth near the border between the plateau to the west and the valleys to the east, in between the site groupings covered in Bertler's work.

Mean chemistry

Spatial differences in mean chemistry among the sites presented here can be divided into differences between two sites along a west-east axis (the Victoria Upper and

the Clark) and differences among three sites along a coastal north-south axis (the Clark, the Commonwealth, and the Blue). Data from the east-west sites examined here confirm previously documented trends in concentration based on distance to the Ross Sea and on elevation. These influences are confirmed both for sites in the Asgaard Range and for sites in the Victoria Valley. While at the Bertler et al. [2004*b*] sites, however, they classified K^+, Mg^{2+}, and Sr as marine species, at my sites it appears these ions share a mixed terrestrial / marine source. Though mean concentration differences between Bertler et al. and this work might be explained by slightly different time periods covered by pits, the likelihood of soil influence playing a role is supported by non-sea-salt species analysis, in which calculated nss-Mg^{2+} comprises 25-50% of total Mg^{2+} and nss-K^+ comprises ~50% of total K^+ at the Clark and Victoria Upper sites; Sr, meanwhile, covaries with the terrestrial metals rather than with the ions in EOF space, arguing against a uniquely marine source, as suggested by Bertler et al. [2004*b*] for Sr on the Victoria Lower Glacier. The contrasting results highlight the potential for metals source variability over small distances (the Victoria Lower Glacier and the Clark Glacier are separated by only ~13 km). The data presented here also supports Welch's [1993] hypothesis that relatively high values for Ca^{2+} and SO_4^{2-} at the Newall Glacier (NG on the map) are related to the nearby MDV soil source. Welch's finding of ~90% nss-SO_4^{2-} is the same value found here for the Blue and Victoria Upper Glaciers [*Welch*, 1993].

When examined alongside these relationships among mean chemistry data, elevation and distance from the coast within the Asgaard Range and the Victoria Valley, the lack of chemistry trends following these two variables along the axis of the coast suggests separate dominant influences. The simplest explanation for north-south

variation at these sites lies in the different local exposures to soil and marine sources from which they draw material. Because soil salt chemistry within the Dry Valleys varies spatially [*Claridge and Campbell*, 1977; *Keys and Williams*, 1981; *Bockheim*, 1997], we would expect to see a correspondingly complex influence on snow and firn chemistry. Examining published data describing the salt composition of a wide selection of MDV soil samples, however, some common patterns can be found. In particular, ratios between Mg:K and Ca:K are both higher in all MDV soil samples than they are in sea-salt (Figure 1.25) [*Claridge and Campbell*, 1977; *Keys and Williams*, 1981; *Bockheim*, 1997; *Abollino et al.*, 2001]. The magnitude of these ratios also provides an identifiable pattern, with marine material showing a Mg:K ratio higher than the Ca:K ratio, and soil material showing the opposite. The relationship between Mg:K and Ca:K in the snow and firn examined here is similar to that shown by samples from the soil source (though lower in magnitude), highlighting the influence of valley soils in determining solute chemistry at these sites.

Differing influences from marine air masses further distinguish each site's chemistry. Sodium, Cl^- and MS^- likely reflect the marine influence. Both the Clark and the Commonwealth glaciers, where Na^+ and Cl^- concentrations are highest, have uninterrupted corridors to the coast through which up-valley winds characterizing summer daytime ground-level flow can carry marine aerosols. The Clark Glacier in particular has two exposures, through the Victoria Valley and the Wright Valley, leading to the highest concentrations of marine species at this site. The Victoria Upper Glacier, though twice as far from the coast as the other sites, likewise sits at the head ofthe Victoria Valley, which may funnel marine species inland. The Blue Glacier, on the other

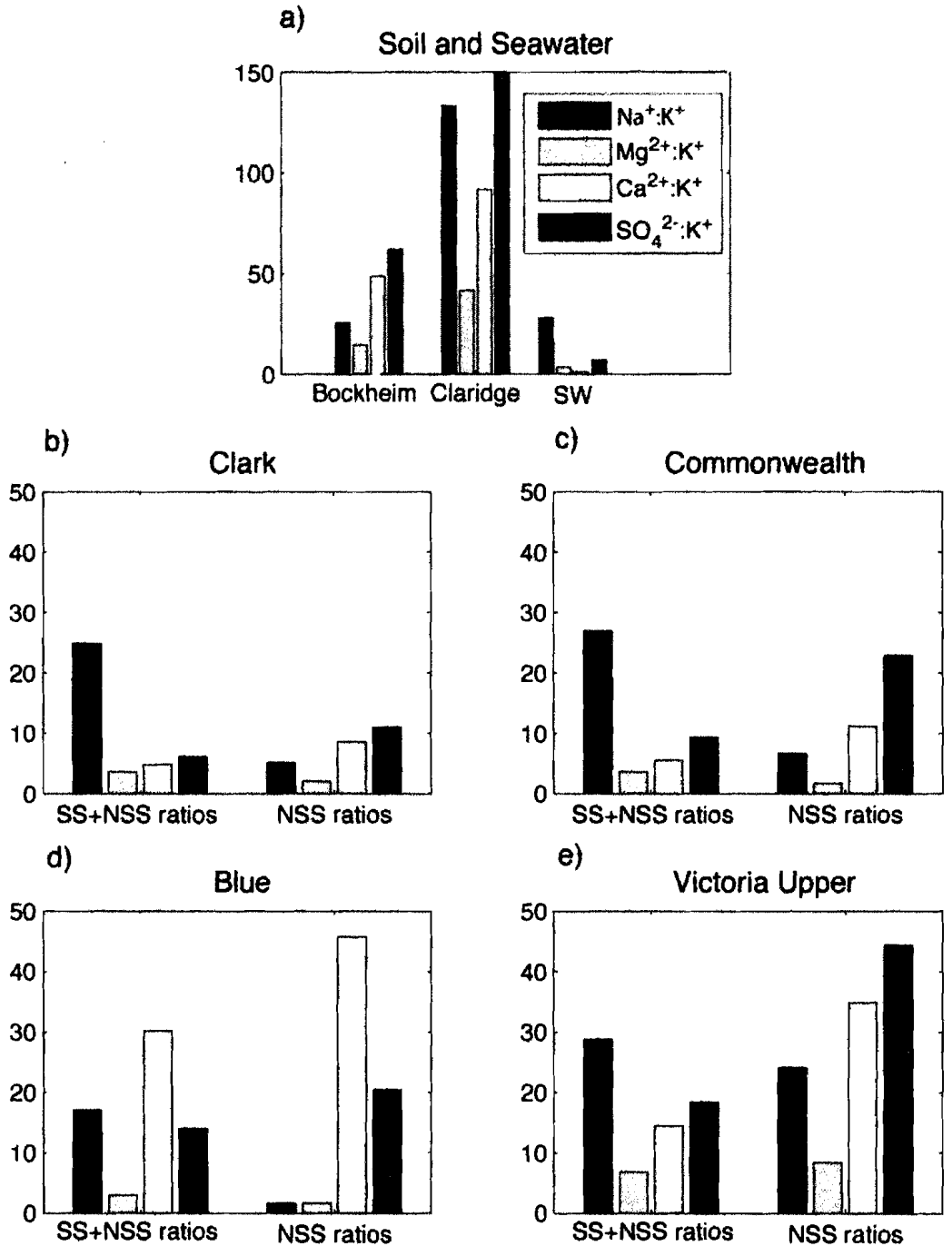

Figure 1.25. Molar ion ratios of material collected at MDV sites -- total (=SS+NSS) and the non-sea-salt component (=NSS) -- compared to those of mean regional soil samples and of seawater. Subfigure a) represents regional soil and seawater ion ratios, b) represents these ratios for material collected at the Clark Glacier, c) ratios for the Commonwealth Glacier, d) ratios for the Blue Glacier, and e) ratios for the Victoria Upper Glacier. Bockheim mean soil ratios include data from 8 sites [Bockheim, 1997], while Claridge mean ratios include data from 20 sites [Claridge and Campbell, 1977]. Note that scale is higher for soil samples (0-150) than for snow pit samples (0-50).

hand, though it is relatively close to the coast, is sheltered from low-elevation marine air to the east by a coastal range of mountains with peaks from 800 to 1500 meters elevation. The combination of this shelter from the marine environment and a presumed high-calcium soil source may give the Blue Glacier its unique ion signature of high Ca^{2+} concentrations alongside low concentrations in other major ions relative to the other sites.

Timing of Deposition

Because trace metals are characterized by their relatively low presence in seawater and, by extension, in sea-salt aerosols, their relatively high concentrations in the MDV likely derive from valley particulates rather than from the marine environment. In contrast, while the major ions have significant local soil sources, as shown above, the marine source is clearly a significant contributor of these analytes. To approach the distinction between marine and local particulate deposition, I will discuss the input timing of dominantly soluble species (the major ions, with a strong influence from the marine environment) relative to that of the dominantly insoluble species (the trace metals, for which the marine environment supplies negligible quantities relative to those found in MDV snow and firn). The EOF analysis presented here allows comparison of the input timing of these two groupings. Because trace metals were sampled at 10-cm resolution to achieve adequate volume for multiple analyses (further examined in chapter 2), this analysis does not characterize sub-annual species variability. Samples for this approach all correspond to the same time period (1989 - 2002), however, so similarities and differences in temporal behavior among the sites can be addressed here on the basis of longer time-scale influences.

Variability in species input timing appears to reflect site exposure to the marine source, with the Clark and Commonwealth sites showing variability relatively well contained in the first two dominant modes while the Blue and the Victoria Upper sites demonstrate more complex deposition patterns. An additional striking result from the temporal analysis presented here lies in the relationships between dominantly soluble species, dominantly insoluble species and the first and second EOFs at all sites. Because all species are similarly associated with the first EOF, interpreting a physical basis for this mode requires a process that acts in a consistent manner for the majority of variates, with both soluble and insoluble species increasing and decreasing in response to a similar forcing. The second EOF, by contrast, splits the species into soluble and insoluble groupings; this separation dictates a process that acts in an opposing manner for soluble species relative to its effect on insoluble species.

Bertler et al. [2004*b*] explain the dominant pattern of variability (their EOF1) according to "monsoonal" circulation, with dominant (in frequency) onshore - offshore winds operating along the axes of the MDV and providing concurrent maxima and minima for both soluble and insoluble species. Major ion data from the four sites described here supports this interpretation. Variance in MS^- is not explained by this model, however, suggesting additional factors be considered for variability in this species.

One possible physical basis to explain EOF2 involves the effect of katabatic wind storms in the MDV. Nylen et al. [2004] note that strong katabatic events overwhelm topographic controls and are often accompanied by a shift in wind direction and a significant increase in wind speed. These changes would naturally influence the quantity

and source of particulates reaching glacier deposition zones. Katabatic winds are also episodic, responding to synoptic scale forcing [*King and Turner*, 1997]; as such, they represent a fundamentally separate mode of variability than that represented in the onshore-offshore flow model.

Published data for katabatic wind frequency for 1989-2001 at Lake Hoare in the Taylor Valley overlap the snow pit chronologies discussed here, representing 1989 - 2002 (Table 1.11). Additional records of katabatic frequency and strength include observations from the year 1999 for a variety of sites surrounding the glaciers discussed here [*Nylen et al.*, 2004]. These data show katabatic wind events occur with an abundance (expressed as the percentage of the total number of recorded wind events) that matches the variability shown by EOF2 (expressed as a percentage of the total variability in chemistry variance) at the four sites examined here. Moreover, because katabatic winds flow consistently from west to east in the MDV, they would retard lower tropospheric marine air mass movement into the valleys described by the monsoonal effect. The combination of this cessation of marine air incursion and increased particulate mobilization associated with higher wind speeds would be recorded in firn records as an increase in insoluble species and a decrease in soluble species.

Unfortunately, because of resolution limitations in the trace metals dataset, samples from these snowpits do not allow adequate calibration to determine if there is a correlation between katabatic events and trace metal concentrations in MDV snow and firn. Alternate hypotheses for mechanisms to explain this portion of chemistry variability in MDV firn include more tightly localized down-glacier air flow (described by Nylen et al. [2004] as interfering with their analysis in defining katabatic events) or processes that

site	time period covered	EOF2 variance explained 1 - total 2 - variates exc MS^- (%)	monthly katabatic frequency(%)
Lake Vida (LV)	1999		0 to 8
Lake Brown (LBr)	1999		4 to 28
Canada Glacier (CaG)	1999		4 to 28
Lake Fryxell (LF)	1999		0 to 20
Commonwealth Glacier (CoG)	1999		0 to 15
Explorer's Cove (EC)	1999		0 to 9
Lake Hoare (LH)	1989 - 2001		4 to 26
Victoria Upper Glacier	1989 - 2002	30.2 0 to 48	
Clark Glacier	1989 - 2002	28.9 0 to 45	
Commonwealth Glacier	1989 - 2002	16.6 0 to 31	
Blue Glacier	1989 - 2002	13.3 0 to 27	

Table 1.11. Comparison of katabatic wind event frequency (represented as range of monthly frequencies) from Nylen et al. [2004] with percentage variance explained by EOF2. EOF figures are presented with and without MS^-, given that this species does not follow the same pattern of variance as other ions at any site.

would temporarily interrupt down-glacier air flow and bring additional particulate material to the site from the valley floor below. The intra-site variability at the Clark and Commonwealth Glaciers points out the possibilities inherent in this second approach.

Conclusions

Snowpits excavated to two and three meters at the Victoria Upper, Clark, Commonwealth and Blue Glaciers in the Dry Valleys provide information on marine and local soil chemistry input into regional surface snow and firn. Measurements from additional pits at locations separated by hundreds of meters at the Clark and Commonwealth glaciers show significant variability, and require both marine and soil inputs to explain. Chronologies based on marine species input, confirmed alongside mass accumulation rates measured directly by networks of mass balance poles, show that these four sites share a common time frame of 1989 - 2002, with some of the sites having slightly longer coverage. Accumulation rates average 2.5, 3.4, 3.1 and 4.6 cm w.e. for the Clark, Commonwealth, Blue and Victoria Upper sites, respectively; the possibility of subsurface melting at the Victoria Upper Glacier dictates caution in interpreting data from this location.

A survey of mean chemistry among the sites shows the Clark and Commonwealth Glaciers with the highest concentrations in marine species (350 μg/L and 167 μg/L for Na^+, 25 μg/L and 21 μg/L for MS^-), while the Blue Glacier shows unexpectedly low concentrations (72 μg/L Na^+, 10 μg/L MS^-), likely related to shelter provided by a coastal range to the east. Trace metals are in highest abundance at the Clark Glacier (Al concentration = 234 μg/L), with the lowest concentrations found at the Commonwealth

Glacier (Al concentration = 45 μg/L). Major ion concentrations at the Victoria Upper, Clark and Commonwealth sites are in good agreement with previously published intra-valley trends in the Victoria Valley and the Asgaard Range, showing broadly decreasing values with increasing distance from the coast and increasing elevation. When considered independently of external datasets, however, trends in chemistry following elevation and distance from the coast do not appear. Instead, variations related to differing soil sources and exposures to the Ross Sea dominate north-south mean chemistry gradients at these sites.

Empirical Orthogonal Function (EOF) analysis demonstrates more complex species input timing variability at the Victoria Upper and Blue Glaciers than at the Clark and Commonwealth Glaciers. Temporal variability in major ions at these sites provides support for the interpretation of the first EOF as representative of the monsoonal circulation proposed by Bertler et al. [2004*b*]. While the second EOF may be related to katabatic wind frequencies, the data here do not allow direct correlation of snow and firn trace metal concentrations and katabatic wind events. Future, higher resolution samples will be examined to study this possibility further.

Continuing work is needed to identify specific sources and pathways for particulate material to each of the glaciers studied here. Grain size analysis and analysis of trace metal and major ion ratios in digested soil samples are planned to help with this process, so as to more tightly constrain input to each individual site. Part of this work will involve separating out the particulate fraction found in glacier firn for separate analysis. This will be discussed in greater depth in chapter 2.

The circumstances defining the MDV climate system, including the onshore - offshore wind regime, widespread aridity and exposed rock and soils, help to give the valleys their unique character. This character also creates a wide selection of individual snow and firn signatures within a small area. Understanding broader climate changes in this area will therefore require continuing attention to local variation in Dry Valleys ice core and snowpit locations so as to be able to tell the difference between regional climate change and local variability in this junction between the Ross Sea to the east and the East Antarctic Ice Sheet to the west.

Chapter 2:

DETERMINATION OF TRACE METAL CONCENTRATIONS IN ANTARCTIC SNOW AND FIRN USING A COMBINATION OF REFRENCE, FILTERED, AND ACIDIFIED SAMPLES

During the past few decades, trace metal analysis has provided valuable information regarding past atmospheric composition [*Boutron*, 1982; *Mayewski and Lyons*, 1982; *Matsumoto and Hinkley*, 2001; *Garbarino et al.*, 2002], petrological study [*Cullers and Podkovyrov*, 2002; *Ghosh et al.*, 2002], and the effect of certain species (Fe in particular) on oceanic CO_2 concentrations and thereby on global climate [*Mayewski and Lyons*, 1982; *Martin*, 1990; *deBaar et al.*, 1995]. A variety of tools has been used for measurement of these elements in ice and snow, including graphite furnace atomic absorption [*Boutron and Lorius*, 1979], colorimetric techniques for reactive species [*Mayewski and Lyons*, 1982], flow injection analysis with spectrophotometric detection [*Edwards et al.*, 1998; *Matsumoto and Hinkley*, 2001], thermal ionization mass spectrometry [*Hinkley and Matsumoto*, 2001], and optical emission spectrometry [*Bertler et al.*, 2004*b*]. Measurements are available from sites in the Arctic, Antarctica, and high-elevation mid-latitudes [*Boutron and Martin*, 1980; *Mayewski and Lyons*, 1982; *Kreutz and Sholkovitz*, 2000; *Garbarino et al.*, 2002].

This diversity of sites leads to variable snow conditions, ranging from locations containing snow and firn with minimal dust and particulate input to those with abundant input [*Mayewski and Lyons*, 1982; *Planchon et al.*, 2002]. In both cleaner ice and snow and that with higher dust inputs, trace metals have provided information regarding the

geographic source of weather systems affecting the areas studied [*Mayewski and Lyons*, 1982; *Basile et al.*, 1997; *Kreutz and Sholkovitz*, 2000] and the associated temporal variability [*Boutron*, 1982; *Planchon et al.*, 2002]. Multiple sources for central Asian dust were identified, for example, using a divide between Nd concentration variability (dominated by loess sources) and Ca and S concentration variability (dominated by non-loess sources) in snow from high- and low-dust samples on the Inilchek Glacier in Kyrgyzstan, central Asia; this information dictated a change in either wind speed or wind direction for the seven years covered by the data [*Kreutz and Sholkovitz*, 2000].

In recent years, researchers have focused specifically on measuring Fe transport and testing the "iron hypothesis"; this argument proposes that as a trace nutrient, iron controls significant amounts of photosynthesis in the southern ocean and thereby controls regional ocean-atmosphere carbon fluxes [*Martin*, 1990; *deBaar et al.*, 1995; *Sedwick et al.*, 2000; *Buessler et al.*, 2004]. Research quantifying iron concentrations in Antarctic ice and snow contributes both a spatial and temporal perspective regarding possible southern ocean iron input [*Mayewski and Lyons*, 1982; *Edwards et al.*, 1998; *Edwards and Sedwick*, 2001]. Only a portion of the iron reaching the southern ocean, however, is available for biological use [*Gao et al.*, 2003; *Bonnet and Guieu*, 2004]. In particular, the difference between dry deposition and wet deposition may be significant, with interactions between acidic cloud droplets and scavenged particles promoting ferrous iron (Fe^{2+}) dissolution, allowing more bioavailable Fe through wet deposition than through dry [*Gao et al.*, 2003].

To account for this difference, investigators have experimented with methods using both filtered and unfiltered samples and involving a variety of acidification and pre-

concentration steps to determine the amount of total and/or dissolved trace metals [*Boutron and Lorius*, 1979; *Boutron and Martin*, 1980; *Boutron*, 1982; *Edwards et al.*, 1998; *Edwards and Sedwick*, 2001; *Gaspari et al.*, 2003; *Marino et al.*, 2003]. Because the application of each technique has commonly been associated with a different sample location, it is difficult to separate effects associated with a given technique from effects associated with different locations. In this chapter, I examine trace metal concentrations from a single set of snowpit samples analyzed both with and without physical filtration in order to identify the effects of this procedural difference. This analysis assesses the accuracy of the method of physical filtration followed by acidification of the filtrate for yielding separate measurements of trace metals present in particles larger than the filter gauge (0.4 μm in this case) and those present either as smaller particles or in a soluble form. I also analyzed the same set of samples with and without acidification of the unfiltered samples to assess concentrations of acid soluble metals.

Samples and Analysis

The samples for this study were collected from the accumulation zone of the Victoria Upper Glacier (77.3005° S, 161.0419° E, 1350m) in the McMurdo Dry Valleys (MDV) of southern Victoria Land, Antarctica (Figure 2.1). This glacier is 60 km from the coast of the Ross Sea, flows east and southeast, and forms the head of Victoria Valley, an arc-shaped valley of exposed bedrock and sand ending at the base of Victoria Lower Glacier, 40 km to the east at the mouth of Victoria Valley. A 2-meter snowpit was excavated in December 2004 as a preliminary assessment of suitability for future ice core drilling [*Kreutz and Mayewski* proposal, 2002]. Visible fine sand occurred at the pit

Figure 2.1. Location map for Victoria Upper Glacier. Site elevation is 1350 m.a.s.l. Imagery from Landsat library and GeographX, NZ.

location, more than 1 km from the surrounding rock walls. From 0 to 25 cm depth, harder layers composed of fine-grained ice crystals alternated with softer layers composed of larger crystals of hoar. Below 25 cm, firn was consistent with crystals up to 4 mm diameter and no discernable layering. Densities in the top 120 cm of the pit ranged between 0.25 and 0.33 g/cc, but the lower part was quite hard, making excavation, even with steel shovels, difficult. The hardness of the firn made density measurements below 120 cm depth impossible. This contrast is consistent with possible subsurface melting at this location.

Using the techniques described in chapter 1, twenty samples were recovered from the Victoria Upper site, representing material from the surface to 200 cm depth. All components used for the analysis here, including vials, pipette tips, and other containers, were cleaned according to the same procedure used for the sampling containers. Samples were kept at –20° C and shipped back to the University of Maine Climate Change Institute (CCI) freezer facility for storage before analysis.

At the CCI, each frozen sample was split into two parts before melting. One part remained in the original sample bottle and the second was transferred into a 50 mL polypropylene centrifuge tube. The contents of both of these aliquots were melted at 25° C (still in closed containers) on wire racks in the CCI's class 10,000 clean room, and three different analyses were conducted (Figure 2.2). First, the original sample bottle, unaltered, was agitated to suspend sediment, and 3.5 mL of reference sample was transferred by pipette to a 4 mL polypropylene vial used to introduce sample into the ICP-MS. After the transfer, 35 μL of Optima grade HNO_3 was added to the ICP-MS analysis vial to create a 1% acidified sample for analysis; acidification ensured that no

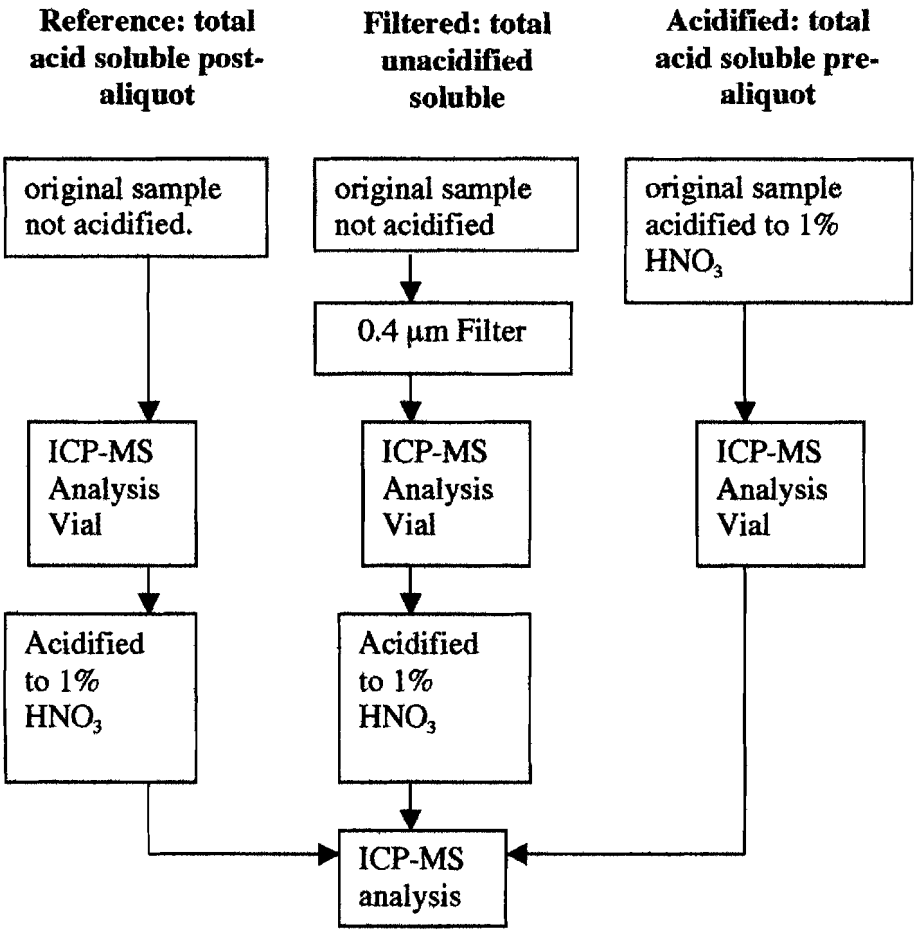

Figure 2.2. Procedural schematic for reference, filtered, and acidified samples.

material was lost to the analysis from adsorption to the analysis vial wall. Acidification also likely dissolved some of the particulate in the analysis vial. Samples were introduced into the ICP-MS including both particulate and liquid, however, so in theory concentrations should not change as a result of the mode in which trace metals reside in the analysis vial. Data generated from these samples, termed "reference", are examined in the discussion to assess the truth of this assumption.

For the second procedure, the original sample bottle was again agitated, and 3.5 mL of the sample water was poured directly into a 10 mL polypropylene syringe attached to a polycarbonate filter holder containing a 0.4 μm Nucleopore® polycarbonate membrane. This sample was filtered through the membrane using thumb pressure on the syringe and the filtrate was collected in ICP-MS vials identical to those used for control samples; the membranes were removed and saved for future analysis. Thirty-five μL of HNO_3 was again added to these analysis vials to bring the samples to 1% HNO_3 concentration. The analysis based on this procedure is termed "filtered".

The third procedure, termed "acidified", used the sample in the 50 mL polypropylene centrifuge tubes. This sample was melted, and enough HNO_3 was added directly to each tube to yield 1% HNO_3 concentration. After 24 hours, these samples were agitated and 3.5 mL of this new acidified sample was transferred by pipette to the ICP-MS vials for analysis. No additional acid was added to the vials after the transfer.

Finally, by subtracting the concentration yielded in the "filtered" analysis from the concentration yielded in the "reference" analysis, I derived an estimate of the material removed from analysis through filtration. This material, termed "insoluble particulate", provides further information regarding the partitioning of trace metals in these samples.

Analysis was conducted on a ThermoFinnigan ELEMENT2™ ICP-MS, with samples injected into the plasma chamber as liquid and any suspended particulates. No additional filtration was conducted prior to samples' introduction into the instrument. Analytes included Al, As, Ba, Bi, Ca, Cd, Co, Cr, Cs, Cu, Fe, Mn, Pb, S, Sb, Sr, Ti, Tl, U, V, Zn and the rare earth elements (REE) – La, Ce, Pr, Nd, Sm, Eu, Gd, Tb, Dy Ho, Er, Tm, Yb and Lu. Because these samples had a large range of concentrations, from < 1 ng/L in some samples and species to 10^2 μg/L in others, two methods were used for analysis. For one run, samples were measured directly, with no reference standard included. These values are considered appropriate for samples with low concentrations, where the addition of a standard to the sample would lead to appreciable contamination and where significant interference from a high density of elements in the plasma is of small concern. For samples with higher concentrations – in which sample interferences with the plasma were of greater concern and the potential contamination introduced is minimal compared to original sample concentrations – a second run was conducted in which samples were spiked before analysis with 1 μg/L of In to provide a material against which sample values could be measured to assess efficiency.

Blanks and variability among duplicate sample runs provide quality control criteria for each of the three preparation methods described above. To account for contamination introduced using each method, reagent blanks were run using the reference (n = 2), filtered (n = 3), and acidified (n = 2) sample preparation procedures and containers. The consistency of results is judged by comparing duplicate runs of three samples for each procedure. Variability in each sample set is defined as the mean of the variabilities of all duplicate pairs, where sample variability is expressed as a percentage, calculated as:

$$\left(\frac{x-\mu}{\mu}\right)*100$$

with x being the concentration of the species in a given sample and μ the average value of the duplicate pair to which it belongs. I also calculated variability as a percentage of the insoluble particulate fraction according to the formula:

$$\left(\frac{x-\mu}{C-\mu}\right)*100$$

where C is the concentration found in the reference sample prior to filtering and x and μ are the sample concentration and average value, respectively, for the associated filtered duplicate pair.

With a better understanding of the variability of each methodology, the difference between concentrations of each species in the filtered and reference samples is then examined. Material not captured by the filter is considered "soluble", and all particulate matter is considered accurately accounted for after contact with the plasma, yielding a total concentration for reference samples. These assumptions are operationally defined, and their ramifications are explored further in the discussion. Finally, differences between reference and filtered samples are compared to differences between reference and acidified samples to better evaluate the effect of filtration on sample concentrations.

Results

Blank values

Blanks are similar for the reference and acidified methods, with all but four species having concentrations <10% of the lowest sample values. For the reference procedure, the highest blanks for Cr, Cu, Sb, and Zn had concentrations of 38%, 42%, >100% and

52% of the lowest samples, respectively. For the acidified procedure, Cr had a blank value of 14% of the lowest sample value (Table 2.1) (Figures 2.3, 2.4). By contrast, blanks for filtered samples had values >25% of the lowest sample values in the majority of species, with values <10% of low samples only for Mn, S, Sr, and U. When compared against average sample values instead of low concentrations, filtered blanks for Ca, Co, Cs, Fe, and the REE are <10%, but the remainder of elements continue to have blanks >10%. Comparing blanks to values for the insoluble particulate fraction, Bi, Cs, Fe, Mn, S, Ti, V and the REE have blanks of <10% of the lowest values, and Al, Ca, Co, Cr, Sr and U have blanks <10% of average sample values.

High blank values in filtered samples relative to the reference and acidified groups occur both because blanks put through the filtration method have higher concentrations (presumably derived from the filtration apparatus) than those for either the reference or the acidified groups, and because the non-blank filtered samples have concentrations lower than do the other groups. With the exception of Mn, S, Sr, and U, absolute values of low-concentration filtered samples represent only a rough approximation of true soluble load, because blanks, reagents, and vessels contribute a significant portion of these sample values. Because the soluble particulate fraction, however, is an order of magnitude larger in many species than is the filtered fraction, this derived value provides more significant information because blanks are relatively insignificant; in addition, the lowest sample concentrations commonly represent anomalously low values for a given element. I will therefore examine filtration for elements in which blank values are <10% of average sample values in either the filtered or the insoluble particulate fraction and for which blank values are not larger than the lowest sample value. Values for As, Cu, Pb,

a)

		Ca, Cd, S, Sr	Ba, Co, Mn, U	Al, Bi, Fe, Cr, Cs, Nd, Ti, V	As, Cu, Tl, Pb, Sb, Zn
Reference samples	high blank : low sample	<0.01 to 0.06	<0.01 to 0.01	<0.01 to 0.65	<0.01 to 1
	high blank : avg sample	<0.01 to 0.03	<0.01 to 0.04	<0.01 to 0.15	<0.01 to 0.04

b)

Acidified samples	high blank : low sample	<0.01 to 0.06	<.01 to 0.03	<0.01 to 0.13	<0.01 to 0.05
	high blank : avg sample	<0.01	<0.01	<0.01 to 0.04	<0.01 to 0.02

c)

Filtered samples	high blank : low sample	<0.01 to 1	0.05 to 0.59	0.33 to 1	0.66 to 1
	high blank : avg sample	<0.01 to 0.66	0.02 to 0.22	<0.01 to 0.76	0.34 to 0.57

d)

Insoluble particulate samples = reference value - filtrate sample value	high blank : low sample	<0.01 to 1	0.09 to 0.30	<0.01 to 0.37	1
	high blank : avg sample	<0.01 to 1	<0.01 to 0.07	<0.01 to 0.07	0.15 to 1

Table 2.1. Blank/sample ratios for a) reference, b) acidified, c) filtered, and d) insoluble particulate samples. Blanks are reported as a percentage of the lowest sample values and as a percentage of average values for four groups of elements. The first three columns of elements are grouped according to the dominance of the soluble versus the insoluble particulate fractions in each. As the table moves to the right, elements are more associated with insoluble particulate in samples. The fourth row includes elements for which blanks hinder further analysis.

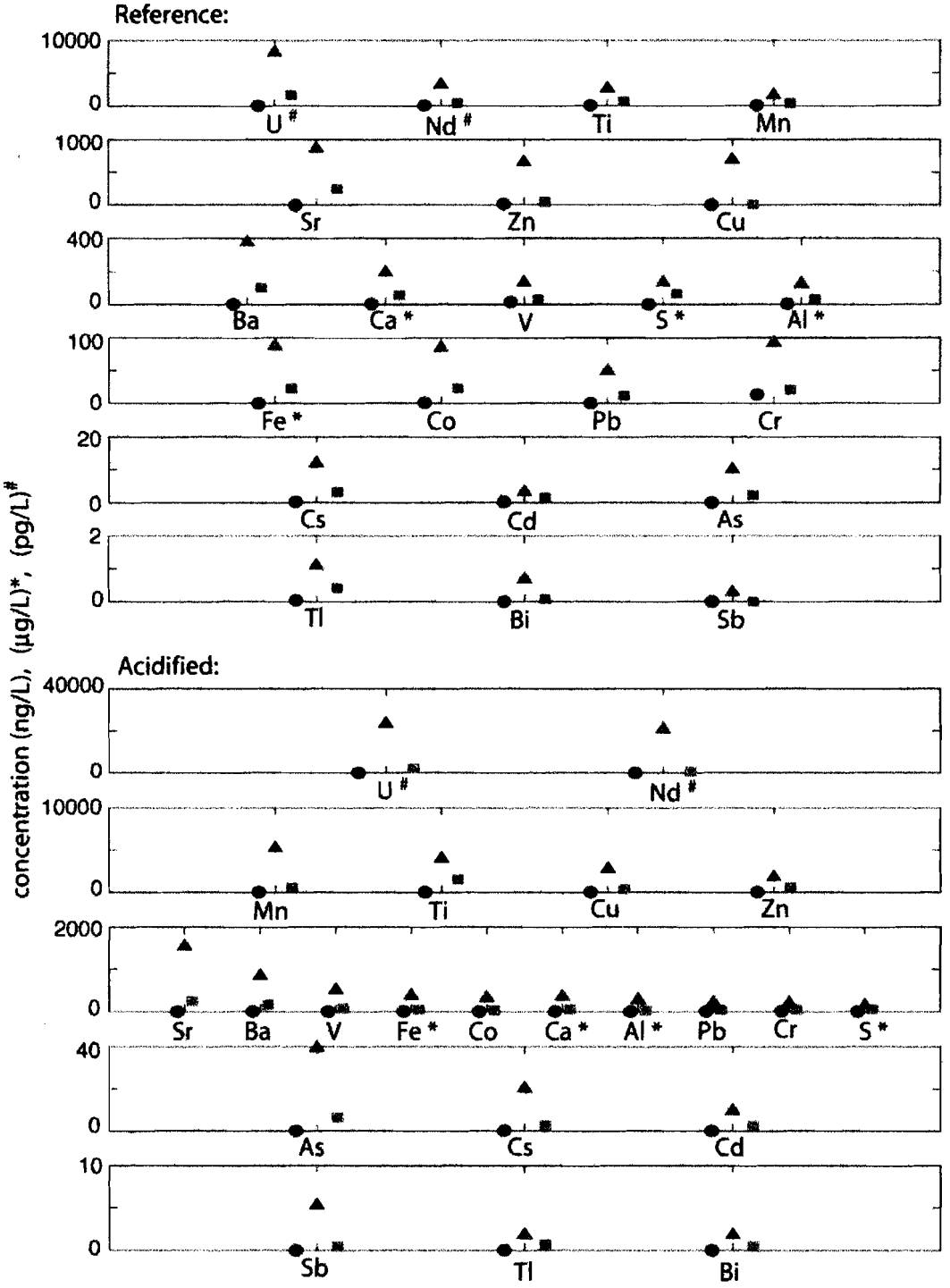

Figure 2.3. Blank values (blue circles), low sample values (green squares), and average sample values (red triangles) for "reference" samples and "acidified" samples. Note that units vary on the same line. Absolute blank values are visually compared only within each element. Also, organization of blank values in these figures is based only on the magnitude of the blanks for each element and thus varies according to which procedure is examined; in each of these figures, average sample concentrations decrease moving to the right.

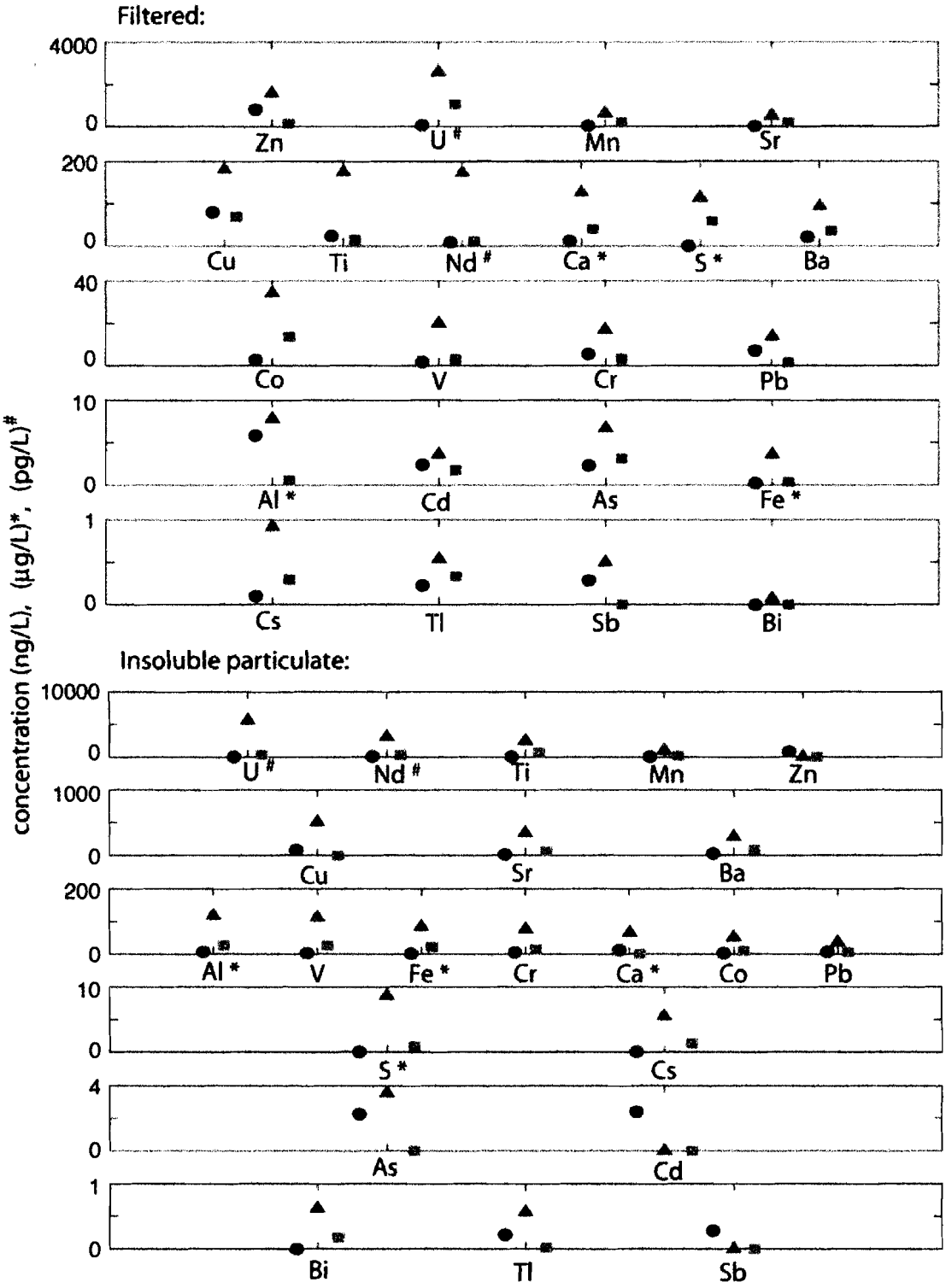

Figure 2.4. Blank values, low sample values, and average sample values for "filtered" and "insoluble particulate" samples.

Sb, Tl, and Zn do not fit these criteria; contamination for these elements is likely a product of the acid cleaning process for analysis vials, in which work is ongoing to isolate vials more thoroughly during the cleaning process. These elements will not be considered in the treatment here regarding the effects of filtration. Although Cd blank values in filtered samples also do not fit the above criteria, they are highly correlated with the reference values for this element ($R^2 = 0.79$, $p < 10^{-6}$); because reference blank values for Cd are <10% of the lowest sample value, Cd behavior will be examined further.

Duplicate samples

Of the three sample processing techniques, the acidified procedure yielded the most reproducible results, with all but three elements (Bi, Sb, Zn) having average duplicate variability <10% (Table 2.2) (Figure 2.5). Within 95% confidence bounds, values for 16 elements and the REE lie within $0.8\mu < x < 1.2\mu$, with μ being the geometric mean of the sample values. Most metals in the reference group showed an increase of between 2% and 10% in average duplicate variability relative to acidified samples. Filtered samples showed the lowest reproducibility, with a median duplicate variability of 28%. For Al, Cu, Pb, Cr, Sb, mean variability for the filtered procedure was >40%. Cs, Fe, and Tl yielded variability <16%. Examining the window within 95% confidence bounds for filtered duplicates, concentrations for 10 metals are outside the bounds of $0 < x < 2\mu$, and the lowest variability (Fe) lies within $0.71\mu < x < 1.29\mu$. When filtered duplicate variability is compared against the insoluble particulate fraction, reproducibility improves, with the majority of metals showing mean variability <15% and only 6 varying >25%. In addition, five of these 6 species – Ca, Cd, S, Sb and Zn –

a)		Ca, Cd, S, Sr	Ba, Co, Mn, U	Al, Bi, Fe, Cr, Cs, Nd, Tl, V	As, Cu, Pb, Sb, Tl, Zn
Reference samples	average variability from mean (%):	2 to 6	7 to 11	9 to 24	7 to 70
	standard deviation (%):	1 to 4	5 to 11	3 to 19	4 to 51
	95% confidence interval surrounding	$0.85\mu < x < 1.15\mu$	$0.67\mu < x < 1.33\mu$	$0.51\mu < x < 1.49\mu$	$0 < x < 2.3\mu$

b)					
Acidified samples	average variability from mean (%):	1 to 8	2 to 7	5 to 16	3 to 13
	standard deviation (%):	1 to 8	2 to 4	4 to 7	3 to 6
	95% confidence interval surrounding	$0.76\mu < x < 1.24\mu$	$0.86\mu < x < 1.14\mu$	$0.75\mu < x < 1.25\mu$	$0.78\mu < x < 1.22\mu$

c)					
Filtered samples	average variability from mean (%):	28 to 31	26 to 32	12 to 67	9 to 67
	standard deviation (%):	38 to 44	27 to 39	9 to 110	12 to 63
	95% confidence interval surrounding	$0 < x < 2.2\mu$	$0 < x < 2.1\mu$	$0 < x < 3.9\mu$	$0 < x < 2.8\mu$

d)					
Insoluble particulate	average variability from mean (%):	17 to 350	3 to 10	0 to 9	6 to 824
	standard deviation (%):	16 to 389	2 to 11	0 to 13	3 to 1391
	95% confidence interval surrounding	$0 < x < 11\mu$	$0.68\mu < x < 1.32\mu$	$0.65\mu < x < 1.35\mu$	$0 < x < 36\mu$

Table 2.2. Duplicate variability for a) reference, b) acidified, c) filtered, and d) insoluble particulate samples. Sample variability is divided into four groups of elements: The first three groups are arranged in order of decreasing sample reproducibility in the insoluble particulate fraction; the fourth includes elements with high variability in all sample methods. 95% confidence intervals are given for the element showing the highest variability in the group. All other elements in each group will have variability equal to or smaller than what is recorded here.

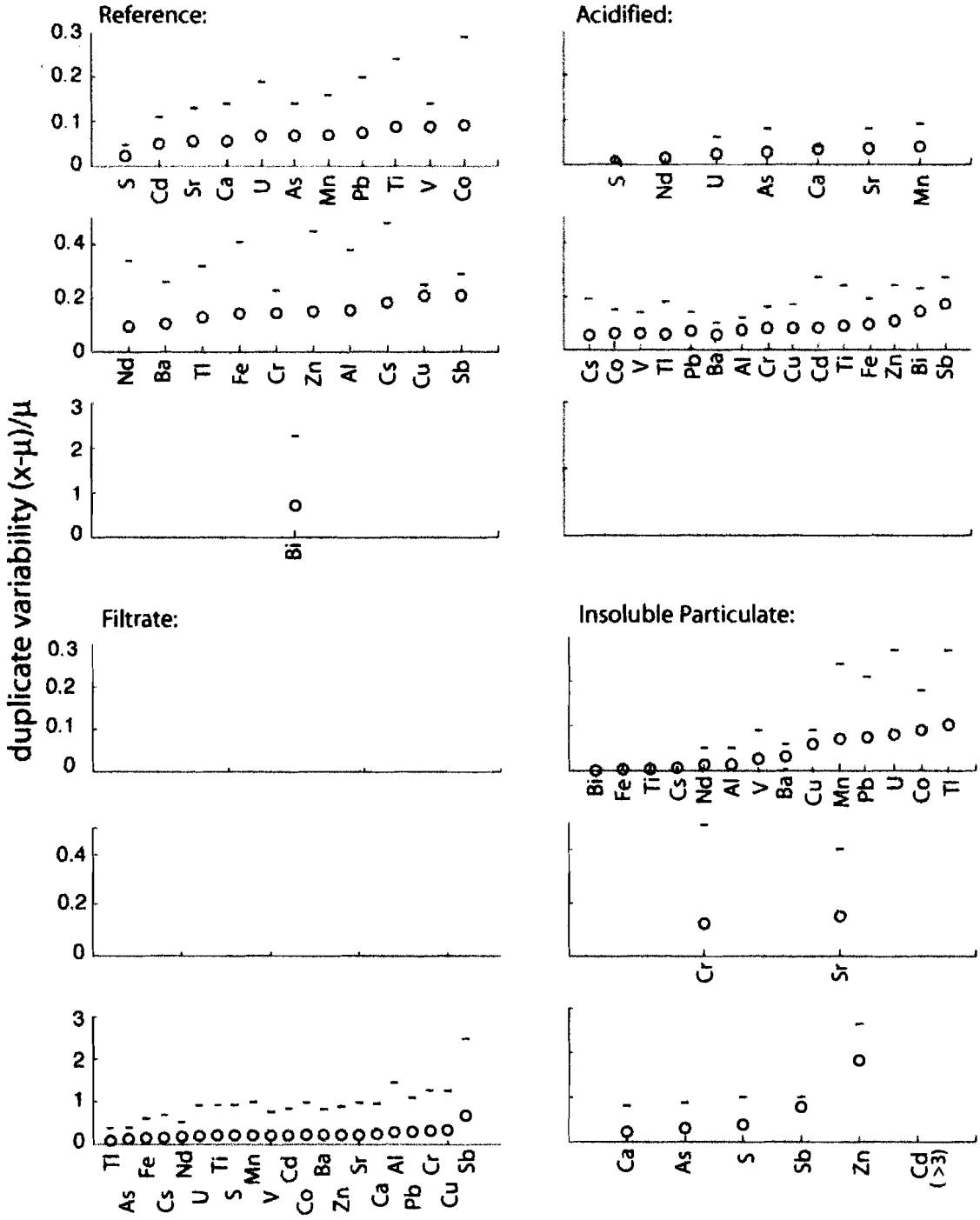

Figure 2.5. Variability for reference, acidified, filtered, and insoluble particulate samples. Substantial improvement is noted in replicate variability for the particulate fraction over that of the filtered fraction.

either contain a relatively small particulate fraction (Ca, Cd, and S, discussed below) or are associated with procedural contamination, as seen in high blank values (Sb and Zn).

Measured in absolute terms rather than as percentages, sample ranges based on variability are from 0.43 to 53 x 10^3 ng/L in reference samples, from 0.29 to 216 x 10^3 ng/L in filtered and insoluble particulate samples, and from 2.27 to 74 x 10^3 ng/L in acidified samples. In reference and acidified samples, variability measured in an absolute sense is in all cases at a minimum of 4x higher than procedural blanks. In the filtrate and particulate groups, however, the data are mixed. For some elements (e.g. Al, Fe), variability and blank values are of a similar magnitude; for others (e.g. Sr, U), variability is significantly greater than are blank values (Table 2.3).

Differences between filtered and control values

Twenty samples were processed using the reference, filtered, and acidified procedures. Of these twenty, sixteen provided data useful for comparison; three of the filters ruptured visibly during the filtering process and a fourth yielded higher values in the filtered process than in the reference process in some species, suggesting contamination during filtration. Based on examination of the intact samples, metals fall into five categories: those that are unaffected by filtration, three groups associated with lesser, moderate and greater removal in filtering, and those that are effectively removed by filtration. The first group includes Cd and S, the second Ca and Sr, the third Ba, Co, Cu, Mn, Tl, and U, the fourth Bi, Cr, Pb, and V, and the fifth Fe, Al, Cs, Ti, and the REE.

	High Blank	range of measured samples	range based on variability
Cd (ng/L)	2.38	2.97	3.09
S (μg/L)	0.00	124.62	159.32
Ca (μg/L)	11.29	285.10	215.60
Sr (ng/L)	10.32	816.88	993.71
Ba (ng/L)	20.71	104.18	56.23
Co (ng/L)	2.56	40.94	31.63
Mn (ng/L)	16.19	772.68	650.49
U (pg/L)	51.24	3437.42	2370.84
Bi (ng/L)	0	0.32	ND
Cr (ng/L)	7.51	16.42	12.47
V (ng/L)	1.58	22.46	22.87
Al (μg/L)	5.88	9.35	10.70
Cs (ng/L)	0.10	0.43	0.29
Fe (μg/L)	0.22	1.49	0.45
Nd (ng/L)	0.21	7.38	1.15
Ti (ng/L)	22.81	47.55	54.78

Table 2.3. Range of absolute variability in filtered samples for each element. This calculation is based on replicate samples compared to range of measured concentrations and to high blank values for the filtered procedure. Replicate sample values represent 95% confidence for the range in each element.

Group 1:

Cd and S -- Values for Cd and S are similar in filtered and reference samples (Table 2.4) (Figure 2.6). Concentrations for S in both procedures are more than two orders of magnitude higher than those for filtered blank samples, while filtered concentrations for Cd fall within the range of blank values. Because filtered samples are strongly correlated to control samples, as discussed above, I consider Cd values to be real; as such, Cd is not significant in the particulate fraction. The correlation between reference and filtrate samples for S is even stronger, with $R^2 = 0.88$ and $p < 10^{-9}$. Insoluble particulate makes an insignificant contribution to concentrations in these species.

Group	Element	R^2	p
1	Cd	0.79	10^{-6}
	S	0.90	10^{-9}
2	Ca	0.72	10^{-5}
	Sr	0.92	10^{-10}
3	Ba	0.28	.02
	Co	0.45	.001
	Mn	0.44	.001
	U	0.02	.53
4	Bi	0.03	.50
	Cr	0.03	.45
	V	0.32	.01
5	Al	0.03	.45
	Cs	0.03	.45
	Fe	0.10	.18
	Ti	0.39	.003
	Nd	0.00	.89

Table 2.4. Correlations between analyses of reference and filtered samples. As samples become increasingly associated with the insoluble particulate fraction (lower in the table), correlation between reference and filtered values decreases.

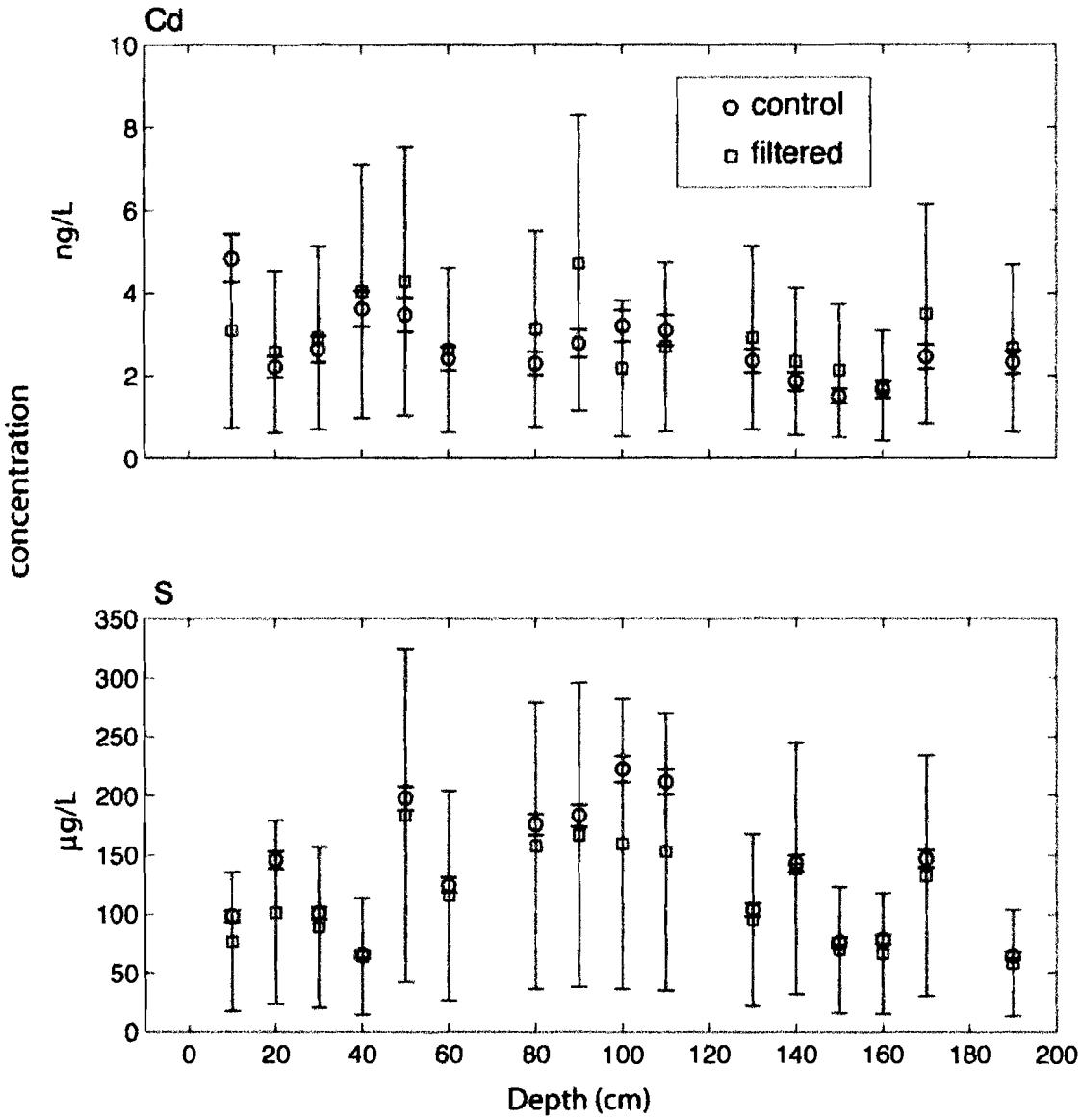

Figure 2.6. Reference and filtered concentrations for Cd and S (group 1). Error bars represent 95% confidence intervals surrounding each measurement (=2σ, based on duplicate percentage variability for each species found in three replicate samples). Note that concentrations for Cd are in given in ng/L, while S is in µg/L. Depth displayed is the depth at the top of each sample interval.

Group 2:

Ca and Sr -- Filtered concentrations consistently comprise from 34 to 98% of reference values (Figure 2.7). Correlations between reference and filtered sample concentrations ($R^2 = 0.72$ and 0.92, $p < 10^{-5}$ for both) are similar to those of Cd and S. The offset in concentrations between reference and filtered samples, however, suggests that insoluble particulate deposition accounts for a consistent portion of Ca and Sr concentrations.

Group 3:

Ba, Co, Mn, and U -- Filtered samples contain from 3% to 83% of reference sample concentrations. Correlations between filtered and reference values are lower for these elements ($0 < R^2 < 0.45$; $0.001 < p < 0.53$) than are the correlations for the elements in groups 1 and 2. In addition, the correlation between reference and filtered samples for U has low significance. Loss of significance in the correlation between the filtered and reference values increases as elements become more and more associated with the insoluble particulate fraction, suggesting that U is the most closely associated with particulates of the group 3 elements. Including only Ba, Co, Mn and Tl, correlations between reference and filtered samples are $0.28 < R^2 < 0.45$ and significances are $0.001 < p < 0.02$. Concentrations in these elements appear to have contributions in roughly equal amounts from soluble and insoluble sources.

Group 4:

Filtered concentrations for Bi, Cr, and V range from 0% to 50% of reference values, while correlation between filtered and reference samples drops to $0.03 < R^2 < 0.32$. The significance of these correlations also continues to be irregular, with

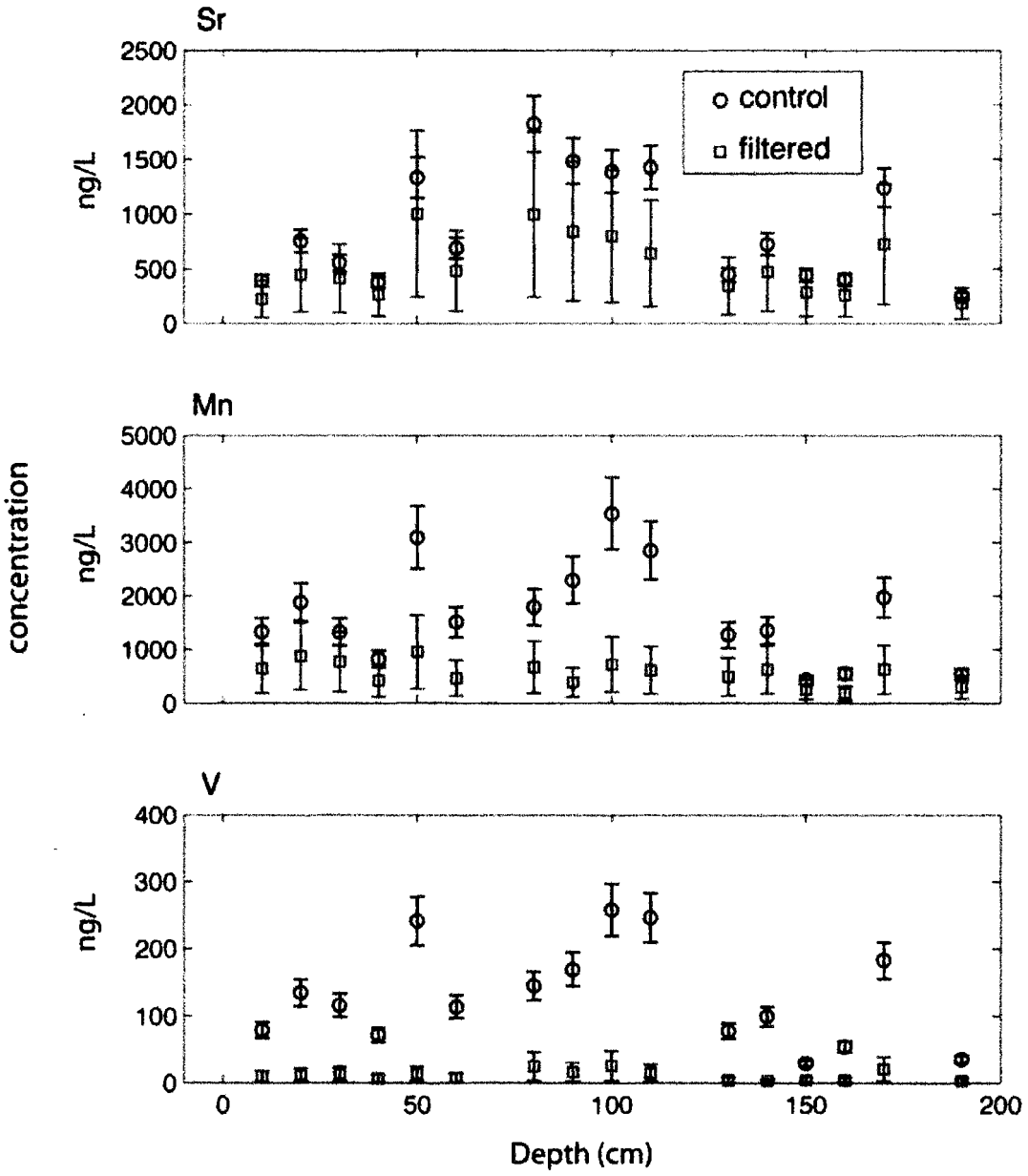

Figure 2.7. Reference and filtered concentrations for Sr, Mn, and V (representing groups 2, 3, and 4).

correlation for V yielding $p \sim 0.01$, but correlations for Bi and Cr yielding $p \sim 0.5$. The poor significance value for Bi is associated with very low filtered values, which registered negative concentrations in several samples. For group 4 elements, there appear to be only small contributions from soluble load, with the majority of concentrations associated with insoluble particulate.

Group 5:

Al, Cs, Fe, Ti, and REE – Iron provides a good reference element for this group of species. Values for Fe range from 22 to 181 μg/L for reference samples and from 0.4 to 1.8 μg/L for filtered samples (Figure 2.8). Al, Cs, and the REE in filtered and reference samples are proportional to Fe, suggesting that these elements share a common deposition mechanism. While values for filtered concentrations are as high as 16% of reference values for Al and Cs and as high as 34% for REE, these higher concentrations are still distinct from those of reference samples when compared using 95% confidence intervals for each measurement. Correlations are poor between reference and filtered values for all elements in this group. Distinction between these two procedural groupings is consistent with the expectation of a dominant particulate source.

Although the tools used for collecting these samples are made of titanium, Ti concentrations for filtered samples range from 0.014 μg/L to 0.071 μg/L while concentrations for reference samples range from 0.7 μg/L to 7.6 μg/L. Because filtered Ti values all fall within 0.060 μg of blank values, soluble Ti contamination is presumed to be negligible. Because samplers were thoroughly cleaned with DI water prior to the field season, particulate Ti contamination is thought to be unlikely, though this cannot be ruled out. As a first estimation, using titanium sampling tools leads to no appreciable

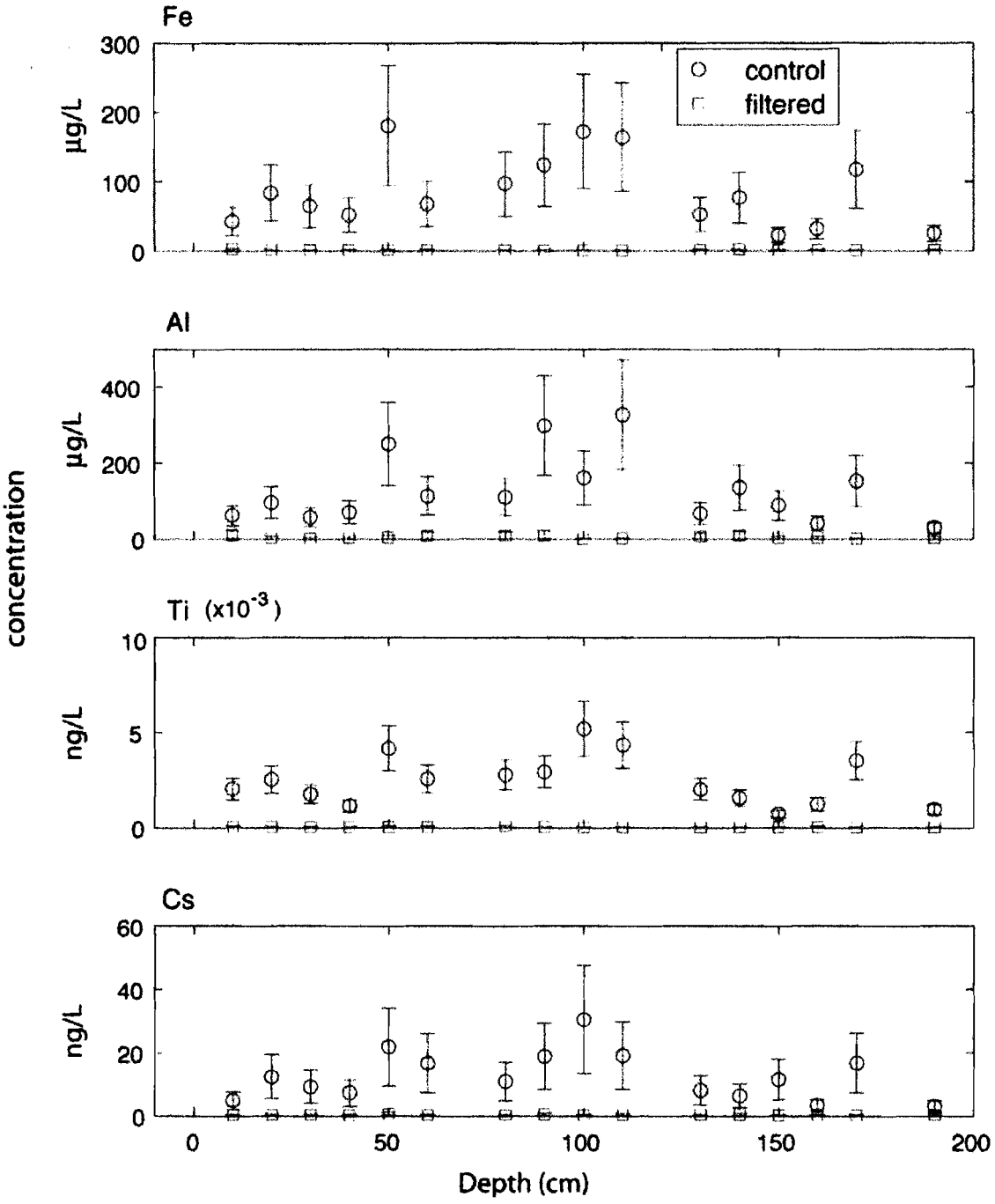

Figure 2.8. Reference and filtered concentrations for Al, Cs, Fe, and Ti (group 5). Nd concentrations (not shown) represent the REE and are similar in pattern and magnitude to those shown for these elements.

difference between the behavior of Ti and the other group 5 elements with respect to soluble and insoluble particulate partitioning.

Discussion

For filtered samples, the majority of trace metals are difficult to quantify with precision better than ~25% using the method described. For several of the elements discussed above, variability in filtered samples based on replicate sample analysis is higher than the range of concentrations for measured samples. Because variability is defined in terms of duplicate runs of the same samples, external variables such as input timing, the sources of constituents to the snow, and post-depositional alteration in the snowpack do not contribute to this uncertainty. In the absence of these variables, low sample concentrations, high contamination, inconsistent particle filtration, and low sample number (3 replicate samples used to determine variability) are possible contributors to imprecise values.

Comparing sample concentrations and relative blank concentrations to replicate variability in both the control and the filtrate case, there are no direct relationships (Figure 2.9). In addition, though high blank values and sample variability are similar in magnitude for some elements in the filtrate fraction, other elements showing equally high variability relative to sample range have insignificant blank contributions. This discrepancy dictates another source of variability in the filtration procedure.

The procedure outlined here does not address variability associated with particle sizes below 0.4 μm. In future work, multiple filter gauges will be used to capture dust of smaller size fractions. With the data here, however, one approach for estimating the

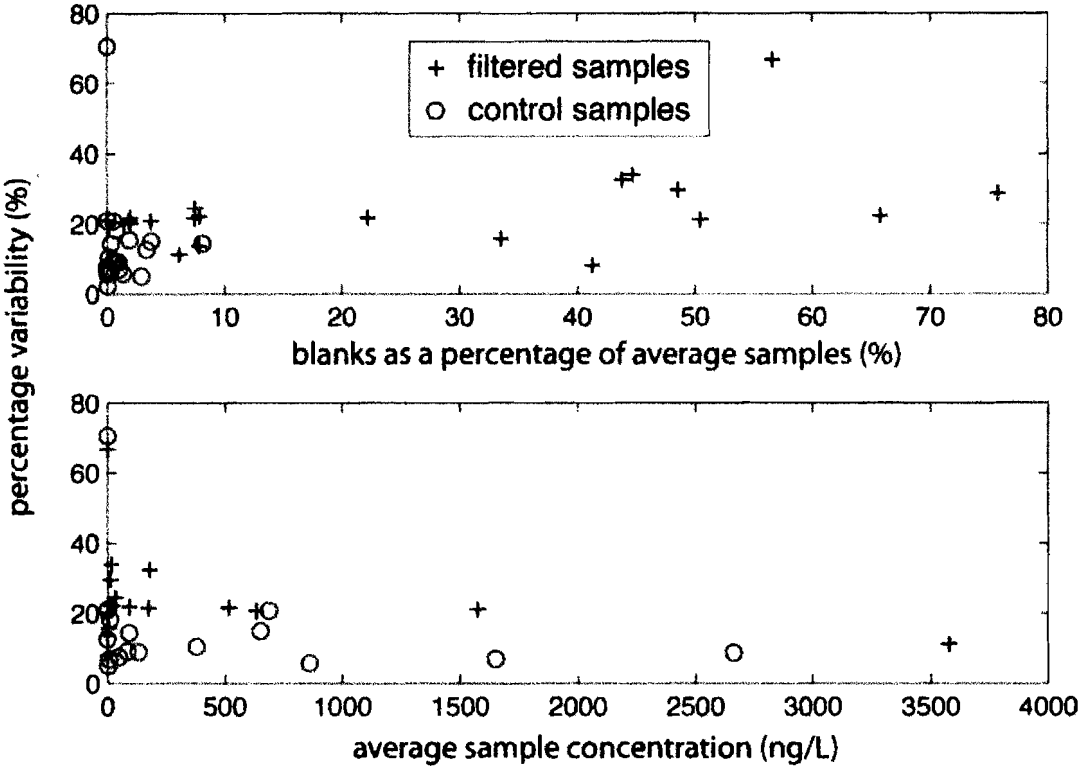

Figure 2.9. Percentage variability as a function of relative blank concentration and of absolute species concentration for filtrate and control samples. The x axis in a) represents the percentage of material represented by highest blanks relative to the average concentration of each element and in b) represents the quantity of the element present in the sample. Each '+' or 'o' represents the average for one element against the variability in that element.

effect of particles smaller than 0.4 μm is to compare the effect of filtration on sample values with the effect of acidifying samples in their original containers. If reference samples captured all soluble and insoluble particulate components of all elements, acidifying the container would in theory have no effect on sample concentrations; only in the case of S, however, is no effect noted with container acidification (Figure 2.10). For Ba, Bi, Cr, Cs, and Ti, acidification mobilized a similar magnitude of material as was captured in filtration of particles >0.4 μm, and for Cd, Fe, and U, consistently more material was released by acidification than was captured by the filter. In the case of Al, Ca, Co, Mn, Sr, and V, most of the record shows a similar magnitude of material

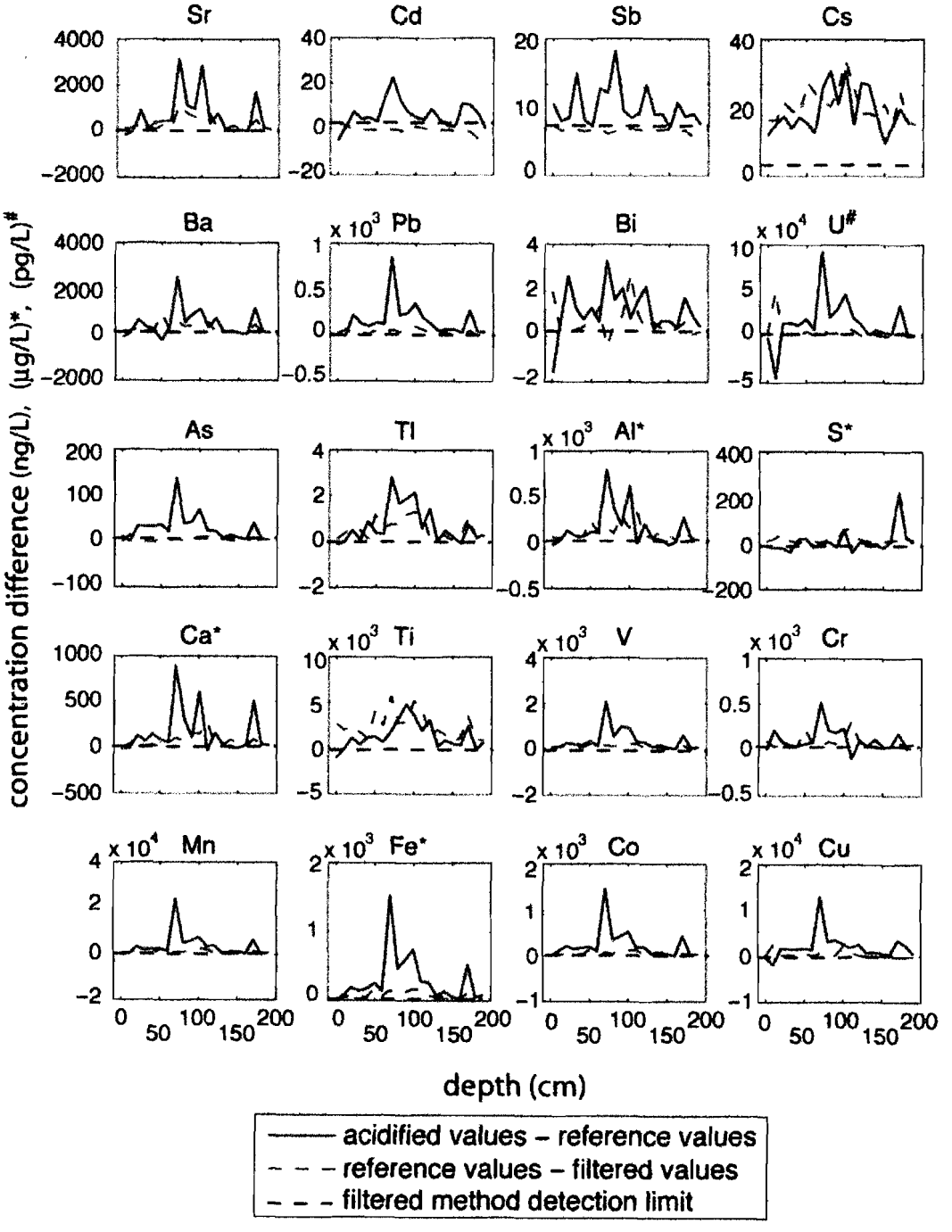

Figure 2.10. Reference samples subtracted from acidified samples compared to filtered samples subtracted from reference samples. Filtered sample values subtracted from the reference values are defined in this paper as insoluble particulate. Filtered procedure detection limits for As, Cd, Sb, and S are high enough to interfere with insoluble particulate measurements, as discussed in the Blanks section.

mobilized by acid as was captured by filtration, but there are samples for which acidification releases far more material than filtration removes. All samples were drawn after 24 hours of contact with HNO_3, so the impact of shorter or longer acidification times was not examined in this procedure; in continuing studies, this variable will also be included.

The source of additional material in acidified containers is not well constrained. First, 1% HNO_3 is adequate to rapidly dissolve some minerals (e.g. carbonates), but others (e.g. framework silicates) are more resistant to this treatment. Second, because acidification simultaneously attacks all particles, distinguishing the relative amount drawn from particles >0.4 μm would require knowledge of an initial population. On a qualitative visual basis, noticeably fewer and smaller particles occurred in acidified samples than in reference samples.

A conceptual view of this process demonstrates locations where material is contained in a hypothetical sample (Figure 2.11). Sekaly et al. [1999] concluded that in the absence of acidification, significant amounts of dissolved (<0.45 μm) Cu, Pb, Cd and Al are trapped in polypropylene containers after filtration and over time periods as short as 30 minutes. After 2 hours, they found 15% of dissolved (i.e. post-filtration) Pb, 25% of dissolved Cu and 20% of dissolved Cd were bound to the polypropylene and not available for measurement [*Sekaly et al.*, 1999]. In my procedure, this material would not have been available in either the reference or the filtered samples (because the original sample container was not acidified), explaining one portion of the increase in acidified samples. Also, in addition to remobilizing this material adsorbed to the container walls,

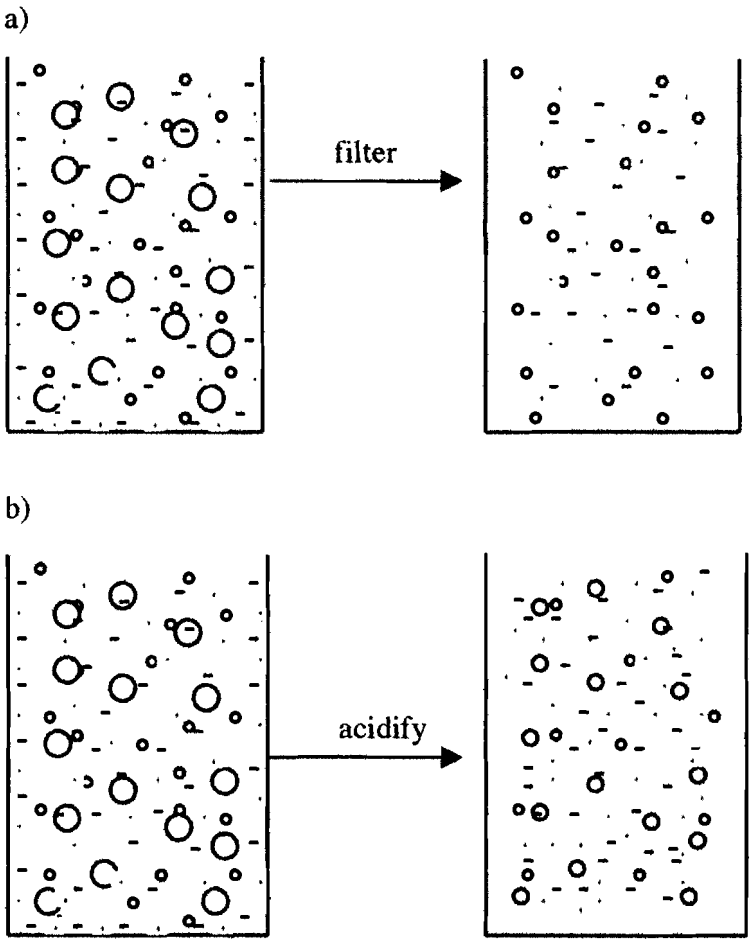

Figure 2.11. Conceptual framework describing acid mobilization of species compared to particulate capture through filtration. On the left in both a) and b) is the same sample container. On the right in a) is the filtrate, now containing none of the material bound to the material of the original container and none of the large particulate matter. On the right in b) is the acidified sample, with the dissolved material from the sides of the original container now in the dissolved matrix, and with both larger and smaller particles having been decreased in size or totally dissolved by acid, thereby also increasing the dissolved load in the liquid. The samples on the right are measured in ICP-MS analysis.

unlike the above study, I added acid to unfiltered samples; as a result of this procedure, material from particulate of all sizes would be mobilized.

Small sample size also plays a role in high sample variability. Of the 3 samples for which replicate variability is calculated, two have far lower variability than the final mean value. One sample with particularly high variability, however, has a disproportionate influence on mean variability (Table 2.5). Other investigators with promising levels of reproducibility in longer datasets for trace metal measurement have witnessed individual sections of the data where agreement in their replicate runs has been equally divergent as the poorest replicate run reported here [*Knusel et al.*, 2003]. With significantly longer replicate datasets, however, these anomalous values were witnessed as isolated events rather than defining values.

Even in these more reliably duplicated trace metal datasets, difficulties remain in accurately determining both the filtered and insoluble particulate fractions. Investigators developing techniques for measurement of trace metals in ice cores have found that methods of ice preparation affect concentrations of Al, La, U, V, Fe, As, Rb, Cd, Sb, Cs, Ba, Ce, Pr, Nd, Sm, Pb, Bi, and Th [*Knusel et al.*, 2003]. Knusel et al. [2003] examined consolidated ice (ρ = 0.88 to 0.9 g/cc), and compared a continuous melter system to a discrete sampling system with the outer section removed by manual scraping with a clean scalpel. The discrete sampling method consistently yielded higher values for the elements in the above list. They concluded that the lack of contact with acid during their continuous melting procedure until after melting and contact with a portion of capillary tubing most likely accounted for the differences, and believed the material they had

sample #	97	97d	100	100d	108	108d
S (μg/L)	157.74	48.12	152.75	181.47	58.42	57.39
Cd (ng/L)	3.13	0.97	2.70	3.44	2.67	2.56
Ca (μg/L)	224.96	76.70	144.72	181.85	39.53	40.58
Sr (ng/L)	994.52	311.06	641.40	798.21	184.55	189.95
Ba (ng/L)	64.50	26.75	47.01	70.14	35.03	37.97
Co (ng/L)	29.95	9.86	33.01	47.97	13.63	14.82
Mn (ng/L)	671.31	226.68	613.32	777.96	297.41	301.28
U (pg/L)	2489.62	877.54	2368.34	3017.02	1039.46	1047.92
Bi(ng/L)	0.00	0.00	0.00	0.00	0.00	0.00
Cr (ng/L)	7.72	2.13	5.93	6.08	5.09	12.96
V (ng/L)	24.57	9.24	14.81	22.20	3.39	3.44
Al (μg/L)	8.19	0.95	0.91	0.89	3.18	2.82
Cs (ng/L)	0.43	0.22	0.46	0.50	0.42	0.38
Fe (μg/L)	0.83	0.58	0.44	0.42	0.91	1.17
Ti (ng/L)	61.64	23.62	16.32	18.35	19.57	25.85
Nd (ng/L)	0.77	0.45	0.46	0.36	2.85	2.03

Table 2.5. Values for three duplicate filtered samples. The duplicates for samples 100 and 108 are roughly equal, but sample 97 is highly variable.

difficulty measuring was associated with the particulate fraction [*Knusel et al.*, 2003]. The work presented here supports this conclusion, as most of the elements in this list are associated either with a sizeable particulate fraction or with replicate sample difficulties in Victoria Upper Glacier snow and firn.

In summary, I can trace a large portion of the variability associated with the procedure outlined here to a lack of information about the total load in each sample, including soluble and insoluble particulate fractions. To approach this value for total load more accurately, plans for continuing work include replacing the HNO_3 acidification step in the procedure outlined here with HF microwave digestion. With this information, I will be in a position to form three equations for the three unknowns -- large particulate (>0.4) (L), small particulate (S) and filtered soluble load (F):

$$\text{HF Digestion Value} = L + S + F$$

$$\text{Control Value} = L + S + f(F)$$

$$\text{Filtered Value} = S + f(F)$$

where f is the fraction of the filtrate load not lost to the material of the container in the absence of acidification. In addition to this modification, further work is planned to refine understanding of the error internal to ICP-MS measurement of high-particulate samples. Preliminary results based on running the same acidified sample 5 times on the ICP-MS suggest that values remain fairly consistent over time, but a higher number of samples and a variety of sample conditions will improve understanding of the amount of variability to be expected from interactions between the plasma of the ICP and particles suspended in samples. The work presented here provides a reasonable estimate of particulate values >0.4 μm for samples from a site characterized by high particulate load; HF digestion, multiple filtering steps using progressively finer membranes, varying acification times, and a greater number of ICP-MS test runs will provide the information required to further distinguish between particulate fraction and the dissolved load in further analyses. This, in turn, will allow a better understanding of the relationship between local insoluble particulate versus marine soluble input in Dry Valleys climate records.

Finally, although the finer fraction of material is hard to quantify using this method, the large amount of material accounted for in the insoluble particulate >0.4 μm provides substantial information even in the absence of a perfect understanding of filtered concentrations. The insoluble particulate fraction described here demonstrates that significant portions of the metals present in snow and firn at this site are contained in >0.4 μm particulates. Filtering removes an average of 82% of Al, Co, Cs, Fe, Mn, Ti, U, V and the REE, ranging from 17% of U in low particulate samples to ~100% of Al, Fe, Ti and REE in high particulate samples. Replicate sample variability in these insoluble

particulate concentrations averages less than 10% for Al, Cs, Fe, Ti, V and the REE and 15% or less for Co, Mn, and U. Likewise, blank values are < 10% of average samples. Conversely, values for filtered Ca, Cd, S and Sr are similar to those of reference values. These elements are either filtered very little (Ca and Sr) or filtered not at all (Cd and S) at the 0.4 μm level. While variability for these measurements is higher (21%, 22%, 21% and 22%, respectively), I believe that the strength of correlations between filtered and reference samples combined with statistically identical values at 95% significance justifies the conclusion that deposition for these elements occurs predominantly in either dissolved or soluble particulate form.

Conclusions

Absolute concentrations for Al, Ba, Ca, Cd, Cs, Co, Cr, Fe, Mn, S, Sr, Ti, U, V, and the REE after filtration with a 0.4 μm filter and acidification of the analysis vial are precise to a median ±28%. Duplicate variability for Al, Cd, Co, Mn, and S -- within 95% confidence intervals -- is higher than the range of concentrations among measured samples. Acidification of samples in the original container accounts for an amount equal to the large particulate fraction in most species, and accounts for more for Cd, Fe, and U. Acidification also provides better reproducibility than do filtrate samples, with duplicate samples in the majority of elements having <15% variability. Given greater confidence in the results associated with acidification, further exploration of acidification and digestion techniques using HF for samples with high particulate load, where contamination introduced by laboratory procedures is not likely to be significant, is warranted.

Filtering using a 0.4 μm filter removes statistically significant amounts of several trace metals analyzed from snow and firn samples from the Victoria Upper Glacier. For Al, Co, Cs, Fe, Mn, Ti, U, V and the REE, an average 82% of sample concentration in a given species was present in insoluble particulate form >0.4 μm. The particulate contribution to total concentration ranged from 17% to 100%. Reproducibility is better than 10% for calculated particulate concentrations of Al, Cs, Fe, Ti, V and the REE, and is 15% or less for Co, Mn and U. Cd and S are not statistically different in filtrate and control samples. Ca and Sr are dominantly present in dissolved form; the particulate component is as low as 2% in some samples.

This analysis demonstrates two important concepts in relation to future study of trace metals in ice and snow. First, at the Victoria Upper Glacier, mobilization of several insoluble trace metals (iron in particular being of interest to several communities) is enhanced dramatically in the presence of winds capable of transporting particle sizes >0.4 μm. In the absence of this particle source, iron input reaches levels approaching measurement blanks. This may provide another criterion along with the results of chapter 1 for discriminating between regional onshore-offshore flow and katabatic flow events. The results here, combined with the results of Knusel et al. [2003], however, show that accurate simultaneous measurement of both insoluble particulate and the soluble fraction of trace metals still requires refinement.

Secondly, while many trace metals are primarily associated with insoluble particulate deposition, Cd and S occur in a soluble mode. This makes them a potential indicator of soluble metal load as opposed to insoluble particulate metal load. Further efforts to decrease replicate variability and to further isolate sample values from blank

values for these elements may provide valuable information to better refine our understanding of trace metal dynamics in Antarctica.

CONCLUSIONS

Although high particulate loads provide challenges for interpretation of snow and ice records in the McMurdo Dry Valleys, determination of local as opposed to marine input can help to unravel these complexities. Here I have examined two different approaches to isolating local aerosol input from broader climate signatures. The first chapter shows that differing local-scale (10^2 to 10^4 meter) exposures to soil and marine aerosols play a significant role in determining chemistry signatures in Dry Valleys glaciers. Based on these results, work on samples representing times of low insoluble particulate input likely will provide the most promising avenue for cataloging "purely" marine climate signals regionally. These relatively dust-free samples can then be compared to regional climate signals to examine how the Dry Valleys fits into the broader context of Antarctic atmospheric chemistry. Samples with high particulate input, on the other hand, will provide the best proxies for historical local-scale processes, including katabatic winds, in the valleys.

In the second chapter, physical filtration yields results isolating the local large-particulate fraction of a number of elements; in some samples, filtration removes virtually all Al, Co, Cs, Fe, Mn, Ti, U, V and the REE. Using the methodology described here, I am still unable to determine the smaller sized but soluble fraction of these materials with precision better than 25%, but more thorough acidification schemes should help lower this value in future efforts. Even mild acidification showed promise here for realizing more consistent results than possible without acid.

Additional work will continue to build on the data presented here. Particulate matter captured during filtration, for example, will be analyzed for chemical and mineralogical composition and compared to soil samples collected as part of the 2004 field season. Additional snow and firn samples will also be used for particle size analysis to better constrain transport distance and direction. Both of these sets of samples will also be compared to maps of regional geology to tie material at these sites to regional source areas where possible. Deeper cores collected from the Clark, Commonwealth and Victoria Upper Glaciers will enable examination of climate regimes from the deeper past at these sites. I will continue to use and refine the methods outlined here in my analysis and interpretation of these deeper samples. Samples will also be compared to meteorology derived from automatic weather stations in place at the Clark and Commonwealth glaciers from November, 2004 to November, 2005. As this process moves forward, confidence in interpreting the meaning of data from these relatively dusty sites will improve, increasing our understanding of historical Antarctic coastal chemistry transfers.

REFERENCES

Abollino, O., M. Aceto, C.L. Gioia, C. Sarzanini, and E. Mentasti, Spatial and seasonal variations of major, minor and trace elements in Antarctic seawater. Chemometric investigation of variable and site correlations, *Advances in Environmental Research, 6*, 29-43, 2001.

Abollino, O., M. Aceto, G. Sacchero, C. Sarzanini, and E. Mentasti, Determination of copper, cadmium, iron, manganese, nickel and zinc in Antarctic sea water. Comparison of electorchemical and spectroscopic procedures, *Analytica Chimica Acta, 305*, 200-206, 1995.

Armienti, P., M. Tamponi, and M. Pompilio, Sand provenance from major and trace element analyses of bulk rock and sand grains from CRP2/2A, Victoria Land Basin, Antarctica, *Terra Antarctica, 8* (4), 569-582, 2001.

Augustin, L., C. Barbante, P.R.F. Barnes, J.M. Barnola, M. Bigler, E. Castellano, O. Cattani, J. Chappellaz, D. Dahl-Jensen, B. Delmonte, G. Dreyfus, G. Durand, S. Falourd, H. Fischer, J. Flueckiger, M.E. Hansson, P. Huybrechts, G. Jugie, S.J. Johnsen, J. Jouzel, P. Kaufmann, J. Kipfstuhl, F. Lambert, V.Y. Lipenkov, G.C. Littot, A. Longinelli, R. Lorrain, V. Maggi, V. Masson-Delmotte, H. Miller, R. Mulvaney, J. Oerlemans, H. Oerter, G. Orombelli, F. Parrenin, D.A. Peel, J.R. Petit, D. Raynaud, C. Ritz, U. Ruth, J. Schwander, U. Siegenthaler, R. Souchez, B. Stauffer, J.P. Steffensen, B. Stenni, T.F. Stocker, I.E. Tabacco, R. Udisti, R.S.W. VanDeWal, M. VanDeBroeke, J. Weiss, F. Wilhelms, J.G. Winther, E.W. Wolff, and M. Zucchelli, Eight glacial cycles from an Antarctic ice core, *Nature, 429* (6992), 623-628, 2004.

Bao, H., D.O. Campbell, J.G. Bockheim, and M.H. Thiemens, Origins of sulphate in Antarctic dry-valley soils as deduced from anomalous 17-O compositions, *Nature, 407*, 499-502, 2000.

Basile, I., E.G. Grousset, M. Revel, J.R. Petit, P.E. Biscaye, and N.I. Barkov, Patagonian origin of glacial dust deposited in East Antarctica (Vostok and Dome C) during glacial stages 2, 4 and 6, *Earth and Planetary Science Letters, 146*, 573-589, 1997.

Bertler, N., P.A. Mayewski, A. Aristrain, P. Barrett, S. Becagli, R. Bernardo, S. Bo, X. C., M. Curran, Q. D., D. Dixon, F. Ferron, H. Fischer, M. Frey, M. Frezzotti, F. Fundel, C. Genthon, R. Gragnani, G. Hamilton, M. Handley, S. Hong, E. Isaksson, K. J., R. J., K. Kamiyama, S. Kanamori, E. Karkas, L. Karlof, S. Kaspari, K. Kreutz, A. Kurbatov, E. Meyerson, Y. Ming, Z. M., H. Motoyama, R. Mulvaney, H. Oerter, E. Osterberg, M. Proposito, A. Pyne, U. Ruth, J. Simoes, B. Smith, S. Sneed, K. Teinila, F. Traufetter, R. Udisti, A. Virkkula, O. Watanabe, B. Williamson, J.-G. Winther, L. Y., E. Wolff, L. Z., and A. Zielinski, Snow Chemistry across Antarctica, *Annals of Glaciology, 41*, 167-179, 2005.

Bertler, N.A.N., P.J. Barrett, P.A. Mayewski, R.L. Fogt, K.J. Kreutz, and J. Shulmeister, El Nino suppresses Antarctic warming, *Geophysical Research Letters*, *31* (L15207), doi:10.1029/2004GL020749, 2004*a*.

Bertler, N.A.N., P.A. Mayewski, P.J. Barrett, S.B. Sneed, M.J. Handley, and K.J. Kreutz, Monsoonal Circulation of the McMurdo Dry Valleys, Ross Sea region, Antarctica: signal from the snow chemistry, *Annals of Glaciology*, *39*, 139-145, 2004*b*.

Bonnet, S., and C. Guieu, Dissolution of atmospheric iron in seawater, *Geophysical Research Letters*, *31* (3), DOI: 03310.01029/02003GL018423, 2004.

Bockheim, J.G., Properties and Classification of Cold Desert Soils from Antarctica, *Soil Science Society of America Journal*, *61*, 224-231, 1997.

Bockheim, J.G., Landform and soil development in the McMurdo dry valleys, Antarctica; a regional synthesis, *Arctic, Antarctic and Alpine Research*, *34* (3), 308-317, 2002.

Boutron, C., and C. Lorius, Trace metals in Antarctic snows since 1914, *nature*, *277*, 551-554, 1979.

Boutron, C., and S. Martin, Sources of twelve trace metals in Antarctic snows determined by principal components analysis, *Journal of Geophysical Research*, *85* (C10), 5631-5638, 1980.

Boutron, C., Atmospheric trace metals in the snow layers deposited at the South Pole from 1928 to 1977, *Atmospheric Environment*, *16* (10), 2451-2459, 1982.

Buessler, K.O., J.E. Andrews, S.M. Pike, and M.A. Charette, The effects of iron fertilization on carbon sequestration in the Southern Ocean, *Science*, *304*, 414-417, 2004.

Claridge, G.G.C., and I.B. Campbell, The salts in Antarctic soils, their distribution and relationship to soil processes, *Soil Science*, *123* (6), 377-384, 1977.

Crozaz, G., C.C.L. Jr, and E. Picciotto, Artificial radioactivity reference horizons in Greenland firn, *Earth and Planetary Science Letters*, *1* (1), 42-48, 1966.

Curran, M.A.J., A.S. Palmer, T.D.v. Ommen, V.I. Morgan, K.L. Phillips, A.A. McMorrow, and P.A. Mayewski, Post-depositional movement of methanesulfonic acid at Law Dome, Antarctica, and the influence of accumulation rate, *Annals of Glaciology*, *35*, 333-339, 2002.

Cullers, R.L., and V.N. Podkovyrov, The source and origin of terrigenous sedimentary rocks in the Mesoproterozoic UI Group, southeastern Russia, *Precambrian Research*, *117* (3-4), 157-183, 2002.

Dansgaard, W., Stable isotopes in precipitation, *TELLUS*, *16*, 436-468, 1964.

deBaar, H.J.W., J.T.M. deJong, D.C.E. Bakker, B.M. Loscher, C. Veth, U. Bathmann, and V. Smetacek, Importance of iron for plankton blooms and carbon dioxide drawdown in the Southern Ocean, *Nature*, *373*, 412-415, 1995.

DeCarlo, E.H., and W.J. Green, Rare earth elements in the water column of Lake Vanda, McMurdo dry valleys, Antarctica, *Geochimica et Cosmochimica Acta*, *66* (8), 1323-1333, 2002.

Dick, A.L., and D.A. Peel, Trace Elements in Antarctic air and snowfall, *Annals of Glaciology*, *7*, 12-19, 1985.

Dixon, D., P.A. Mayewski, S. Kaspari, K. Kreutz, G. Hamilton, K. Maasch, S.B. Sneed, and M.J. Handley, A 200 year sulfate record from 16 Antarctic ice cores and associations with Southern Ocean sea-ice extent, *Annals of Glaciology*, *41* (1), 155-166, 2005.

Dixon, D.A., P.A. Mayewski, S. Kaspari, S.B. Sneed, and M. Handley, A 200 year sub-annual record of sulfate in West Antarctica, from 16 ice cores, *Annals of Glaciology*, *39*, 545-556, 2004.

Doran, P.T., C.P. McKay, G.D. Clow, G.L. Dana, A.G. Fountain, T. Nylen, and W.B. Lyons, Valley floor climate observations from the McMurdo dry valleys, Antarctica, *Journal of Geophysical Research*, *107* (D24), doi:10.1029/2001JD002045, 2002.

Edwards, R., and P. Sedwick, Iron in East Antarctic snow: Implications for atmospheric iron deposition and algal production in Antarctic waters, *Geophysical Research Letters*, *28* (20), 3907-3910, 2001.

Edwards, R., P.N. Sedwick, V. Morgan, C.F. Boutron, and S. Hong, Iron in ice cores from Law Dome, East Antarctica: implications for past deposition of aerosol iron, *Annals of Glaciology*, *27*, 365-370, 1998.

Fountain, A.G., Mass Balance Stake Data for Commonwealth Glacier, 2005.

Fountain, A.G., Lake Brownworth Meteorological Station Measurements, *knb-lter-mcm.7005.1*, 2006.

Gao, Y., S.M. Fan, and J.L. Sarmiento, Aeolian iron input to the ocean through precipitation scavenging: A modeling perspective and its implication for natural iron fertilization in the ocean, *Journal of Geophysical Research, 108* (7), DOI: 10.1029/2002JD002420, 2003.

Garbarino, J.R., E. Snyder-Conn, T.J. Leiker, and G.L. Hoffman, Contaminants in arctic snow collected over northwest Alaskan sea ice, *Water, Air and Soil Pollution, 139*, 183-214, 2002.

Gaspari, V., C. Barbante, G. Cozzi, and P. Cescon, Temporal variability of iron and other bioactive trace elements in Antarctic continental ice, *Terra Antarctica Reports, 8*, 33-36, 2003.

Ghosh, P., S.K. Bhattacharya, A.M. Dayal, J.R. Trivedi, M. Ebihara, M.M. Sarin, and A. Chakrabarti, Trace element and isotopic studies of Permo-Carboniferous carbonate nodules from Talchir sediments of peninsular India: Environmental and provenance implications, *Proceedings of the Indian Academy of Science – Earth and Planetary Sciences, 111* (2), 87-101, 2002.

Gooseff, M.N., J.E. Barrett, P.T. Doran, A.G. Fountain, W.B. Lyons, A.N. Parsons, D.L. Porazinska, R.A. Virginia, and D.H. Wall, Snow-patch influence on soil biogeochemical processes and invertebrate distribution in the McMurdo dry valleys, Antarctica, *Arctic, Antarctic and Alpine Research, 35* (1), 91-99, 2003.

Green, W.J., B.R. Stage, A. Preston, S. Wagers, J. Shacat, and S. Newell, Geochemical processes in the Onyx River, Wright Valley, Antarctica: major ions, nutrients, trace metals, *Geochimica et Cosmochimica Acta, 69* (4), 839-850, 2005.

Grootes, P.M., M. Stuiver, L.G. Thompson, and E.M. Thompson, Oxygen isotope changes in tropical ice, Quelccaya, Peru, *Journal of Geophysical Research, 94* (D1), 1187-1194, 1989.

Guerzoni, S., R. Lenaz, G. Quarantotto, M. Taviani, G. Rampazzo, M.C. Facchini, and S. Fuzzi, Geochemistry of airborne particles from the lower troposphere of Terra Nova Bay, Antarctica, *Tellus, Series B: Chemical and Physical Meteorology, 44* (4), 304-310, 1992.

Hall, B.L., and G.H. Denton, Surficial geology and geomorphology of eastern and central Wright Valley, Antarctica, *Geomorphology, 64* (1-2), 25-65, 2005.

Hall, B.L., G.H. Denton, and C.H. Hendy, Evidence from Taylor Valley for a grounded ice sheet in the Ross Sea, Antarctica, *Geografiska Annaler, 82A* (2-3), 275-303, 2000.

Hall, B.L., G.H. Denton, B. Overturf, and C.H. Hendy, Glacial Lake Victoria, a high-level Antarctic lake inferred from lacustrine deposits in Victoria Valley, *Journal of Quaternary Science*, *17* (7), 697-706, 2002.

Hinkley, T.K., and A. Matsumoto, Atmospheric regime of dust and salt through 75,000 years of Taylor Dome ice core: Refinement by measurement of major, minor, and trace metal suites, *Journal of Geophysical Research*, *106* (D16), 18487-18493, 2001.

Johnsen, S.J., Stable isotope homogenization of polar firn and ice, isotopes and impurities in snow and ice, *IAHS Publ.*, *118*, 210-219, 1977.

Jouzel, J., R.B. Alley, K.M. Cuffey, W. Dansgaard, P. Grootes, G. Hoffman, S.J. Johnsen, R.D. Koster, D. Peel, C.A. Shuman, M. Stievenard, M. Stuiver, and J. White, Validity of the temperature reconstruction from water isotopes in ice cores, *Journal of Geophysical Research*, *102* (C12), 26471-26487, 1997.

Jouzel, J., L. Merlivat, and C. Lorius, Deuterium excess in an East Antarctic ice core suggests higher relative humidity at the oceanic surface during the last glacial maximum, *Nature*, *299*, 688-691, 1982.

Keys, J.R., and K. Williams, Origin of crystalline, cold desert salts in the McMurdo region, Antarctica, *Geochimica et Cosmochimica Acta*, *45*, 2299-2309, 1981.

King, J.C., and J. Turner, *Antarctic Meteorology and Climatology*, 409 pp., Cambridge University Press, New York, 1997.

Knusel, S., D.E. Piguet, M. Schwikowski, and H.W. Gaggeler, Accuracy of Continuous Ice-Core Trace-Element Analysis by Inductively Coupled Plasma Sector Field Mass Spectrometry, *Environmental Science and Technology*, *37*, 2267-2273, 2003.

Kreutz, K., and P.A. Mayewski, Spatial variability of Antarctic surface snow glaciochemistry: implications for palaeoatmospheric circulation reconstructions, *Antarctic Science*, *11* (1), 105-118, 1999.

Kreutz, K.J., P.A. Mayewski, L.D. Meeker, M.S. Twickler, S.I. Whitlow, and I.P. Pittalwala, Bipolar changes in atmospheric circulation during the Little Ice Age, *Science*, *271*, 1294-1296, 1997.

Kreutz, K.J., and P.A. Mayewski, Grant Proposal: Dry Valleys Late Holocene Climate Variability, *NSF*, *02-086*, 2002.

Kreutz, K.J., P.A. Mayewski, I.I. Pittalwala, L.D. Meeker, M.S. Twickler, and S.I. Whitlow, Sea level pressure variability in the Amundsen Sea region inferred from a West Antarctic glaciochemical record, *Journal of Geophysical Research, 105* (D3), 4047-4059, 2000.

Kreutz, K.J., and E.R. Sholkovitz, Major element, rare earth element, and sulfur isotopic composition of a high-elevation firn core: Sources and transport of mineral dust in central Asia, *Geochemistry, Geophysics, Geosystems, 1*, Paper #2000GC000082, 2000.

Lancaster, N., Flux of eolian sediment in the McMurdo dry valleys, Antarctica; a preliminary assessment, *Arctic, Antarctic, and Alpine Research, 34* (3), 318-323, 2002.

Legrand, M., and R.J. Delmas, The ionic balance of antarctic snow: A 10-year detailed record, *Atmospheric Environment, 18*, 1867-1874, 1984.

Legrand, M.R., and R.J. Delmas, Formation of HCl in the Antarctic atmosphere, *Journal of Geophysical Research, 93* (D6), 7153-7168, 1988.

Legrand, M., and P.A. Mayewski, Glaciochemistry of polar ice cores: a review, *Reviews of Geophysics, 35* (3), 219-243, 1997.

Legrand, M.R., and R.J. Delmas, Spatial variations of snow chemistry in Adelie Land, *Annals of Glaciology, 7*, 20-25, 1985.

Liston, G.E., J. Winther, O. Bruland, H. Elvehøy, and K. Sand, Below-surface ice melt on the coastal Antarctic ice sheet, *Journal of Glaciology, 45* (150), 273-285, 1999.

LTER, LTER Project Overview, 2005.

Lyons, W.B., K.A. Welch, A.G. Fountain, G.L. Dana, B.H. Vaughn, and D.M. McKnight, Surface glaciochemistry of Taylor Valley, southern Victoria Land, Antarctica and its relationship to stream chemistry, *Hydrological Processes, 17*, 115-130, 2003.

Lyons, W.B., K.A. Welch, J.C. Priscu, J. Labourn-Parry, D. Moorhead, D.M. McKnight, P.T. Doran, and M. Tranter, The McMurdo dry valleys Long-Term Ecological Research Program; new understanding of the biogeochemistry of the dry valley lakes; a review, *Polar Geography (1995), 25* (3), 202-217, 2001.

Marino, F., G. Ghermandi, and V. Maggi, Elemental characterization of insoluble atmospheric aerosol in EPICA ice core samples using PIXE analyses, *Terra Antarctica Reports, 8*, 95-100, 2003.

Martin, J.H., Glacial-Interglacial CO2 change: the iron hypothesis, *Paleoceanography, 5* (1), 1-13, 1990.

Matsumoto, A., and T.K. Hinkley, Trace metal suites in Antarctic pre-industrial ice are consistent with emissions from quiescent degassing of volcanoes worldwide, *Earth and Planetary Science Letters, 186*, 33-43, 2001.

Mayewski, P.A., and W.B. Lyons, Source and climatic implication of the reactive iron and reactive silicate concentration found in a core from Meserve Glacier, Antarctica, *Geophysical Research Letters, 9* (3), 190-192, 1982.

Mayewski, P.A., W.B. Lyons, G. Zielinski, M. Twickler, S. Whitlow, J. Dibb, P. Grootes, K. Taylor, P.-Y. Whung, L. Fosberry, C. Wake, and K. Welch, An ice-core based, late Holocene history for the Transantarctic Mountains, Antarctica, *Contributions to Antarctic Research IV, Antarctic Res. Series, 67*, 33-45, 1995.

Mayewski, P.A., M.S. Twickler, S.I. Whitlow, L.D. Meeker, Q. Yang, J. Thomas, K. Kreutz, P.M. Grootes, D.L. Morse, E.J. Steig, E.D. Waddington, E.S. Saltzman, P.-Y. Whung, and K.C. Taylor, Climate change during the last deglaciation in Antarctica, *Science, 272* (5268), 1636-1638, 1996.

Mayewski, P.A., Antarctic oversnow traverse-based Southern Hemisphere climate reconstruction, *EOS, Transactions, American Geophysical Union, 84* (22), 205,210, 2003.

McKelvey, B.C., and P.N. Webb, Geological investigations in south Victoria Land, Antarctica; part 1, Geology of Victoria Dry valley, *New Zealand Journal of Geology and Geophysics, 2* (1), 120-136, 1959.

McKelvey, B.C., and P.N. Webb, Geological investigations in southern Victoria Land, Antarctica; part 3, Geology of Wright valley, *New Zealand Journal of Geology and Geophysics, 5* (1), 143-162, 1962.

McKendry, I.G., and W.D. Lewthwaite, The vertical structure of summertime local winds in the Wright Valley, Antarctica, *Boundary-Layer Meteorology, 51*, 321-342, 1990.

Meeker, L.D., P.A. Mayewski, and P. Bloomfield, A new approach to glaciochemical time series analysis, in *Ice Core Studies of Global Biogeochemical Cycles*, edited by R.J. Delmas, pp. 383-400, Springer-Verlag, Berlin, 1995.

Mulvaney, R., E.C. Pasteur, D.A. Peel, E.S. Saltzman, and P.Y. Whung, The ratio of MSA to non sea salt sulphate in Antarctic Peninsula ice cores, *Tellus, 44*, 295-303, 1992.

Mulvaney, R., and E.W. Wolff, Spatial variability of the major chemistry of the Antarctic ice sheet, *Annals of Glaciology, 20*, 440-447, 1994.

Nylen, T.H., A.G. Fountain, and P.T. Doran, Climatology of katabatic winds in the McMurdo dry valleys, southern Victoria Land, Antarctica, *Journal of Geophysical Research, 109* (D03114), doi: 10.1029/2003JD003937, 2004.

Pasteur, E.C., and R. Mulvaney, Laboratory study of migration of methane sulfonate in firn, *Journal of Glaciology, 45* (150), 214-218, 1999.

Pasteur, E.C., and R. Mulvaney, Migration of methae sulphonate in Antarctic firn and ice, *Journal of Geophysical Research, 105* (D9), 11525-11534, 2000.

Paterson, W.S.B., *The Physics of Glaciers*, Pegamon Press, New York, 1981.

Peixoto, J.P., and A.H. Oort, *Physics of Climate*, American Institute of Physics, New York, 1992.

Petit, J.R., J. Jouzel, D. Raynaud, N.I. Barkov, J.M. Barnola, I. Basile, M. Bender, J. Chappellaz, M. Davis, G. Delaygue, M. Delmotte, V.M. Kotlyakov, M. Legrand, V.Y. Lipenkov, C. Lorius, L. Pepin, C. Ritz, E. Saltzman, and M. Stievenard, Climate and atmospheric history of the past 420,000 years from the Vostok ice core, Antarctica, *Nature, 399*, 429-436, 1999.

Planchon, F.A.M., C.F. Boutron, C. Barbante, G. Cozzi, V. Gaspari, E.W. Wolff, C.P. Ferrari, and P. Cescon, Changes in heavy metals in Antarctic snow from Coats Land since the mid-19th to the late 20th century, *Earth and Planetary Science Letters, 200*, 207-222, 2002.

Sedwick, P.N., G.R. DiTullio, and D.J. Mackey, Iron and manganese in the Ross Sea, Antarctica: Seasonal iron limitation in Antarctic shelf waters, *Journal of Geophysical Research, 105* (C5), 11321-11336, 2000.

Sekaly, A.L.R., C.L. Chakrabarti, M.H. Back, D.C. Gregoire, J.Y. Lu, and W.H. Schroeder, Stability of dissolved metals in environmental aqueous samples: Rideau River surface water, rain and snow, *Analytica Chimica Acta, 402*, 223-231, 1999.

Smilley, R.W., Petrological evolution of basement granitoids, southern Victoria Land, *New Zealand Antarctic Record, 8* (1), 66-71, 1987.

Smith, B.T., Methane Sulphonic Acid Movement in Solid Ice Cores, *Annals of Glaciology, 39*, Preprint, 2004.

Steig, E.J., C.P. Hart, J.W.C. White, W.L. Cunningham, M.D. Davis, and E.S. Saltzman, Changes in climate ocean and ice-sheet conditions in the Ross Embayment, Antarctica, at 6 ka, *Annals of Glaciology, 27*, 305-310, 1998.

Steig, E.J., P.A. Mayewski, D.A. Dixon, S.D. Kaspari, M.M. Frey, D.P. Schneider, S.A. Arcone, G.S. Hamilton, V.B. Spikes, M. Albert, D. Meese, A.J. Gow, C.A. Shuman, J.W.C. White, S. Sneed, J. Flaherty, and M. Wumkes, High-resolution ice cores from US ITASE (West Antarctica): development and validation of chronologies and determination of precision and accuracy, *Annals of Glaciology, 41*, 77-84, 2005.

Steig, E.J., D.L. Morse, E.D. Waddington, M. Stuiver, P.M. Grootes, P.A. Mayewski, M.S. Twickler, and S.I. Whitlow, Wisconsinan and Holocene climate history from an ice core at Taylor Dome, western Ross Embayment, Antarctica, *Geografiska Annaler, 82A* (2-3), 213-235, 2000.

Thompson, D.C., R.M.F. Craig, and A.M. Bromley, Climate and surface heat balance in an Antarctic Dry Valley, *new zealand Journal of Science, 14*, 245-251, 1971.

VonStorch, H., and F.W. Zwiers, *Statistical analysis in climate research*, Cambridge University Press, Cambridge, 1999.

Wagenbach, D., F. Ducroz, R. Mulvaney, L. Keck, A. Minikin, M. Legrand, J.S. Hall, and E.W. Wolff, Sea-salt aerosol in coastal Antarctic regions, *Journal of Geophysical Research, 103* (D9), 10961-10974, 1998.

Wedepohl, K.H., The composition of the continental crust, *Geochimica et Cosmochimica Acta, 59* (7), 1217-1232, 1995.

Weisel, C.P., R.A. Duce, J.L. Fasching, and R.W. Heaton, Estimates of the transport of trace metals from the ocean to the atmosphere, *Journal of Geophysical Research, 89* (D7), 11607-11618, 1984.

Welch, K., W.B. Lyons, J.C. Priscu, R. Edwards, D.M. McKnight, H. House, and J. R.A. Wharton, Inorganic geochemical studies with special reference to calcium carbonate dynamics, *Antarctic Journal of the United States, Review 1994*, 237-239, 1994.

Welch, K.A., P.A. Mayewski, and S.I. Whitlow, Methanesulfonic acid in coastal Antarctic snow related to sea-ice extent, *Geophysical Research Letters, 20* (6), 443-446, 1993.

Welch, K.A., Glaciochemical investigations of the Newall Glacier, southern Victoria Land, Antarctica, University of New Hampshire, 1993.

Yang, Q., P.A. Mayewski, E. Linder, S. Whitlow, and M. Twickler, Chemical species spatial distribution and relationship to elevation and snow accumulation rate over the Greenland Ice Sheet, *Journal of Geophysical Research, 101* (D13), 18629-18637, 1996.

APPENDICES

Appendix A:

DATA FROM DRY VALLEYS MASS BALANCE POLES

Table A.1. Mass balance pole networks on the Victoria Upper and Clark Glaciers.

Site	Pole Number	Pole latitude °N	Pole longitude °E	distance from snow pit m	2003 - 2004 mass balance cm w.e.	2004 - 2005 mass balance cm w.e.
Victoria Upper Glacier	VUMB 1	-77.30002	161.04723	141	ND	0
	VUMB 2	-77.29972	161.04338	98	ND	0.7
	VUMB 3	-77.29943	161.03963	134	ND	-0.7
	VUMB 4	-77.30085	161.04573	99	ND	1.4
	VUMB 5	-77.30053	161.04188	0	ND	-3.5
	VUMB 6	-77.30023	161.03798	100	ND	0.35
	VUMB 7	-77.30167	161.04400	136	ND	5.25
	VUMB 8	-77.30138	161.04012	104	ND	0.7
	VUMB 9	-77.30105	161.03630	146	ND	1.05
Clark Glacier	CLMB 1	-77.40381	162.34678	504	18.36	4.32
	CLMB 2	-77.40459	162.35619	261	-0.27	4.86
	CLMB 3	-77.40622	162.35291	333	6.21	3.24
	CLMB 4	-77.40299	162.35942	321	4.59	5.13
	CLMB 5	-77.40538	162.36556	20	2.43	6.21
	CLMB 6	-77.40694	162.38425	462	5.4	3.78
	CLMB 7	-77.40849	162.40278	940	2.97	8.1
	CLMB 8	-77.40789	162.34956	485	ND	9.45
	CLMB 9	-77.40705	162.33990	659	ND	1.62
	CLMB 10	-77.40542	162.34333	552	ND	4.05
	CLMB 11	-77.40216	162.35027	533	ND	2.7
	CLMB 12	-77.40372	162.36893	204	ND	9.18
	CLMB 13	-77.40702	162.36218	201	ND	8.64
	CLMB 14	-77.40870	162.35914	401	ND	4.32
	CLMB 15	-77.41035	162.35577	602	ND	6.21
	CLMB 16	-77.40954	162.34626	663	ND	7.83
	CLMB 17	-77.40869	162.33647	802	ND	0.81
	CLMB 18	-77.40794	162.32798	962	ND	2.97
	CLMB 19	-77.40627	162.33089	856	ND	2.43
	CLMB 20	-77.40464	162.33374	788	ND	6.75
	CLMB 21	-77.40296	162.33666	765	ND	6
	CLMB 22	-77.40128	162.33958	794	ND	4.32

Table A.2. Mass balance pole networks on the Commonwealth and Blue Glaciers.

Site	Pole Number	Pole latitude °N	Pole longitude °E	distance from snow pit m	2003 - 2004 mass balance cm w.e.	2004 - 2005 mass balance cm w.e.
Commonwealth Glacier	CMMB 1	-77.54256	163.03041	191	-2.7	-0.8
	CMMB 2	-77.53842	163.02584	440	-6.75	9.7
	CMMB 3	-77.54585	163.02135	398	-5.67	ND
	CMMB 4	-77.54195	163.03443	288	ND	2.8
	CMMB 5	-77.54016	163.03437	371	ND	-1
	CMMB 6	-77.53838	163.03414	518	ND	9.7
	CMMB 7	-77.53660	163.03399	693	ND	10.5
	CMMB 8	-77.53481	163.03383	879	ND	11.9
	CMMB 9	-77.54200	163.02628	95	ND	-0.7
	CMMB 10	-77.54021	163.02603	247	ND	1.4
	CMMB 11	-77.53664	163.02570	636	ND	12.1
	CMMB 12	-77.53485	163.02558	835	ND	12.2
	CMMB 13	-77.54206	163.01795	114	ND	-2.4
	CMMB 14	-77.54027	163.01776	253	ND	0.3
	CMMB 15	-77.53849	163.01759	441	ND	13.2
	CMMB 16	-77.53670	163.01740	637	ND	2.9
	CMMB 17	-77.53490	163.01724	835	ND	10.9
	CMMB 18	-77.54214	163.00963	311	ND	-0.8
	CMMB 19	-77.54035	163.00948	382	ND	-0.7
	CMMB 20	-77.53856	163.00932	524	ND	0.1
	CMMB 21	-77.53678	163.00918	695	ND	0.9
	CMMB 22	-77.53500	163.00905	877	ND	23.6
Blue Glacier	BLMB 1	-78.07506	163.28139	936	2.7	0
	BLMB 2	-78.07498	163.29865	910	-1.89	7.29
	BLMB 3	-78.07951	163.29169	397	2.16	0
	BLMB 4	-78.08298	163.30150	199	1.35	0.27
	BLMB 5	-78.08323	163.28439	213	-2.7	2.7

Appendix B:

p VALUES FOR VARIATION IN THE MEANS OF MAJOR IONIC SPECIES IN SNOW AND FIRN REPRESENTING 1989 - 2002 FROM PRIMARY PITS ON THE CLARK, COMMONWEALTH, BLUE, AND VICTORIA UPPER GLACIERS

Figure B.1. Differences between means indicated in red are significant at the 95% confidence level ($p < 0.05$) in a) Na^+:Cl^- ratio, b) Ca^{2+}:($Na^+ + K^+ + Mg^{2+}$) ratio, c) Na^+ concentration, d) MS^- concentration, e) K^+ concentration, f) Cl^- concentration, g) Mg^{2+} concentration, h) NO_3^- concentration, i) Ca^{2+} concentration, and j) SO_4^{2-} concentration.

	# samples in calculation
Clark	51
CMW	87
Blue	65
Upper Vic	82

Na^+

	Clark	CMW	Blue	VU
Clark 350.1 ± 620.4	1			
CMW 166.8 ± 344.9	<.01	1		
Blue 72.3 ± 83.4	<.01	<.01	1	
Upper Victoria 118.9 ± 138.9	<.01	0.049	<.01	1

MS^-

	Clark	CMW	Blue	VU
Clark 33.5 ± 27.4	1			
CMW 30.9 ± 36.2	0.25	1		
Blue 14.2 ± 16.6	<.01	<.01	1	
Upper Victoria 13.7 ± 19.7	<.01	<.01	0.054	1

K^+

	Clark	CMW	Blue	VU
Clark 26.5 ± 37.3	1			
CMW 11.4 ± 15.7	<.01	1		
Blue 7.7 ± 6.0	<.01	<.01	1	
Upper Victoria 8.6 ± 6.0	<.01	0.04	<.01	1

Cl^-

	Clark	CMW	Blue	VU
Clark 684.9 ± 955.3	1.00			
CMW 336.1 ± 600.3	<.01	1.00		
Blue 160.0 ± 173.4	<.01	<.01	1.00	
Upper Victoria 220.4 ± 176.0	<.01	<.01	<.01	1.00

Mg^{2+}

	Clark	CMW	Blue	VU
Clark 54.9 ± 77.2	1			
CMW 24.4 ± 36.4	<.01	1		
Blue 13.8 ± 10.1	<.01	<.01	1	
Upper Victoria 35.0 ± 35.3	<.01	<.01	<.01	1

NO_3^-

	Clark	CMW	Blue	VU
Clark 177.3 ± 157.8	1			
CMW 93.0 ± 88.4	<.01	1		
Blue 82.4 ± 84.5	<.01	0.33	1	
Upper Victoria 160.9 ± 111.4	0.28	<.01	<.01	1

Ca^{2+}

	Clark	CMW	Blue	VU
Clark 120.1 ± 206.5	1			
CMW 51.8 ± 111.5	<.01	1		
Blue 192.1 ± 412.1	0.03	<.01	1	
Upper Victoria 114.4 ± 152.2	0.61	<.01	<.01	1

SO_4^{2-}

	Clark	CMW	Blue	VU
Clark 339.8 ± 348.3	1			
CMW 219.2 ± 223.8	<.01	1		
Blue 233.1 ± 243.5	<.01	0.43	1	
Upper Victoria 366.7 ± 332.6	0.42	<.01	<.01	1

BIOGRAPHY OF THE AUTHOR

Bruce R. Williamson was born in New York City, NY on January 24, 1968. He grew up in New York and New England. He graduated from high school (Phillips Exeter Academy) in 1986. After attending Stanford University for a year and a half, the author relocated to Williams College, where he received a Bachelor of Arts degree in History in 1990. For the next ten years, he lived in New York and Seattle, where he found employment as a Research Associate Editor at Reader's Digest Magazine in Pleasantville, NY and then as a luthier at Arnquist Guitars in Seattle.

In 2001, the author entered classes at the University of Washington, from which he received a Bachelor of Science degree in Earth and Space Science in May, 2003. Upon completion of a Master's degree at the University of Maine, he will be entering the Earth Science Department at the University of Maine in pursuit of a Ph.D. He is a candidate for the Master of Science degree in Earth Sciences from The University of Maine in August, 2006.